From the Clinic for Gastroenterology, Hepatology and Infectious Diseases at
Heinrich Heine University Düsseldorf

BAF function in HIV-1 replication

Dissertation

to obtain the academic title of Doctor of Philosophy (PhD) in Medical Sciences from the Faculty of Medicine at Heinrich Heine University Düsseldorf

submitted by

Xiao Tang

2025

As an inaugural dissertation printed by permission of the Faculty of Medicine at Heinrich Heine University Düsseldorf

signed:

Dean:

Prof. Dr. med. Nikolaj Klöcker

First examiner:

Univ.-Prof. Dr. Carsten Münk

Clinic for Gastroenterology, Hepatology and Infectiology

Faculty of Medicine, Heinrich Heine University Düsseldorf

Second examiner:

Univ.-Prof. Dr. Philipp Lang

Institute of Molecular Medicine II

Faculty of Medicine, Heinrich Heine University Düsseldorf

Zusammenfassung

Diese Dissertation untersucht die vielfältigen Funktionen des „Barrier to Autointegration Factor 1“ (BAF) im Kontext retroviraler Infektionen und der Regulation der angeborenen Immunantwort, mit besonderem Fokus auf seine Interaktion mit HIV-1. BAF ist ein hochkonserviertes, DNA-bindendes Protein, das die Autointegration retroviraler DNA verhindert und deren korrekte Integration in das Wirtsgenom unterstützt. Mittels molekularbiologischer und zellulärer Experimente konnte gezeigt werden, dass eine HIV-1-Infektion den endogenen BAF-Proteinspiegel in HEK293T-Zellen senkt – jedoch nur, wenn die Viruspartikel über das Drei-Plasmid-System erzeugt wurden, nicht aber bei Transfektion mit vollständigen HIV-1-Konstrukten.

Entgegen früheren Annahmen konnte zudem nachgewiesen werden, dass BAF unter Überexpressionsbedingungen in HIV-1-Virionen eingebaut wird. Funktionelle Studien zeigen, dass BAF für die Replikation von HIV-1 in Zielzellen essenziell ist, jedoch nicht in virusproduzierenden Zellen benötigt wird. Ein Knockout von BAF in THP-1-Zellen führt zu einer deutlichen Reduktion der HIV-1-Replikation, ein Effekt, der durch erneute Expression von BAF teilweise rückgängig gemacht werden kann. Im Gegensatz dazu fördert der BAF-Knockout die Replikation des murinen Leukämievirus (MLV), was auf virusartspezifische Regulationsmechanismen hinweist.

Neben seiner Rolle bei der retroviralen Integration wirkt BAF auch als wichtiger Regulator der angeborenen Immunantwort. Der Verlust von BAF führt zur Hochregulierung interferonstimulierter Gene (ISGs) wie ISG15 und ISG54, selbst ohne eine gleichzeitige Erhöhung der Typ-I-Interferon-Produktion. Dies deutet auf eine mögliche posttranskriptionale oder chromatinvermittelte Regulation dieser Gene durch BAF hin. Darüber hinaus erhöht das Fehlen von BAF die Aktivierung des cGAS–STING-Signalwegs, was BAF als negativen Regulator dieser antiviralen Achse ausweist.

Zusammenfassend beschreibt diese Arbeit BAF als doppelt wirkenden Wirtsfaktor: Einerseits unterstützt er die retrovirale Integration, andererseits dämpft er übermäßige Immunaktivierung. Diese Erkenntnisse liefern neue Einblicke in die Wechselwirkungen zwischen Virus und Wirt und identifizieren mögliche Zielstrukturen für therapeutische Ansätze bei viralen Infektionen und Immunregulation.

Summary

This dissertation investigates the multifaceted roles of Barrier to Autointegration Factor 1 (BAF) in the context of retroviral infection and innate immune regulation, with a particular focus on its interaction with HIV-1. BAF is a highly conserved DNA-binding protein known to prevent retroviral DNA autointegration and promote proper integration into the host genome. Through a series of molecular and cellular experiments, I demonstrate that HIV-1 infection downregulates endogenous BAF protein levels in HEK293T cells, specifically when viral particles are produced via the 3-plasmid system, but not with full-length HIV-1 constructs. Notably, BAF can be incorporated into HIV-1 virions under overexpression conditions, contrary to previous assumptions.

Functional studies reveal that BAF is essential in HIV-1 target cells but not in virus-producing cells, underscoring its critical role in the post-entry phase of infection. Knockout of BAF in THP-1 cells significantly impairs HIV-1 replication, an effect that is partially rescued by BAF re-expression. In contrast, BAF knockout enhances replication of Murine Leukemia Virus (MLV), suggesting virus-specific interactions and regulatory mechanisms.

Beyond its role in retroviral integration, BAF also emerges as a key modulator of innate immunity. Loss of BAF results in upregulation of interferon-stimulated genes (ISGs) such as ISG15 and ISG54, even in the absence of increased type I interferon production. This highlights a potential post-transcriptional or chromatin-level regulatory function for BAF in ISG expression. Furthermore, BAF deficiency sensitizes cells to enhanced cGAS–STING pathway activation, supporting its role as a negative regulator of this critical antiviral signaling axis.

In summary, this work defines BAF as a dual-function host factor: facilitating retroviral integration while restraining innate immune activation. These findings offer new insights into host-virus interactions and uncover potential targets for therapeutic modulation in viral infection and immune regulation.

List of abbreviations

APS	Ammonium persulphate solution
A3A	AOBEC3A
BAF1	Barrier-to-autointegration factor 1
cGAMP	2',3'-cyclic-GMP-AMP
cGAS	Cyclic GMP–AMP synthase
cps	counts per second
CRFK	Crandell-Rees Feline Kidney cells
DMEM	Dulbecco's modified eagle complete medium
DMSO	Dimethyl sulfoxide
DNA-PK	DNA-dependent protein kinase
dNTP	Deoxynucleoside triphosphate
DHFR	dihydrofolate reductase
ER	Endoplasmic reticulum
Gag	Group-specific antigen
HIV	Human immunodeficiency virus
HIV-1	Human immunodeficiency virus type 1
HS-DNA	Herring sperm DNA
IFN-β	Interferon beta
ISGs	Interferon-stimulated genes
Ku	Ku70/80
kDa	Kilodalton
LB	luria-bertani
M	Mole
min	Minute
ml	Milliliter
mM	Millimolar
MVA	Modified vaccinia virus Ankara
min/kb	Kilobase per minute
NHEJ	non-homologous end-joining
ng	Nanogram
nm	Nanometer
Native SDS PAGE	Native polyacrylamide gel electrophoresis
NF-κB	Nuclear factor kappa B
OMK	Oleanolic acid methyl ester derivative
rcf	Relative centrifugal force
rpm	Revolutions per minute
p53	Tumor protein p53
PAMPs	Pathogen-associated molecular patterns
PRRs	Pattern recognition receptors
RPMI	Roswell Park Memorial Institute
RT	Room temperature
s	Second

SDS	Sodium dodecyl-sulfate
SDS–PAGE	Sodium dodecyl-sulfate polyacrylamide gel electrophoresis
STING	Stimulator of interferon genes
TEMED	N, N, N′, N′-Tetramethyl ethylenediamine
Tris-HCl	Tris (hydroxymethyl) aminomethane
U/ml	Unit per milliliter
V	Voltage
µg	Microgram
µg/ml	Microgram pro milliliter
µl	Microliter
µM	Micromolar

Table of contents

1 Introduction

1.1 HIV-1 replication

Replication of HIV-1 (human immunodeficiency virus type 1, a retrovirus) is a complex multi-step process that involves several key steps[1–8](Fig. 2). Infection with HIV-1 causes systemic T cell destruction and reduced cell-mediated immunity that leads to a wide range of opportunistic infections and cancers[9]. In addition to the structural genes *gag*, *pol*, and *env* that are found in all retroviruses, HIV-1 possesses two regulatory genes, *tat,* and *rev*, which are essential for viral replication, along with four accessory genes, *vif*, *vpr*, *vpu*, and *nef* (see Fig. 1)[10]. While these accessory genes are unnecessary for viral growth *in vitro*, they are crucial for replication and pathogenesis *in vivo*[10].

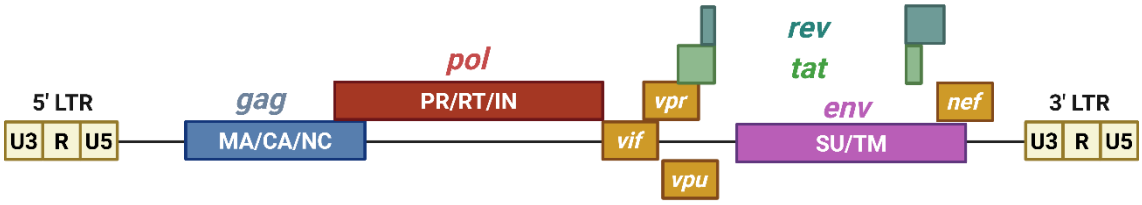

Fig. 1: **Schematic representation of the HIV-1 genome organization.** The HIV-1 genome is composed of the following structural, accessory, and regulatory genes: *gag* (blue) encodes the matrix (MA), capsid (CA), and nucleocapsid (NC) proteins, which are essential for virus assembly and structure. *pol* (red) encodes protease (PR), reverse transcriptase (RT), and integrase (IN), which are critical for viral replication and integration. *env* (purple) encodes the surface (SU) and transmembrane (TM) proteins, which facilitate host cell entry. Accessory genes (*vif*, *vpr*, *vpu*, and *nef* in yellow) and regulatory genes (*rev* and in green) contribute to viral replication, immune evasion, and regulation of transcription. The genome is flanked by 5' and 3' LTRs (light yellow), which contain regulatory sequences necessary for transcription and replication. Created with BioRender.com.

A virus must undergo the replication process to create new, infectious virions that can infect other body cells or subsequent hosts[11].

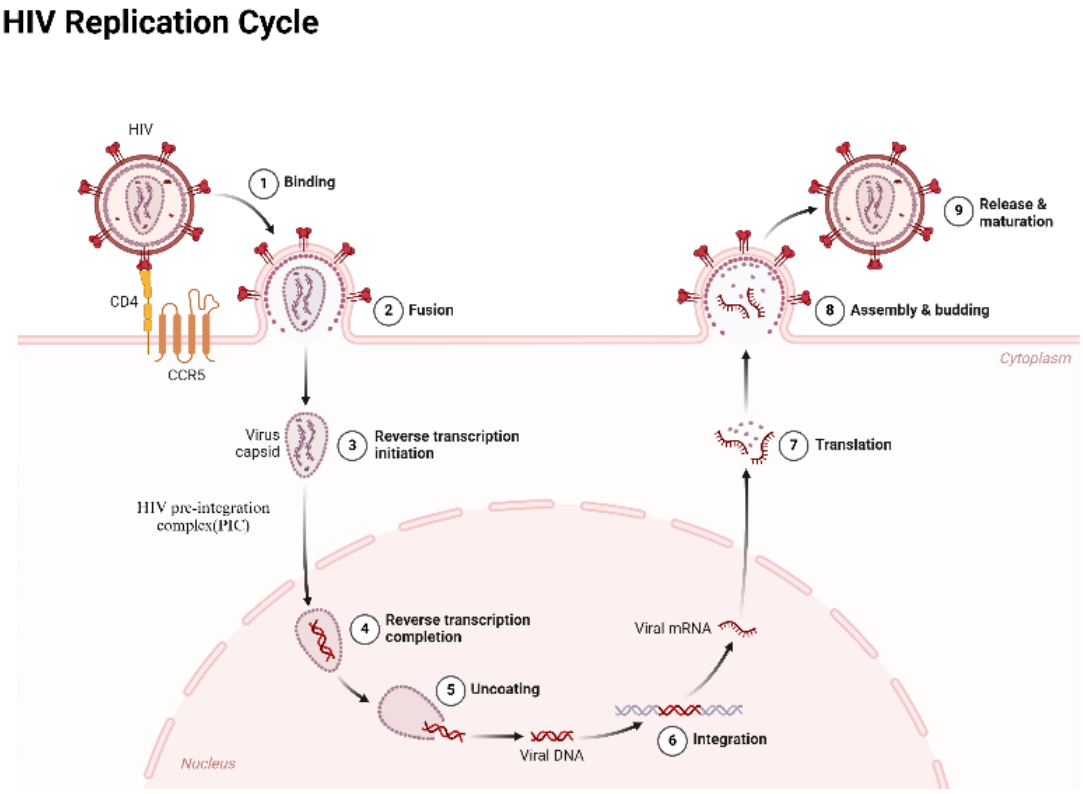

Fig. 2： Schematic overview of the HIV-1-1 replication cycle[2]. The figure illustrates the main steps in the HIV-1-1 replication cycle: binding to the CD4 receptor and co-receptors; fusion with the host cell membrane; possible gradual uncoating of the viral capsid; reverse transcription of HIV-1 RNA to DNA; formation of the pre-integration complex (PIC); and translocation into the nucleus. Once in the nucleus, the main uncoating step is required before the viral DNA is integrated into the host DNA and subsequently transcribed and translated to form new viral RNA and viral proteins that translocate to the cell surface to assemble into new immature virus forms. The new viruses bud off and are released. Finally, during maturation, the protease enzyme cleaves the structural polyprotein to form mature Gag proteins, producing new infectious virions. Created with BioRender.com[2].

1.1.1 HIV-1 entry into host cells

Enveloped viruses, such as HIV-1, utilize membrane fusion to gain entry into host cells[12–14]. HIV-1 infection begins with the attachment of the virion to a host cell via its envelope glycoprotein (*Env*), which subsequently induces the fusion of the viral and cell membranes, facilitating viral entry[15]. The HIV-1 *Env* is the only glycoprotein

displayed on the surface of the HIV-1 virion[16–18]. The viral *Env* specifically binds to the CD4 receptor on the surface of a target cell[19]. This binding induces a conformational change in *Env*, allowing it to interact with a co-receptor on the host cell surface[20,21]. The two main co-receptors are CCR5 and CXCR4[22]. The choice of co-receptor depends on the HIV-1 strain: R5-tropic HIV-1 strains use CCR5[23], while X4-tropic strains use CXCR4[24]. Dual-tropic strains can interact with both CCR5 and CXCR4[25]. Binding to the co-receptor triggers further conformational changes in another viral glycoprotein, gp41[26]. This glycoprotein facilitates the fusion of the viral envelope with the host cell membrane[27]. Gp41 inserts itself into the host cell membrane, folding back on itself to bring the viral and cellular membranes closer, allowing them to fuse[26,28].

1.1.2 Integration， assembly, and maturation

After entry into the host cell, the uncoating of the viral capsid occurs gradually, with partial disassembly of the capsid as it moves toward the nucleus.[8,29]. Other models, however, claim that all uncoating happens in the nucleus[30,31]. The viral RNA genome is reverse-transcribed within the reverse transcription complex (RTC) to double-stranded DNA by the viral enzyme reverse transcriptase[32]. The RTC matures into the pre-integration complex (PIC), which delivers the viral DNA to the nucleus for the viral enzyme integrase integration into the host cell's chromosome [33,34]. The pre-integration complex may also sequester and protect the viral DNA from cellular DNA-modifying enzymes[35] and cytoplasmic DNA sensors[36–38] that could trigger antiviral innate immunity.

The late phase in the HIV-1 morphogenesis includes the assembly of new viral particles, their release from the host cell's plasma membrane, and maturation coupled with infectious activity[39]. HIV-1 assembly and replication proceed by forming morphologically distinct immature and mature viral capsids organized by the Gag polyprotein (immature) and the fully processed CA protein (mature)[40]. Immature

particles dramatically rearrange upon budding to form mature, infectious virions[40]. The maturation process changed the arrangement of the structural components inside the virion: the radially arranged Gag molecules were dismantled, and a conical core structure was assembled in the center of the viral particle[39]. These capsids enclose the viral genome and facilitate delivery into new host cells[40,41].

1.1.2.1 HIV-1 integration and autointegration

The retrovirus family is characterized by reverse transcription of the viral RNA genome to cDNA that is flanked by directly repeated sequences termed long terminal repeats (LTRs)[42,43] (Fig. 1) and its integration into the host cell genome[44]. The reverse transcribed cDNA integration is mediated by the viral encoded and imported integrase enzyme[45]. Integrase excises a dinucleotide from the 3' terminus of the cDNA in a step known as 3' processing[46,47]. Subsequently, integrase cleaves the host genomic DNA at the integration site, generating staggered single-stranded breaks. The 3' processed viral DNA is then covalently linked to the cleaved host DNA in a process known as strand transfer[48]. Single-stranded DNA breaks in the host genome at the site of viral integration are subsequently repaired by host cellular mechanisms[49,50]. The viral genome preferentially integrates into transcriptionally active, open chromatin regions[51–53]. Following integration, the transcription of viral genes is driven by host transcription factors, leading to the synthesis of the viral transactivating protein *Tat*[44,54]. *Tat* does not function as a transcription factor itself; instead, it binds to CDK9 and the cyclin T1 subunit of the P-TEFb complex, as well as RNA polymerase II (RNA Pol II), thereby enhancing the phosphorylation of the C-terminal domain (CTD) of RNA Pol II[53]. This phosphorylation increases the processivity of RNA Pol II, allowing efficient elongation of viral transcripts from the LTR promoter[55]. This sequence of events ensures that the viral genes integrated into the host genome are actively transcribed, ultimately producing viral proteins and completing the viral replication cycle.

However, early in the cell infection, most viral cDNA is unintegrated [56–60]. Multiple forms of unintegrated viral DNA exist, including linear cDNA[44]. Linear cDNA is the

most abundant form, the direct product of reverse-transcribed viral RNA, the precursor to an integrated provirus, and the substrate for the integration reaction[61–63]. All other unintegrated DNA products derive from linear cDNA and are circular[44].

Unintegrated circles can be produced through autointegration, also called suicidal integration, in which the 3'-ends of the viral DNA integrate into itself instead of the host genome[64], producing either internally rearranged or less than full-length DNA circles[65]. This process can occur if the integration machinery mistakenly targets viral DNA instead of host DNA. Autointegration is seen in murine Moloney leukemia virus (MoMLV) and HIV-1 infections and is thus a likely common feature of retroviral replication[33,66–69]. Linear cDNA can also be recombined to produce 1-LTR circles[70]. In addition, the non-homologous end-joining pathway can form 2-LTR circles. (Fig. 3). It is believed that all circular viral DNAs are dead-end products[71].

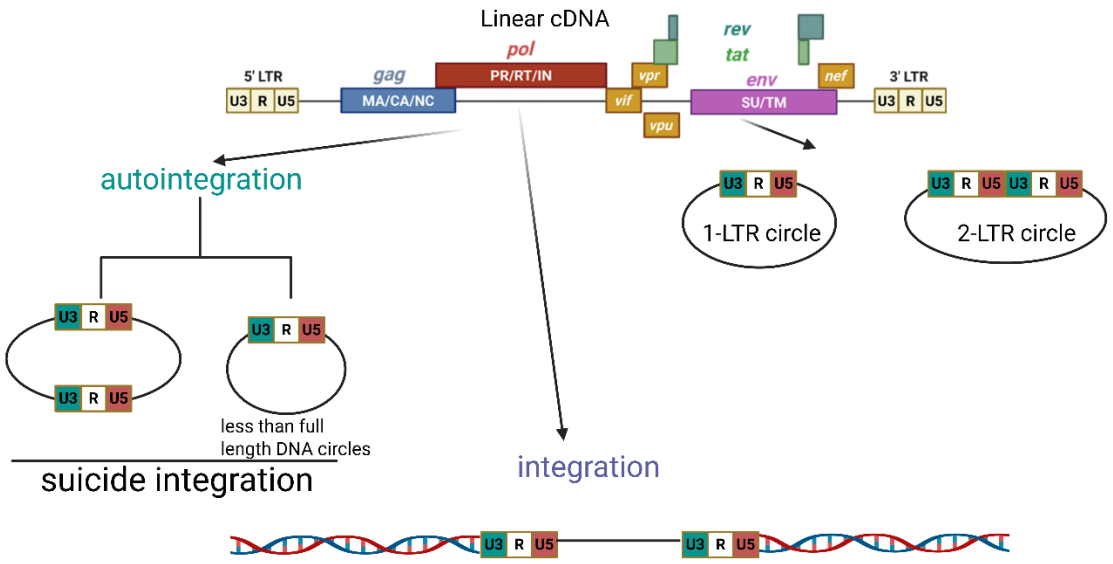

Fig. 3: HIV-1 autointegration and integration. Linear cDNA is the product of reverse transcription. Autointegration leads to the formation of the internally or truncated rearranged circular circle. Recombination and host factors contribute to 1-LTR and 2-LTR circle formation. The viral DNA is also integrated into the host cell's genome. The figure was reproduced with permission from Sloan, R.D., Wainberg, M.A[44]. Created with BioRender.com.

1.2 Immunity

Mammalian cells detect and respond to RNA virus infections by recognizing non-self RNA elements through various pathogen recognition receptors (PRRs)[72]. These include the cell surface and endosomal RNA sensors Toll-like receptors 3 and 7 (TLR3 and TLR7)[73,74], as well as the cytoplasmic RNA sensors retinoic acid-inducible gene I (RIG-I)[75] and melanoma differentiation-associated gene 5 (MDA5)[72]. Binding single- and double-stranded viral RNA to PRRs leads to the downstream activation of transcription factors, including interferon (IFN) regulatory factors 3 and 7 (IRF-3 and IRF-7) and NF-κB[76]. This activation induces the production of IFN-α and IFN-β[77]. The secreted IFNs then engage the IFN-α/β receptor (IFNAR) in autocrine and paracrine manners, activating JAK/STAT-dependent signal transduction cascades[78]. These cascades induce the expression of hundreds of interferon-stimulated genes (*ISGs*), many of which possess antiviral properties[79].

In addition to utilizing RNA sensors to detect RNA viruses, cells also employ DNA-sensing machinery to detect DNA viruses or detect intracellular damage caused early in infection by both RNA and DNA viruses[80]. For example, Cyclic GMP-AMP synthase (cGAS) functions as a DNA sensor[81], which triggers the Stimulator of interferon genes (STING) and induction of type I IFN and ISGs.

At each stage of the immune response, stimulatory and inhibitory signals finely regulate the response's magnitude, quality, and nature. Positive regulators enhance the immune response to effectively eliminate viral infections, while negative regulators mitigate inflammatory responses to prevent immune-mediated tissue damage and spontaneous autoimmunity[82].

1.2.1 cGAS-STING pathway

Innate immunity serves as the first line of defense against invading pathogens. In response to infection, cells utilize various DNA sensors to detect microbial DNA or mislocalized

cellular DNA, initiating antiviral immune responses. The cGAS/STING pathway has emerged as a central innate immune sensing pathway for cytosolic double-stranded DNA (dsDNA) and downstream IFN responses[83–88](Fig. 3). Initially, cytosolic DNA is recognized by the enzyme cGAS, which catalyzes the cyclic dinucleotide 2,3'-cGAMP production from ATP and GTP[89,90]. 2',3'-cGAMP is the second messenger, which induces the dimerization and activation of the endoplasmic reticulum (ER) protein-anchored STING[91,92], also known as MITA[93]. Once activated, dimeric STING translocates to a perinuclear Golgi-like compartment, which oligomerizes to recruit and activate TANK-binding kinase 1(TBK1) and IKKβ. TBK1 subsequently phosphorylates the interferon regulatory factor 3(IRF3), stimulating a type I interferon (IFN) [94–98] and IFN-stimulated genes response[99].

Detection of foreign nucleic acids is an ancient form of host defense. In vertebrates, this detection triggers an antiviral defense program to neutralize the spread of infection. This antiviral response is coordinated by type I interferons (IFNs), which orchestrate a multifaceted strategy to inhibit viral replication within infected cells, alert neighboring cells to the presence of the infection, and expand effector lymphocytes to provide long-term, specific protection against the virus[38].

Some RNA viruses also trigger cGAS-mediated antiviral immunity dependent on the release of mitochondrial DNA (mtDNA) during the viral infection[80,100]. Since cGAS activation potently suppresses viral replication, viruses have evolved intricate strategies to antagonize cGAS-mediated immune signaling[101].

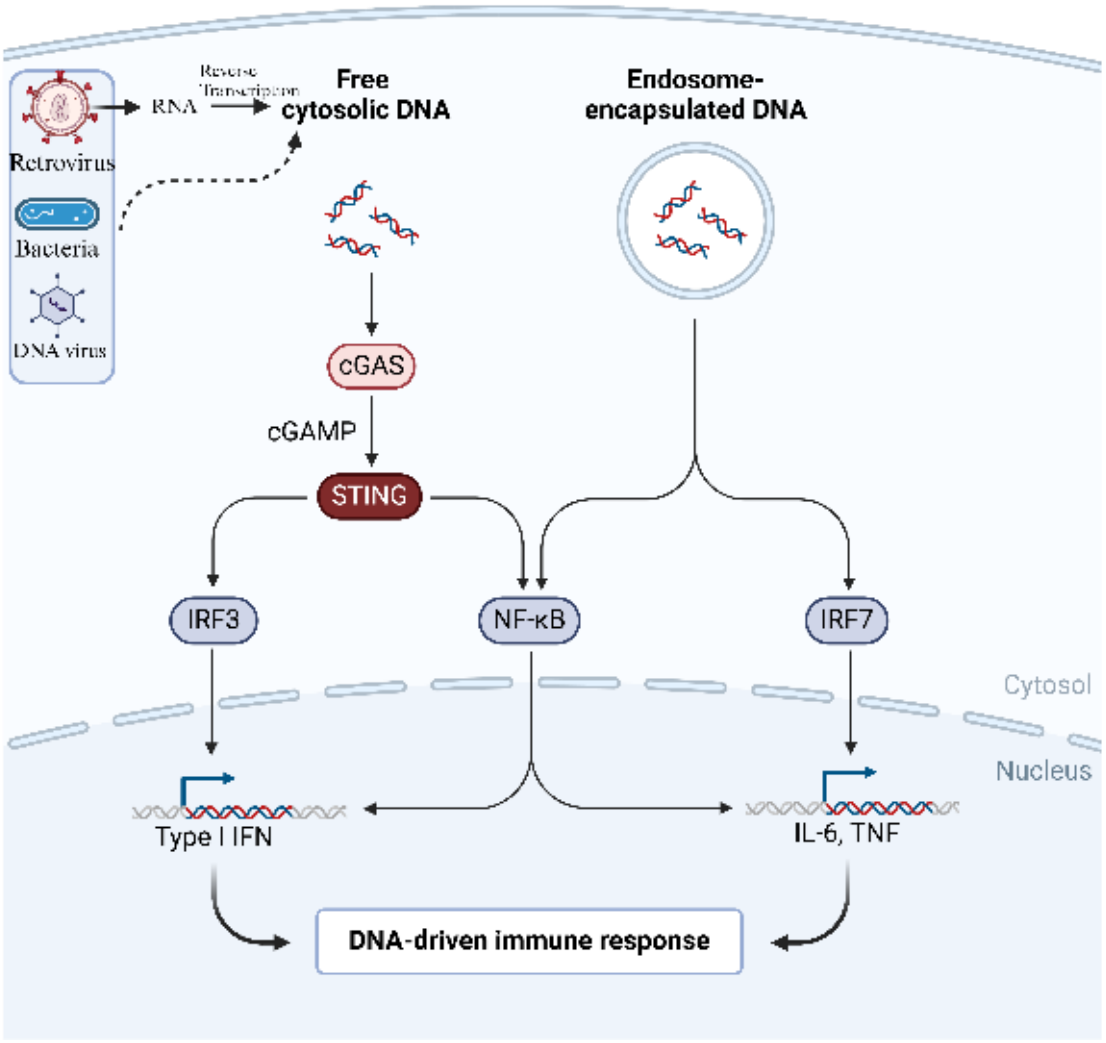

Fig. 4: **The cGAS-STING signaling pathway.** The innate immune sensor cyclic GMP-AMP synthase (cGAS) can sense various cytoplasmic DNAs. Upon binding of dsDNA, cGAS undergoes a conformational change that leads to its enzymatic activation, producing the second messenger 2',3'-cyclic-GMP-AMP (cGAMP). Upon cGAMP binding, the stimulator of interferon genes (STING) translocates from the endoplasmic reticulum (ER) to the Golgi apparatus via coat protein complex-II (COP-II) vesicles, where it recruits TANK-binding kinase 1 (TBK1), promoting TBK1 autophosphorylation and STING phosphorylation. Phosphorylated STING recruits interferon regulatory factor 3 (IRF3), which TBK1 further phosphorylates. In addition to IRF3, TBK1 activates nuclear factor kappa B (NF-κB) signaling. Subsequently, nuclear translocation of IRF3 and NF-κB induces the expression of type I interferons and inflammatory cytokines. Activation of STING also leads to the formation of microtubule-associated protein 1A/1B-light chain 3 (LC3+) vesicles by autophagy. Created with BioRender.com

1.2.1.1 Interferon production

Interferons (IFN) are cytokines that play a crucial role in the immune system[102]. They induce antiviral and antitumor effects and promote the development of immune responses. Through their action, IFN helps control viral infections, inhibit tumor growth, and enhance the activity of various immune cells, contributing to innate and adaptive immunity[103–105]. IFN regulates a broad range of physiological processes, including cytokine and chemokine synthesis[106], mRNA translation[107], RNA and protein stability[108,109], antigen presentation[110], nuclear trafficking[111], cell differentiation[112,113], and cell division and apoptosis[114,115]. IFNs are pivotal in immune modulation and maintaining cellular homeostasis through these mechanisms.

There are three main classes of interferons: type I (predominantly IFN-α, IFN-β, and IFN-κ), type II (IFN-γ)[116], and type III (IFN-λ1 and IFN-λ2, also known as IL-28 and IL-29).

1.2.2 DNA-PK

The DNA-dependent protein kinase (DNA-PK) is a serine/threonine protein kinase primarily known for its role in non-homologous end joining, essential for double-strand break (DSB) repair and V(D)J recombination[117]. DNA-PK is a heterotrimeric protein complex composed of Ku70, Ku80, and the catalytic subunit DNA-PKcs. Besides its nuclear localization, DNA-PK partly localizes in the cytoplasm[118,119]. DNA damage and detection of foreign DNA trigger distinct modalities of DNA-PK activity[120]. Previous studies have suggested a role for DNA-PK in the antiviral response triggered by detecting intracellular DNA[118,121,122].

1.3 BAF/BANF1, Barrier-to-autointegration factor 1

Barrier-to-autointegration factor, encoded by the *BANF1* gene and called *BAF*[123], is an

essential, highly conserved protein among metazoans[124,125]. BAF was first identified in mammalian cells because of its association with the pre-integration complexes (PICs) of retroviruses and its ability to block suicidal autointegration, thus earning the name 'barrier-to-autointegration factor 1[124,126,127]. In the cytoplasm, it appears to bind to the proviral DNA within the PICs and prevent autointegration[124]; once within the nucleus, it appears to facilitate the integration of the proviral DNA into the host chromosome[128]. BAF also has intriguing roles in physiology since BAF missense mutations appear sufficient to cause human progeroid syndrome[129–131]. In addition, BAF can bind to exogenous double-stranded DNA in the cytosol following endosomal breakdown to evade autophagy[132].

BAF is a small (10-kDa), conserved, and abundant DNA-binding protein with 89 amino acids that is a dimer in solution[125]. BAF is a ubiquitously expressed protein in almost all eukaryotic cell types[133–137], with multiple functions necessary for maintaining the integrity of the cellular genome[138,139]. Although its localization can be variable, depending on cell type, age, and cell cycle stage, BAF is found throughout the cytoplasm and nucleoplasm and enriched on the nuclear envelope (NE)[140]. BAF localization depended on the age of the cell, localizing primarily in the nucleus of >90% of young proliferating cells but only 20-25% of aged senescent cells[136].

1.3.1 BAF and pre-integration complexes

Integration of a DNA copy of the viral genome into a host chromosome is an essential step in the retrovirus life cycle. The machinery that carries out the integration reaction is an integrase nucleoprotein complex derived from the core of the infecting virion[141–143]. In *vivo*, integration is mediated by large subviral pre-integration complexes (PICs) that can integrate their endogenous cDNA into an added target DNA in *vitro*[144–148]. In addition to the integrase enzyme, retroviral PICs contain various viral and host cell proteins[149–154]. To successfully integrate into host DNA, the viral DNA within this complex must avoid self-destructive integration into itself, a reaction termed autointegration. BAF is a factor that prevents viral autointegration. In 1994, Lee provided

evidence that the PIC of MoMLV contains a cellular barrier-to-autointegration factor (BAF) that prevents suicidal autointegration[155]. Evidence of BAF as a cellular component in HIV-1 PICs was obtained through co-immunoprecipitation of integrase activity using anti-BAF antibodies[156]. PICs were isolated from cytoplasmic extracts of HIV-1-infected cells 7 hours post-infection. Antibodies targeting known PIC components, such as the viral integrase and matrix proteins, were employed to immunoprecipitate active complexes. The presence of viral cDNA was detected by Southern blotting, while integrase and BAF were identified through Western blotting. Crucially, controls using normal IgG failed to precipitate detectable levels of cDNA or proteins, confirming specificity. Additionally, PIC activity and the association of BAF were corroborated using antibodies against other components, including Ku-80 and Vpr. Ultrafiltration improved the yield of immunoprecipitated complexes, demonstrating that approximately 30% of PICs were co-immunoprecipitated with anti-BAF antibodies. These results provided robust evidence that BAF is a bona fide component of PIC derived from cells infected with either MoMLV or HIV-1[128,156].

BAF binds with low micromolar affinity to p55 Gag, the structural precursor of HIV-1 virions, and to the matrix derived from Gag and may constitute a component of the pre-integration complex (PIC)[157–159]. BAF was recently discovered at low stoichiometry (0–3 per virion) in mature HIV-1 virions[157].

BAF was also implicated in restoring the salt-inactivated PIC activity of HIV-1[160]. This conclusion was supported by biochemical reconstitution experiments, where HIV-1 PICs were first stripped of host factors through exposure to 1.2 M KCl, abolishing their integration activity in vitro. The addition of purified recombinant human BAF at low nanomolar concentrations (5–20 nM) successfully restored the intermolecular integration activity, as evidenced by Southern blot analysis of integration products. Furthermore, Mu-mediated PCR (MM-PCR) footprinting revealed that BAF, but not other DNA-binding proteins such as HMG I(Y) or RNase A, could reconstitute the specific protein-DNA structure (intasome) at the ends of viral DNA. These biochemical findings indicate that BAF directly interacts with HIV-1 PICs to restore their function in vitro, suggesting its role as a natural host cofactor for HIV-1 integration.

BAF protects the PIC from being targeted by its integrase *in vitro*. More generally, BAF positively enhances integrase-dependent integration of PIC from both MoMLV and HIV-1 into target DNA rather than into the viral DNA *in vitro*[124,126,127]. It has been proposed that each BAF dimer has two binding sites for double-stranded DNA (dsDNA) and functions by sterically 'cross-bridging' DNA within the pre-integration complex (PIC), thereby protecting retroviral DNA from integrase[124]. BAF may play sophisticated roles in retrovirus infection due to its ability to bind DNA and protein components of the pre-integration complex (PIC). Based on its presence in mature virions and its predicted ability to recruit more BAF (through oligomerization) from the cytoplasm of newly invaded cells, BAF is proposed to contribute to very early events, such as the conversion of reverse transcriptase (RT) complexes into pre-integration complexes (PICs), as well as later events like facilitate the integration of the proviral DNA into the host chromosome[157]. Although BAF is directly involved in stimulating the intermolecular integration in the *in vitro* PIC assay, it is most probable that the *in vivo* role will be indirect. However, BAF does not stimulate the activity of recombinant integrase[161].

The pre-integration complex (PIC) characterization has evolved significantly with advancements in our understanding of HIV-1 infection mechanisms. Early studies characterized the PIC as a cytoplasmic or nuclear nucleoprotein complex containing viral double-stranded DNA (dsDNA), viral integrase (IN), and host factors necessary for integration activity in vitro[162]. These PICs were extracted and partially purified from infected cells using biochemical approaches such as high-salt stripping and Nycodenz gradient centrifugation, followed by functional reconstitution with host cell extracts or specific host proteins like BAF. BAF was identified as a critical host cofactor that restored the integration activity of salt-treated PICs and reconstituted the native protein-DNA structure at the ends of the viral DNA[162,163]. However, emerging data have reshaped our understanding of HIV-1 replication complexes, particularly with the discovery that an intact or nearly intact viral capsid can enter the nucleus[163–165]. Studies now suggest that the reverse transcription of viral RNA into DNA and the transition of the reverse transcription complex (RTC) to the PIC may occur within the nucleus rather than in the cytoplasm, challenging the canonical view of early events in HIV-1 infection[163,166].

Notably, the capsid appears to shield the viral genome and facilitate nuclear transport until it undergoes controlled disassembly within the nuclear environment[163]. This new understanding raises important questions about the interaction of host factors like BAF with the PIC. If the viral core remains largely intact during nuclear entry, BAF is more likely to interact with the PIC after partially uncoating the capsid in the nucleus. This interaction could stabilize the viral DNA ends, protect against autointegration, and facilitate the assembly of the integration machinery at chromatin-associated sites. However, the precise timing and location of BAF's engagement remain unclear and likely depend on the spatiotemporal dynamics of capsid uncoating and PIC maturation. In light of these findings, the definition of the PIC may need to be updated to incorporate its dynamic nature and its dependence on nuclear uncoating events. Future studies using advanced imaging and biochemical techniques will be essential to resolve how host factors like BAF coordinate with capsid disassembly and PIC maturation in the nucleus.

1.3.2 BAF function

BAF participates in multiple cellular pathways (Fig. 5), including gene regulation, chromatin structure maintenance, nuclear assembly, and viral infection processes[138]. A family of nuclear proteins containing a folded motif known as the LEM domain has been identified to directly bind BAF[167–169]. LEM domain proteins include lamina-associated polypeptide (LAP)2β, emerin, and MAN1 (Fig. 4). LAP2α, distinct from other LEM-domain proteins, lacks a transmembrane domain and is found abundantly in the nuclear interior, where it stably binds to lamin A[170]. These LEM-domain proteins play structural roles during nuclear assembly and are crucial for DNA replication competence[171–173]. All LEM-domain proteins interact with BAF, which is thought to connect chromatin to LEM-domain proteins in the nuclear envelope[174]. LAP2α and BAF co-regulate the assembly of specialized components in nuclear envelope architecture, including membrane-anchored LEM-domain proteins and A-type lamin filaments. BAF's capacity to bridge DNA[175], together with findings that LEM-domain proteins associated with the nuclear lamina interact with BAF in two-hybrid screens[176],

suggests a potential role for BAF in nuclear structure organization. Furthermore, RNA interference (RNAi)-mediated downregulation of BAF in *Caenorhabditis elegans* embryos[175] or the generation of BAF-null *Drosophila* embryos[177] leads to lethal phenotypes, underscoring BAF's essential role in nuclear assembly.

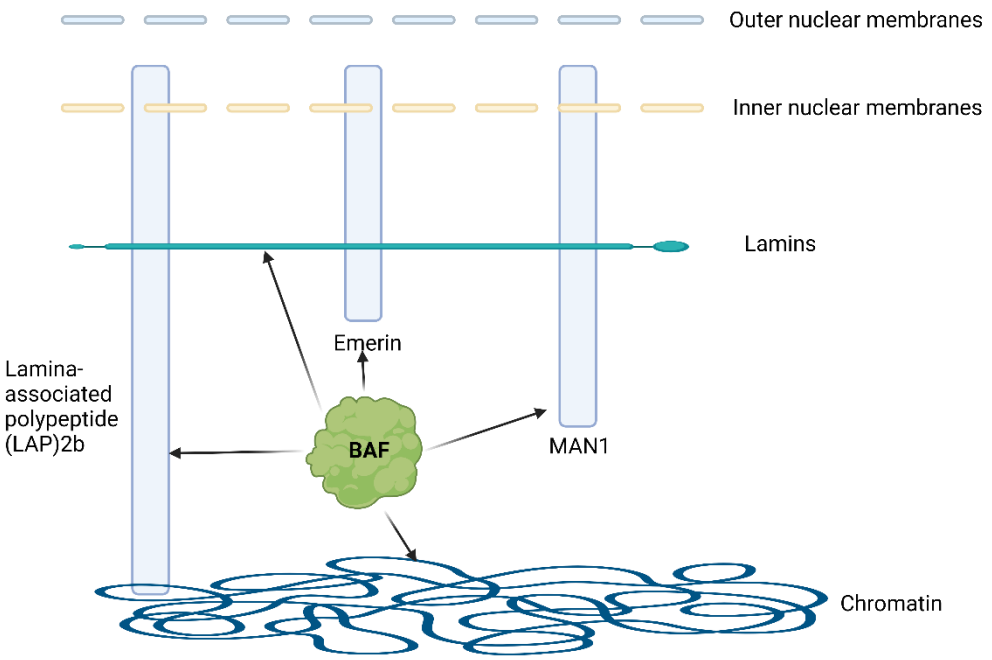

Fig. 5: All LEM-domain proteins bind BAF, and BAF interacts with chromatin. The nuclear envelope, including the outer and inner nuclear membranes. LEM domain proteins lamina-associated polypeptide (LAP)2b emerin and MAN1, and lamin. These LEM-domain proteins are anchored in the INM by transmembrane domain(s). The figure was reproduced with permission from Miriam Segura-Totten and Katherine L. Wilson[138], created with BioRender.com.

Early studies showed that BAF forms homodimers, each subunit of which binds double-stranded DNA in a sequence-independent manner[175,178]. BAF can compact or loop DNA *in vitro*[179,179]. Specifically, each BAF monomer has a helix-hairpin-helix DNA-binding domain, allowing BAF dimers to bind and `bridge' two strands of DNA either intra-molecularly or inter-molecularly[180].

In addition to their roles in nuclear assembly, LEM-domain proteins are important for gene regulation. Like its LEM-domain partners, BAF also regulates gene expression. BAF binds directly to Crx, a homeodomain protein, and represses Crx-dependent gene activation in differentiating retinal cells[181].

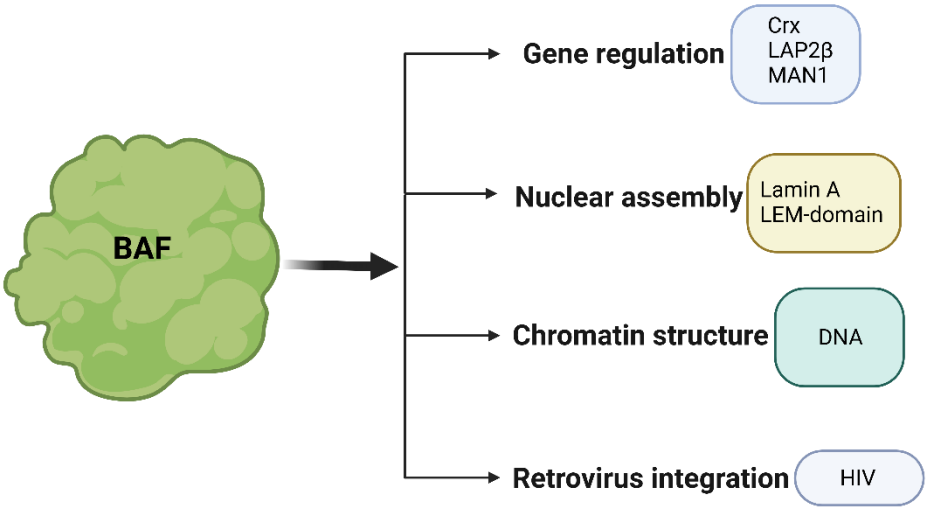

Fig. 6: BAF has a multi-function. BAF (Barrier-to-Autointegration Factor 1) serves multiple intra-cellular functions, including gene regulation, modulation of chromatin structure, nuclear assembly, and promotion of retroviral integration. Created with BioRender.com.

1.3.3 Vaccinia Related Kinases 1 (VRK1) phosphorylation BAF and nuclear functions of BAF

Phosphorylation can modulate diverse properties of a protein, such as localization, turnover, enzymatic activity, protein-protein, and protein-nucleic acid interaction[182]. Cycles of phosphorylation and dephosphorylation control BAF function[183]. BAF is

phosphorylated by the Vaccinia Related Kinases 1 (VRK1) on its N-terminal serine[184–187]. BAF dephosphorylation is done by Protein Phosphatase 2A (PP2A) and Protein Phosphatase 4 (PP4).

The VRK1 is part of the casein kinase family, characterized by its homology to the vaccinia B1 kinase[185]. VRK1, a nuclear and enzymatically active mitotic kinase that phosphorylates serine and threonine residues, plays a vital role in cell cycle progression by participating in various cell division processes[188,189]. The VRK1 orthologues in *Caenorhabditis elegans* and *Drosophila melanogaster* play an essential role in cell division[185]. VRK1 has been shown to phosphorylate many substrates, highlighting its multifaceted regulatory functions. Key substrates include histone H3, where VRK1 phosphorylates serine 10 (H3S10) to promote chromatin condensation and mitotic progression[190]. Additionally, VRK1 phosphorylates p53 at threonine 18, modulating its stability and transcriptional activity under stress conditions[191]. Furthermore, VRK1 phosphorylates transcription factors such as ATF2 and CREB, linking it to stress response pathways and gene regulation[192]. These substrates underscore the diverse roles of VRK1 in cell cycle control, chromatin remodeling, and stress response[193].

The functional form of BAF is a homodimer that binds to double-stranded DNA in a sequence-independent manner, making contact with the phosphate backbone at the minor groove[175,180]. In addition to binding to DNA, BAF can bind to protein components of the inner nuclear membrane (INM) via their LEM domains[177,194–196]. Phosphorylation at the BAF N-terminal residues reduces its affinity for binding to double-stranded DNA[185,197]. Overexpression of VRK1 partially releases BAF from chromatin and redistributes it from the nucleus to the cytoplasm. In contrast, depletion of VRK1 impedes the release of BAF from chromosomes during mitosis[187]. This increases the number of anaphase bridges and multipolar spindles, frequently resulting in aberrant nuclear envelope morphology without affecting the localization of lamin A/C and emerin. VRK1 activity tightly regulates the dynamic status of BAF during cell cycle progression. VRK1 participates in nuclear envelope (NE) dynamics, including NE

assembly and disassembly, by phosphorylating the BAF during interphase and mitotic entry and exit[185]. BAF is a chromatin-associated protein that serves as a link between DNA and the NE[198]. Phosphorylation of BAF by VRK1 promotes chromatin release from the nuclear envelope (NE) and the recruitment of NE-associated proteins into the core region during telophase[199].

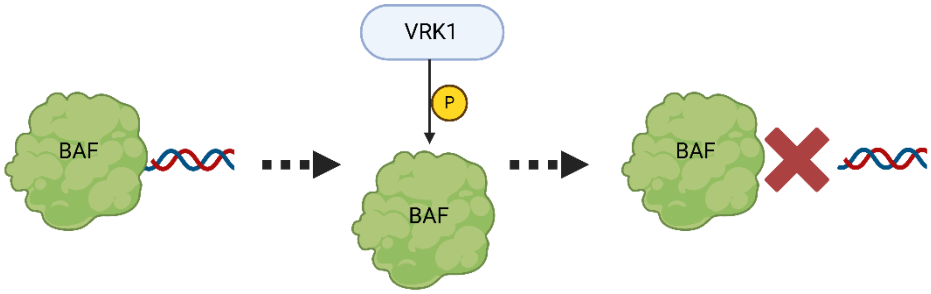

Fig. 7: BAF binding to DNA and its phosphorylation by VRK1. BAF (Barrier-to-Autointegration Factor 1) can bind to DNA under normal conditions. Upon phosphorylation by Vaccinia-Related Kinase 1 (VRK1), BAF undergoes a conformational change that prevents it from binding to DNA. The phospho-group (P) is added to specific amino acid residues within the BAF protein, altering its DNA-binding capability.

1.3.2.1 VRK1 inhibitor: Luteolin

Luteolin (3',4',5,7-tetrahydroxyflavone)[200] is a small-molecule inhibitor of VRK1 kinase activity. This naturally occurring flavonoid is widely distributed in plants and is well-known for its potent antioxidant properties[201]. In traditional Asian medicine, herbs rich in luteolin have been used to treat various disorders, including pain, inflammatory diseases, hypertension, and cancer[202]. Numerous lines of evidence have demonstrated the wide range of pharmacological effects of luteolin, including its anticancer, anti-inflammatory, and anti-allergy activities[202,203]. Although it is known that the anticancer properties of luteolin are associated with pro-apoptotic and anti-

proliferative effects, as well as the inhibition of angiogenesis and metastasis, the molecular mechanisms underlying these activities have not been fully elucidated[204,205]. Luteolin markedly inhibits VRK1-mediated phosphorylation of cell cycle-related substrates, BAF, histone H3, and directly interacts with the catalytic domain of VRK1[206]. Luteolin may induce cell cycle arrest by inhibiting VRK1 kinase activity, suppressing cancer cell growth, and promoting apoptosis.

1.3.3 Mutual impact between BAF, DNA-PK, and cGAS-STING

1.3.3.1 BAF inhibits DNA-PK

BAF's interaction with DNA plays a role in recruiting DNA-PK to sites of DNA damage[207]. BAF can bind to and directly inhibit the activity of DNA-PKcs[208,209]. In the presence of BAF, DNA-PKcs are less active, leading to HR (homologous recombination pathway). Conversely, when BAF is depleted, DNA-PKcs are more active, promoting NHEJ (non-homologous end joining)[207].

Phosphorylation of BAF by VRK1 impairs its DNA-binding ability[185], thereby affecting the recruitment and activation of DNA-PK. This can lead to altered DNA repair mechanisms and potentially influence the cellular response to HIV-1-induced DNA damage.

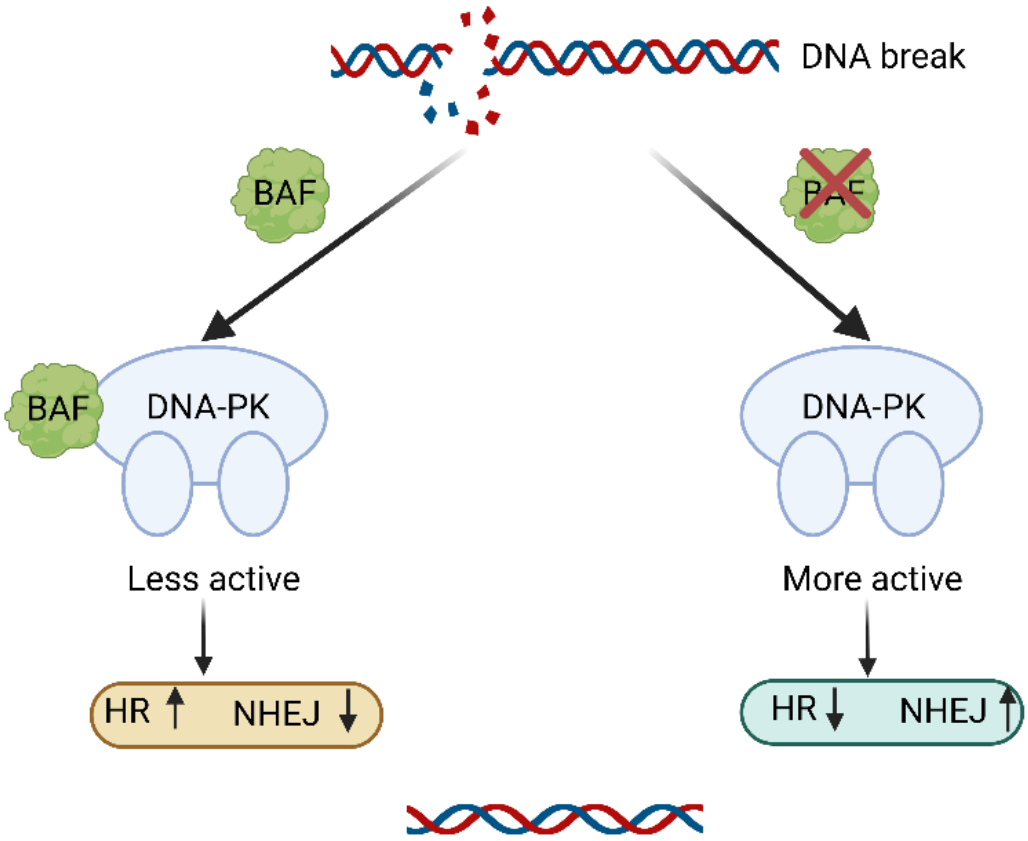

Fig. 8: Model of BAF-mediated control of DSB repair pathway choice[207]**.** In the presence of BAF, DNA-PKcs is less active, leading to HR. Conversely, when BAF is depleted, DNA-PKcs is more active in promoting NHEJ.

1.3.3.2 DNA-PK reduces cGAS-STING signaling

DNA-PK phosphorylates cGAS and suppresses cGAMP synthesis[210,211]. DNA-PK deficiency reduces cGAS phosphorylation and promotes antiviral innate immune responses, thereby potently restricting viral replication[210]. DNA-PK can sense foreign DNA and induce an immune response in cells lacking STING while restricting cGAS signaling in cells with STING[211].

1.3.3.3 BAF protects against cGAS-STING

The absence of BAF led to chromatin activation near host defense genes, which was

associated with increased expression of interferon-stimulated genes (*ISGs*), including *OAS2, RSAD2* (viperin), *IFIT1*, and *ISG15*[72,212]. This phenotype in BAF-deficient cells was mediated by a signaling axis dependent on cGAS, STING, and IRF3. Additionally, it was linked to a reduced infection rate of both RNA and DNA viruses and was reversed when BAF was reintroduced into the cells[72]. The enhanced expression of ISGs was mediated by a pathway requiring cGAS, STING, and IRF3[213]. Decreased expression of BAF was also associated with increased levels of cytosolic double-stranded DNA[132], likely triggering recognition by cGAS. These results suggest that BAF and its established roles in inhibiting retrovirus integration and DNA virus replication regulate baseline levels of endogenous cytoplasmic double-stranded DNA. This regulation prevents unintended cGAS-STING activation and subsequent cellular ISG responses.

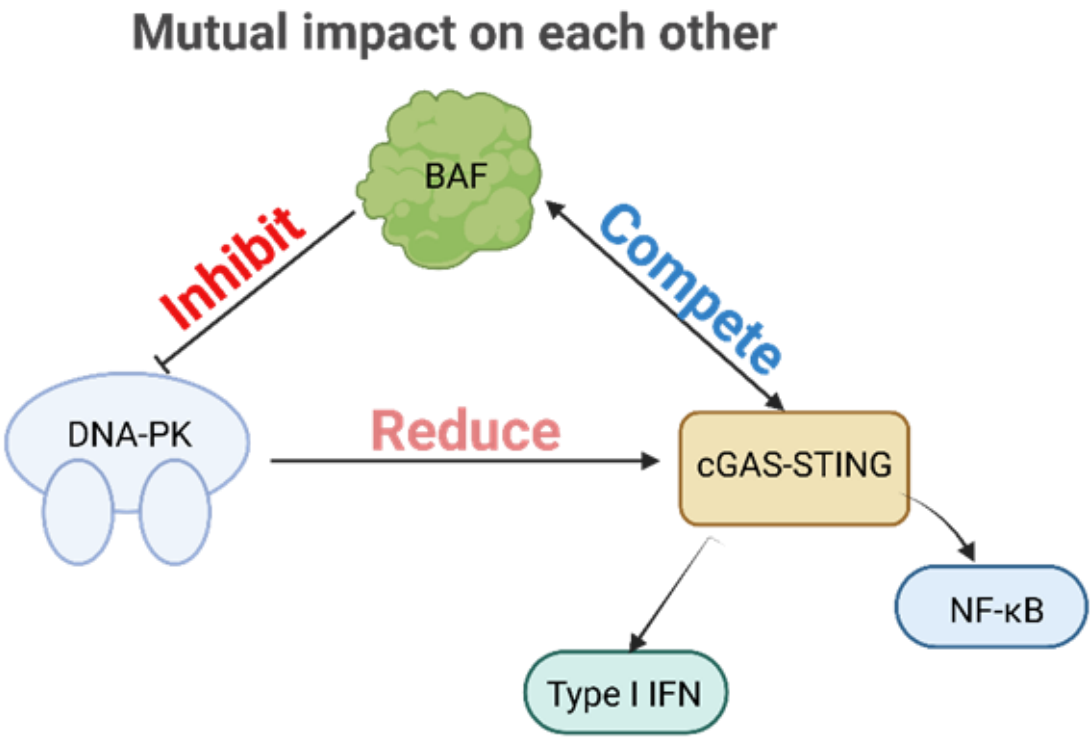

Fig. 9: This diagram illustrates the complex regulatory interactions between BAF, DNA-PK, and the cGAS-STING pathway. BAF inhibits DNA-PK activity, which plays a key role in DNA damage repair and non-homologous end joining (NHEJ). Simultaneously, BAF competes with cGAS-STING by binding to cytoplasmic DNA, thereby reducing the activation of the cGAS-STING pathway[72]. Ablation of BAF resulted in chromatin

activation near host defense genes with associated increased expression of ISGs. Additionally, DNA-PK can sense foreign DNA and induce an immune response in cells lacking STING while restricting cGAS signaling in cells with the presence of STING.

1.5 Aims of the thesis

The primary objective of this thesis is to investigate the role of Barrier-to-Autointegration Factor 1 (BAF) in HIV-1 replication and host immune responses. Specifically, this study aims to determine whether BAF is essential for HIV-1 infection across different cell types, including immune and non-immune cells. A key focus is to assess how the phosphorylation state of BAF influences viral replication, DNA repair (DNA-PK), and antiviral immune signaling (cGAS-STING). Additionally, this work explores whether BAF plays a broader role in infections caused by other viruses. By elucidating these molecular mechanisms, this study seeks to advance our understanding of host-pathogen interactions and inform potential antiviral strategies.

2 Material and Methods

2.1 Molecular biology

2.1.1 Plasmid construction

Plasmid construction involved digesting DNA fragments with restriction enzymes at specific sites and ligating the resulting fragments. Briefly, DNA fragments were amplified using polymerase chain reaction (PCR), separated via gel electrophoresis, and purified through gel extraction. The digested vector and insert fragments were then ligated using T4 ligase. Subsequently, the ligated DNA constructs were transformed into *E. coli* and single colonies were selected on Luria-Bertani (LB) agar plates containing antibiotics. Finally, positive plasmids were identified by double restriction digestion and confirmed through Sanger sequencing.

Table 1: List of plasmids.

Plasmid	Resistancegene	Reference/Origin
pMDLg/pRRE	Ampicillin	[214] Luigi Naldini, Cell Genesys, Foster City,California, USA
pRSV-Rev	Ampicillin	[214] Luigi Naldini, Cell Genesys, Foster City,California, USA
pMD.G	Ampicillin	[214] Luigi Naldini, Cell Genesys, Foster City,California, USA
pSIN.PPT.CMV.Luc.IRES.GF P	Ampicillin	[215] Carsten Münk, Heinrich-Heine- Universität Düsseldorf, Düsseldorf/Germany
pcDNA6/myc-His-VPX	Ampicillin	[216] Nathaniel R Landau, New York University School of Medicine, New York, USA
pMDLx	Ampicillin	[216] Nathaniel R Landau, New York University School of Medicine, New York, USA
psPAX2	Ampicillin	Obtained from the NIH, AIDS Reagent Program repository. Catalog Number: 11348
pcDNA3.1 empty	Ampicillin	Invitrogen. Catalog Number: V79520
pcBAF-HA	Ampicillin	This work
pLentiCRISPR v2	Ampicillin	Addgene. Catalog Number: 52961

pNL-Bal	Ampicillin	[217]Tara G. Edmonds, Department of Molecular and Cellular Pathology, Birmingham, USA
pNL-LucR-E-	Ampicillin	[218]Dr. Nathaniel Landau, Aaron Diamond AIDS Research Center, California, USA
pHIT60	Ampicillin	[219]Jonathan Stoye, Francis Crick Institute, London, London/England

Table 2: List of oligo primers for plasmid generation.

Primer	**Forward 5' to 3'**	**Reverse 5' to 3'**
BAF-HA	TATCCGTATGATGTGCCGGATTATGC GACAACCTCCCAAAAGCA	TCACAAGAAGGCGTCGCACC
sgRNA for HEK293T KO	CACCGGCTTCGGATGCCTTCGAGAG	AAACCTCTCGAAGGCATCCGAAGCC
sgRNA for THP-1 KO	CACCGCCAAAAGCACCGAGACTTCG	AAACCGAAGTCTCGGTGCTTTTGGC

2.1.1.1 Polymerase chain reaction (PCR)

PCR was used to synthesize new DNA fragments for various purposes, including cloning the DNA sequence into an expression vector. Q5® High-Fidelity DNA Polymerase (New England Biolabs, Ipswich, USA) was used to amplify DNA fragments according to the manufacturer's instructions.

Table 3: **50 microliter (µl) PCR reaction mixture**

50 microliter (μl) reaction mixture	
Forward primer	10 micromolar (μM)
Reverse primer	10 micromolar (μM)
Q5 High-Fidelity DNA Polymerase	0.5 microliter (μl)
5X reaction buffer	10 microliters (μl)
deoxynucleoside triphosphate (dNTPs) (New England Biolabs, Ipswich, USA)	10 millimolar (mM)
Plasmid or genomic DNA template	10 nanograms (ng)
Nuclease-free water	To 50 ul

The reaction mixture was gently mixed and transferred to a PCR machine (Bioer GeneTouch™ Thermal Cycler, Hangzhou, China) with the following program: (i) initial denaturation at 98°C for 30 seconds (s); (ii) 30 cycles of denaturation at 98°C for 10 s, annealing at 50-70°C for 10 s, and extension at 72°C at 1 kilobase per minute (min/kb); (iii) final extension at 72°C for 2 minutes; and (iv) hold at 4°C.

2.1.1.2 Agarose gel electrophoresis and gel extraction

DNA fragments can be separated by gel electrophoresis according to their size. After PCR, a mix of DNA gel loading buffers with PCR products and a 1 kilobase plus DNA ladder (Thermo Fisher Scientific, Waltham, USA) were loaded into wells of an agarose gel. Electrophoretic separation of DNA was conducted at a constant 150 volts (V) for 30 minutes. The gel image was captured using gel documentation system, and DNA fragments were excised from the gel with guidance from the DNA ladder.

The DNA-containing agarose gel was purified using a modified protocol of the QIAquick Gel Extraction Kit (QIAGEN, Venlo, Netherlands). 300-500 microliter (μl) of QG buffer were added to each tube, followed by incubation on a shaker at 500 revolutions per minute (rpm) for 10 minutes at 50°C. The entire solution was transferred to a QIAquick spin

column and centrifuged at maximum speed for 1 minute. Then, 600 µl of PE buffer was added, and the centrifugation step was repeated twice at maximum speed for 1 minute each. Finally, 25 µl of EB buffer was added to the columns and after centrifuging at maximum speed for 1 minute, the DNA was eluted. The concentration of DNA was measured photometrically at 260 nanometers (nm).

2.1.1.3 Double restriction enzyme digestion reaction

According to the manufacturer's instructions, 1 microgram (µg) of purified insert and 1 µg of donor plasmid backbone (vector) were digested using double-restriction enzymes.

Table 4: **20 µl Double restriction enzyme digestion reaction system**

20 µl reaction system	
insert or vector	1 µg
2X enzyme-specific buffer as the double digest calculator recommended	10 µl
each restriction enzyme	1 µl
nuclease-free water	To 20ul

The components were mixed by pipetting and incubated at 37°C for 1-2 hours (h). Following incubation, the digested DNA was evaluated by gel electrophoresis and subsequently purified by gel extraction.

2.1.1.4 Ligation of vector and insert

The ligation system was performed with T4 DNA ligase according to the manufacturer's instructions.

Table 5: **20 µl ligation system**

20 µl ligation system	
purified sticky-end insert or donor plasmid backbone (vector)	100 ng
10X T4 DNA ligase buffer	2 µl
T4 ligase	1 µl
Nuclease-free water	To 20ul

Mix thoroughly, spin briefly, and incubate at room temperature (RT) for 2 h. Use 20 µl of the mixture to transform an aliquot of competent cells.

2.1.1.5 *E. coli* transformation

The ligated DNA constructs were transformed into Top10 or Stable 2 chemically competent cells (Thermo Fisher Scientific, Waltham, USA) following the manufacturer's instructions. First, competent cells were thawed on ice. A 10 µl aliquot of ligated DNA constructs was mixed with competent cells using a pipette and incubated on ice for 10 minutes for Top10 cells or 30 minutes for Stable 2 cells. After a heat shock at 42°C for 1 minute, cells were cooled on ice for 2 minutes for Top10 or 10 minutes for Stbl2 cells. Subsequently, 500 µl of fresh Luria-Bertani (LB) liquid medium was added to the DNA-cell mixture and cultured in a shaker at 500 rpm for 1 hour at 37°C for Top10 cells or 30°C for Stbl2 cells. The resulting cells were plated onto LB agar plates supplemented with 100 µg/ml ampicillin or 100 µg/ml kanamycin and incubated overnight at 37°C for Top10 cells or 30°C for Stbl2 cells. Single colonies were picked and inoculated into 4 ml of LB medium containing 100 µg/ml ampicillin or kanamycin, followed by vigorous shaking at 180 rpm overnight at 37°C for Top10 cells or 30°C for Stbl2 cells.

2.1.1.6 DNA extraction

2.1.1.6.1 DNA extraction from bacteria

DNA extraction from bacteria was performed using a modified protocol of the ZR Plasmid Miniprep-Classic kit (Zymo Research, Irvine, USA).

Bacterial cultures (2 ml) were harvested by centrifugation at full speed for 20 seconds. The pelleted bacteria were resuspended in 200 µl of P1 buffer, followed by the addition of 200 µl of P2 buffer. The tube was inverted 2-4 times to mix and incubated for 2 minutes. Subsequently, 400 µl of P3 buffer was added, gently mixed and incubated at room temperature for 2 minutes before centrifugation at full speed. After centrifugation, the supernatant was transferred to a Zymo-Spin™ IIN column and centrifuged at full speed for 1 minute. The flow-through was discarded, and the column was washed with 200 µl of the endo-wash buffer by centrifuging at full speed for 1 minute. Next, 400 µl of plasmid wash buffer was added to the column and centrifuged at full speed for 1 minute. Finally, the plasmid DNA was eluted in 30 µl of nuclease-free water by centrifugation for 1 minute at full speed into a 1.5 ml microcentrifuge tube. The DNA concentration was measured at 260 nm using a spectrophotometer.

For large-scale purification of plasmids, the PureYield™ Plasmid Maxiprep system (Promega, Madison, USA) was utilized according to the manufacturer's instructions.

2.1.1.6.2 DNA extraction from cells

Genomic DNA extraction from cells was performed using the DNeasy Blood & Tissue kit protocol (QIAGEN, Venlo, Netherlands).

Cells were resuspended in 200 µl of Dulbecco's phosphate-buffered saline (DPBS) (PAN-Biotech, Aidenbach, Germany). 20 µl of Proteinase K was added, followed by 200 µl of buffer AL. The mixture was vortexed to mix thoroughly and then incubated at 56°C for 10 minutes. After the incubation, 200 µl of 96% ethanol was added and mixed by vortexing. The sample was transferred into a DNeasy Mini spin column and centrifuged at 12,000 rpm for 1 minute to remove the flow-through. Next, 500 µl of buffer AW1 was added, centrifuged at 12,000 rpm for 1 minute and discarded the flow-through. Subsequently, 500 µl of buffer AW2 was added, and the DNeasy membrane was dried by

centrifugation at 14,000 rpm for 2 minutes. Finally, the genomic DNA was eluted in 50 µl elution buffer by centrifugation at 12,000 rpm for 1 minute.

2.1.1.7 Verification of the plasmid

After purifying the DNA, 300 ng of plasmid was subjected to verification by double restriction digestion.

Table 6: **10 µl plasmid verification reaction mixture**

10 µl reaction mixture	
Plasmid	300 ng
Each restriction enzyme	0.25 µl
1X or 2X enzyme-specific buffer	as recommended by the double digest calculator
Nuclease-free water	To 10 µl

The components were mixed by pipetting, briefly spun down, and then incubated at 37°C for 1 hour.

Verification of plasmids was performed by gel electrophoresis of digested plasmid DNA based on expected fragment sizes. Plasmids were further confirmed by Sanger sequencing at Eurofins company (Eurofins, Luxembourg), and pairwise sequence alignment was conducted using DNASTAR Lasergene software (DNASTAR, Inc., Madison, USA).

2.1.2 Quantitative real-time PCR

2.1.2.1 RNA isolation

Total RNA was purified from cells using the QIAGEN RNeasy® Mini Kit (QIAGEN, Venlo, Netherlands). First, 350 µl of RLT buffer was added to the cells, followed by

vortexing to lyse them. Then, 350 µl of 70% ethanol was added and mixed. Up to 700 µl of the sample was transferred to a RNeasy spin column with a 2 ml collection tube, centrifuged at 12,000 rpm for 1 minute, and the flow-through was discarded. Next, 700 µl of RW1 buffer was added to the spin column, centrifuged at 12,000 rpm for 1 minute, and discarded the flow-through. The spin column was washed twice with 500 µl of RPE buffer, each time centrifuging at 12,000 rpm for 1 minute and discarding the flow-through. Finally, 30 µl of RNase-free water was added to the spin column and centrifuged at full speed for 1 minute to elute the RNA into a new 1.5 ml collection tube. The total RNA was stored at -80°C for future use.

2.1.2.2 First Strand cDNA synthesis

For each sample, 1,500 ng of RNA was reverse transcribed using the RevertAid H Minus First Strand cDNA Synthesis Kit (Thermo Fisher Scientific, Waltham, USA).

Table 7: 20 µl cDNA synthesis reaction mixture

20 µl cDNA synthesis reaction mix	
RNA	1500 ng
Primer (oligo(dT)$_{18}$ primer)	1 µl
5X Reaction Buffer	4 µl
RiboLock RNase inhibitor	1 µl
RevertAid H Minus M-MuLV reverse transcriptase	1 µl
10 mM dNTP mix	2 µl
nuclease-free water	To 20 µl

The mixture was incubated at 42°C for 1 hour, followed by 70°C for 5 minutes. The synthesized cDNA was stored at -80°C for future use.

2.1.2.3 Real-time PCR

Real-time PCR was used to analyze gene expression.

Firstly, cDNA was dissolved in nuclease-free water and diluted to a concentration of 10 ng/µl. SYBR Green is a fluorescent dye that binds to double-stranded DNA, allowing real-time quantification of DNA amplification during PCR.

Table 8: 20 µl real-time PCR mixture

20 µl real-time PCR mixture	
cDNA	1 µl
Primer pair mix (10 pmol/µl each primer)	1 µl
SYBR™ Green PCR Master Mix (Thermo Fisher Scientific, Waltham, USA)	10 µl
Nuclease-free water	8 µl

Amplification was carried out on the ABI PRISM 7700 with the following program.

Table 9: PCR program

Initial hold	95°C for 10 minutes
95°C for 15 seconds	40 cycles
60°C for 1 minute	
Final hold	72°C for 10 minutes

Relative quantification was performed using the 2(Delta Delta C(T)) method with GAPDH as the housekeeping gene. The qPCR primers used in this study are listed in Table 10. qPCR primers were synthesized by Eurofins (Eurofins, Luxembourg).

Table 10: List of qPCR primers.

Gene	Forward (5' to 3')	Reverse (5' to 3')
GAPDH	CAACAGCGACACCCACTCCT	CACCCTGTTGCTGTAGCCAAA

ISG15	GTGGACAAATGCGACGAACC	TCGAAGGTCAGCCAGAACAG
ISG54	TCAGGTCAAGGATAGTCTGGAG	AGGTTGTGTATTCCCACACTGTA
IFNB1	CCTGTGGCAATTGAATGGGAGGC	CCAGGCACAGTGACTGTACTCCTT
Autointegration	TTTCAAGTCCCTGTTCGGGCGCCA	CTACCTTGTTATGTCCTGCTTG/CTCTAC AGTACTTGGCACTAGC
2-LTR	GAGATCCCTCAGACCCTTTTAG	TCCACAGATCAAGGATCTCTTGTC
Late RT	CAGTGTGGAAAATCTCTAGCAGTGG	GCCGTGCGCGCTTCAGCAAGC

2.2 Cell culture and virological methods

2.2.1 Cell culture of continuous immortalized cell lines

HEK293T cells were obtained from the American Type Culture Collection (ATCC) and maintained in Dulbecco's Modified Eagle Medium (DMEM) (PAN-Biotech, Aidenbach, Germany), supplemented with 10% fetal bovine serum (FBS) (PAN-Biotech, Aidenbach, Germany), 2 mM L-glutamine (PAN-Biotech, Aidenbach, Germany), and 100 units per milliliter (U/ml) penicillin-streptomycin (PAN-Biotech, Aidenbach, Germany).

Human monocytic THP-1 cells were obtained from ATCC and cultured in Roswell Park Memorial Institute (RPMI) 1640 medium (Thermo Fisher Scientific, Waltham, USA) supplemented with 10% fetal bovine serum (FBS), 2 mM L-glutamine, and 100 U/ml penicillin-streptomycin.

HEK-Blue™ IFN-α/β cells (Invivogene, San Diego, USA) were cultured in DMEM supplemented with 10% FBS, 2 mM L-glutamine, 100 U/ml penicillin-streptomycin, 30 µg/ml of blasticidin S hydrochloride (Sigma-Aldrich, Carlsbad, USA) and 100 µg/ml of Zeocin™ (Invivogene, San Diego, USA).

All cells were grown at 37°C in 5% CO2 and handled under sterile conditions.

For serial passaging, adherent cells were washed with DPBS and incubated with 0.05% trypsin (PAN-Biotech, Aidenbach, Germany) for 1-2 minutes at 37°C. Suspension cells were harvested by centrifugation at 500 rcf for 5 minutes and resuspended in a fresh

medium. For long-term storage, cells were centrifuged at 500 rcf for 5 minutes, then resuspended in 1 ml of 10% dimethyl sulfoxide (DMSO) (PanReac AppliChem, Chicago, IL, USA) in FBS per cryo vial. Vials were placed in a Nalgene Mr. Frosty freezing container containing 100% isopropyl alcohol and stored at -80°C for 48 hours before being transferred to liquid nitrogen.

2.2.2 Transfection of plasmid

HEK293T cells were seeded at a density of 800,000 cells per well into 6-well plates (Sigma-Aldrich, Carlsbad, USA) and grown to 80% confluence before transfection. For each well of a 6-well plate, 2000 ng of DNA was gently diluted into 100 µl of DMEM and vortexed. Separately, 4 µl of PolyJet™ reagent was diluted into 100 µl of DMEM and vortexed gently. PolyJet™ *in vitro* DNA transfection reagent (SignaGen Laboratories, Frederick, USA) was used according to the manufacturer's instructions. The diluted PolyJet™ reagent was then added to the diluted DNA solution, gently vortexed, and incubated at room temperature for 10 minutes. The PolyJet™/DNA transfection complexes were subsequently added to the cells.

2.2.3 Transfection of herring sperm DNA (HS-DNA)

I am conducting a study to investigate the effects of BAF on other DNA. Undifferentiated and PMA-differentiated THP-1 cells were transfected with 4 µg/ml herring sperm DNA (HS-DNA) (Thermo Fisher Scientific, Waltham, USA) using PolyJet™ reagent.

Day 1: Seeding $4x10^5$ undifferentiated and PMA-differentiated THP-1 cells per well in a 24-well plate.

Day 2: THP-1 cells were centrifuged at 150 rcf at room temperature for 10 minutes before transfection. The supernatant was completely removed, 300 µl of pre-warmed fresh complete cell growth medium was added, and the plate was incubated at 37°C.

For each well of a 24-well plate, 8 µg of HS-DNA was diluted into 100 µl of DMEM and vortexed gently. Separately, 6 µl of PolyJet™ reagent was diluted into 100 µl free DMEM and vortexed gently. The diluted PolyJet™ reagent was then added to the diluted DNA solution and vortexed gently, followed by a 10-minute incubation at room temperature. The PolyJet™/DNA transfection complexes were added to the cells and incubated at 37°C with 5% CO_2 for 15 minutes. After incubation, pre-warmed fresh complete cell growth medium was added to each well, and the plate was incubated at 37°C with 5% CO2 for the indicated time.

2.2.4 Virus production and transduction

2.2.4.1 Lentiviral vector production in S2 lab

HIV-1 based lentiviral luciferase reporter vectors were produced by transfecting HEK293T cells in a 6-well plate. The production utilized a three-plasmid system consisting of 700 ng of pMDLg/pRRE and 700 ng of pSIN.PPT.CMV.Luc.IRES.GFP, 200 ng of pMDG.VSV-G, and 350 ng of pRSV-Rev, using PolyJet™ transfection reagent.

For infecting THP-1 cells, viral particles were produced using a four-plasmid system: 700 ng of pMDL-X, 700 ng of pSIN.PPT.CMV.Luc.IRES.GFP, 200 ng of pMDG.VSV-G, 350 ng of pRSV-Rev, and 500 ng of myc-His-VPX, also using PolyJet™ transfection reagent.

The production of HIV-1-based lentiviral vectors for generating stable expression cell lines involved co-transfection of HEK293T cells with 1000 ng of packaging plasmid psPAX2 and 200 ng of pMDG.VSV-G, 200 ng of pRSV-Rev, and 1000 ng of pLV2 empty vector or pLV2 vector containing the inserted gene, using PolyJet™ transfection reagent. Supernatants were harvested 48 hours post-transfection, purified by centrifugation at 5500 rpm for 10 minutes at 4°C to remove cells, concentrated by centrifugation at 14,000 rpm for 4 hours at 4°C, resuspended in DMEM, and stored at -80°C.

To generate stable THP-1 cell lines with sustained gene expression, THP-1 cells were transduced with HIV-1-based lentiviral vectors and subjected to spinoculation, which uses

centrifugation to enhance viral entry by forcing viral particles onto the target cells. Specifically, cells were centrifuged at 1,200 rcf for 2 hours at 30°C. In reporter virus infection assays, THP-1 cells were similarly spinoculated with HIV-1 luciferase reporter viruses under the same conditions. Two hours before infection, the cells were incubated at 37°C with 5% CO_2 for the indicated time.

The Modified Vaccinia Virus Ankara (MVA), a gift from Prof. Dr. Ingo Drexler at Heinrich-Heine-Universität Düsseldorf, was routinely propagated and purified.
The murine leukemia virus (MLV) packaging construct pHIT60, encoding the *gag-pol* of Moloney MLV, was provided by Jonathan Stoye. The production of MLV-based viruses for generating stable expression cell lines involved co-transfection of HEK293T cells with 1100 ng pHIT60 and 200 ng of pMDG.VSV-G and 1100 ng of pLNCX2 empty vector or pLNCX2 vector containing the inserted gene.

2.2.4.2 Virus production in S3 lab

HIV-1 full-length viruses were produced by transfecting HEK293T cells in a 6-well plate. For Luciferase reporter virus: The production utilized a two-plasmid system of 2000 ng pNL-Luc R-E- and 200 ng of pMDG.VSV-G. For replication competent HIV-1: pNL-Bal plasmid was used.
48 hours after transfection, the supernatant was collected. Subsequently, to ensure consistency, the virus's reverse transcriptase (RT) activity was quantified using a SYBR Green I-based product-enhanced reverse transcriptase assay[220].

2.2.5 HIV-1 luciferase activity assay

To determine the regulation of proteins of interest during HIV-1 infection, HEK293T and undifferentiated or differentiated THP-1 cells were infected with HIV-1 luciferase

reporter viruses of Luciferase lentiviral vectors. The efficiency of infection or transduction was analyzed using the Steady-Glo Luciferase Assay System (Promega, Madison, USA) according to the manufacturer's instructions.

For HEK293T cells, 10^4 cells were seeded in 96-well plates with 50 µl of pre-warmed fresh cell medium and cultured overnight. HEK292T cells were infected with 50 µl of HIV-1 luciferase reporter virus the next day. Then incubated at 37°C with 5% CO2. After 72 hours, the DMEM was completely removed, infected cells were lysed with 100 µl of luciferase reagent and incubated at room temperature for 15 minutes in the dark.

For PMA-differentiated THP-1 cells, 10^5 cells per well were seeded with 50 µl of pre-warmed fresh cell medium containing 25 ng/ml PMA (Calbiochem, Darmstadt, Germany) and incubated for 24 hours at 37°C with 5% CO2. After 24 hours, the PMA-containing medium was completely removed, and the cells were washed once with pre-warmed DPBS. The wells were refilled with 50 µl of pre-warmed cell medium and infected with 50 µl of HIV-1 luciferase reporter virus, with or without Vpx. The cells were spinoculated at 1,200 rcf for 2 hours at 30°C, then incubated at 37°C with 5% CO2. After 72 hours, the RPMI was completely removed, infected cells were lysed with 100 µl of luciferase reagent and incubated at room temperature for 15 minutes in the dark.

For undifferentiated THP-1 cells, 10^5 cells were seeded in 96-well plates with 50 µl of pre-warmed fresh cell medium and cultured overnight. The next day, undifferentiated THP-1 cells were infected with 50 µl of HIV-1 luciferase reporter virus, with or without Vpx. The cells were spinoculated at 1,200 rcf for 2 hours at 30°C, then incubated at 37°C with 5% CO2. After 72 hours, infected cells were lysed with 80 µl of luciferase reagent and incubated at room temperature for 15 minutes in the dark.

Following incubation, 100 µl of cell lysate was transferred into black 96-well polypropylene microplates (Greiner Bio-One, Kremsmünster, Austria), and luminescence was measured for 10 seconds per well using a Centro XS3 LB 960 microplate luminometer (Berthold Technologies Bioanalytic, Bad Wildbad, Germany).

2.2.6 Generation of reconstituted BAF THP-1 cells

Reconstituted BAF THP-1 cells were generated by transduction of BAF KO THP-1 cells with a retroviral vector. MLV (Moloney murine leukemia virus)-based retroviral vector particles were produced by transfecting HEK293T cells with 1100 ng pLNCX2 vector or pLNCX2 vector containing insert gene, 1100 ng packaging plasmid pHIT60, and 200ng pMDG.VSV-G. At 48 h post-transfection, viral supernatants were harvested and concentrated. BAF KO THP-1 cells were transduced with the MLV pseudovirus for 48 h. Transduced cells were selected in a fresh complete cell growth medium containing 800 µg/ml G418Sulfate for 10 days. The efficiency of reconstituted BAF expression of the gene was tested by immunoblot analysis.

2.2.7 Type I interferon production assay

The Type I IFN production assay was performed using HEK-Blue™ IFN-α/β cells. These cells stably express a reporter gene encoding secreted embryonic alkaline phosphatase (SEAP) under the control of the *ISG54* promoter.

Briefly, THP-1 cells were infected with HIV-1, lentiviral vectors or MVA, transfected with 4 µg/ml HS-DNA, or stimulated with 3.6 µM STING agonist SR-717 for the indicated times (Prof. Dr. Thomas Kurz, Heinrich-Heine-Universität Düsseldorf, Düsseldorf, Germany kindly provided STING agonist SR-717).

For the assay, 20 µl of supernatant from the treated THP-1 cells was added to 180 µl of fresh complete cell growth medium containing 50,000 HEK-Blue™ IFN-α/β cells per well in a flat-bottom 96-well plate (Sigma-Aldrich, Carlsbad, USA). After 20 hours of incubation at 37°C with 5% CO2, 20 µl of the induced supernatant was transferred to 180 µl of resuspended QUANTI-Blue™ solution (Invivogen, San Diego, USA) in a flat-bottom 96-well plate and incubated for 1 hour at 37°C. SEAP levels were then determined using a Multiskan Spectrum spectrophotometer (Thermo Fisher Scientific, Waltham, USA) at 630 nm.

2.3 Protein biochemistry

2.3.1 Cell lysis and micro-volume protein concentration determination

The indicated cells were harvested, washed with cold DPBS, and lysed on ice for 20 minutes with 100 µl of cold mild lysis buffer (50 mM Tris-HCl [pH 8], 150 mM sodium chloride (Carl Roth, Karlsruhe, Germany), 0.8% NP-40 (PanReac AppliChem, Chicago, IL, USA), 10% glycerol (PanReac AppliChem, Chicago, IL, USA), 1 mM phenylmethanesulfonyl fluoride, a tablet of protease inhibitor cocktail III (Sigma-Aldrich, Carlsbad, USA), and 1% phosphatase inhibitor cocktail I (MedChemExpress, South Brunswick Township, USA)). Cell lysates were cleared by centrifugation at 14,000 rpm for 20 minutes at 4°C. Protein concentrations were then determined using the protein A280 application on a NanoDrop 1000 spectrophotometer (Thermo Fisher Scientific, Waltham, USA). A blank was established using water, and 2 µl of each sample was used for protein concentration determination.

2.3.2 Western blotting assay

Polyacrylamide gels were prepared according to the instructions in Table 11. For the sodium dodecyl sulfate-polyacrylamide gel electrophoresis (SDS-PAGE) assay, equal amounts of protein were mixed with ROTI®Load 1 reduced loading buffer (Carl Roth, Karlsruhe, Germany) and heated at 95°C for 5 minutes. Samples and a prestained protein molecular weight marker (Thermo Fisher Scientific, Waltham, USA) were loaded into the gel wells. Electrophoretic separation of proteins was performed on ice at a constant 130 V in 1X SDS running buffer.

Proteins were transferred from gels to a polyvinylidene fluoride (PVDF) membrane (Sigma-Aldrich, Carlsbad, USA) at a constant 20 V for 1 hour using a Bio-Rad semidry transfer cell (Bio-Rad, Hercules, USA). The semidry transfer method consisted of the following layers: SDS-containing transfer buffer prewetted filter paper (Bio-Rad,

Hercules, USA), methanol (Carl Roth, Karlsruhe, Germany) prewetted PVDF membrane, SDS gel, and SDS-containing transfer buffer prewetted filter paper.

Membranes were blocked with a 5% non-fat milk (PanReac AppliChem, Chicago IL, USA) solution or a 5% bovine serum albumin (BSA) (Thermo Fisher Scientific, Waltham, USA) solution for 1 hour at room temperature. The membranes were then incubated in primary antibody solution overnight at 4°C with gentle agitation. The next day, membranes were washed three times for 10 minutes each with TBST buffer before incubating with HRP-linked secondary antibody for 1 hour at room temperature with gentle agitation. Afterward, the membranes were washed thrice for 10 minutes each with TBST.

Finally, the membranes were incubated with the Amersham™ ECL Prime Western Blot detection reagent (GE Healthcare, Chicago, USA) according to the manufacturer's directions, and the signal was captured using a ChemiDoc MP imaging system (Bio-Rad, Hercules, USA).

Antibodies used in this study are shown in Table 12.

Table 11: Pipetting scheme for SDS gels (per piece)

	Stacking gel	Resolving gel 15%
Rotiphorese® Gel 30 (37.5:1) (Carl Roth, Karlsruhe, Germany)	420 µl	3.75 ml
1.5 mole (M) Tris-HCl pH 8.8 (PanReac AppliChem, Chicago IL, USA)	/	1.875 ml
1 M Tris-HCl pH 6.8 (PanReac AppliChem, Chicago IL, USA)	315 µl	/
10% SDS (PanReac AppliChem, Chicago IL, USA)	25 µl	75 µl
20% Ammonium persulphate solution (APS) (Sigma-Aldrich, Carlsbad, USA)	12.5 µl	37.5 µl
N, N, N′, N′- Tetramethylethylenediamine (TEMED) (VWR, Radnor, PA/USA)	2.5 µl	7.5 µl

H_2O	1.75 ml	1.8 ml

Table 12: Antibodies for Western blotting

Antibody	Source & Identifier& Supplier	Dilution
α-BAF	sc-166324 (Santa Cruz Biotechnology, Dallas, USA)	1/200
α-TBK1	3504S (Cell Signaling Technology, Danvers, USA)	1/1,000
α-p-TBK1	5483S (Cell Signaling Technology, Danvers, USA)	1/1,000
α-ISG15	15981-1-AP (Proteintech, Rosemont, USA)	1/1,000
α-MX2	sc-47197 (Santa Cruz Biotechnology, Dallas, USA)	1/1,000
α-DNA-PK	4602T (Cell Signaling Technology, Danvers, USA)	1/1,000
α-p-DNA-PK	PA1-29541 (ThermoFisher, USA)	1/1,000
α-STING	13647S (Cell Signaling Technology, Danvers, USA)	1/1,000
α-USP18	4813S (Cell Signaling Technology, Danvers, USA)	1/1,000
α-p53	OP43 (Oncogene, California, USA)	1/500
α-GAPDH	EB06377 (Everest Biotech, Bicester, UK)	1/10,000
α-Tubulin	T6074 (Sigma-Aldrich, Carlsbad, USA)	1/10,000
α-HA	51064-2-AP (Proteintech, Rosemont, USA)	1/5,000
HRP-conjugated sheep α-mouse IgG	NA931V (GE Healthcare, Chicago, USA)	1/10,000
HRP-conjugated donkey α-rabbit IgG	NA9340V (GE Healthcare, Chicago, USA)	1/10,000
HRP-conjugated mouse α-goat IgG	sc-2354 (Santa Cruz Biotechnology, Dallas, USA)	1/10,000

2.4 Statistical analysis

Statistical analysis was performed using GraphPad Prism 8.0 (GraphPad Software Inc., La Jolla, CA, USA). Data are presented as individual points, with mean ± standard deviation summaries. An alpha level of 0.05 was used to determine statistical significance. Unpaired Student's t-tests were utilized to compare the two groups. If sample sizes in both conditions were equal, an unpaired two-tailed Student's t-test was applied. For values normalized to an internal control, one-sample t-tests were used. Multiple comparisons were conducted using one-way or two-way analysis of variance (ANOVA).

3. Results

3.1 The effect of HIV-1 on endogenous BAF and BAF packaged into HIV-1 particles

Studying the impact of HIV-1 on endogenous BAF can help us understand the complex interactions between the virus and host cells. By investigating the changes in BAF during HIV-1 infection, I can gain insights into the virus-host dynamics. I transfected HEK293T cells with a 3-plasmid system HIV-1 (Fig. 10A) and pNL-Bal full-length HIV-1 (Fig. 10C) and analyzed the BAF protein levels in the transfected cells 48 hr post-transfection. Alternatively, the lentiviral vector plasmids were co-transfected with a BAF plasmid with an HA tag. All groups, including the control, were transfected with the same total amount of DNA by supplementing with the empty vector pcDNA3.1 to ensure equal transfection conditions. BAF protein levels were analyzed by immunoblot using an anti-BAF antibody. Interestingly, the results revealed a marked reduction in BAF protein levels in cells transfected with the 3-plasmid HIV-1 system compared to controls (Fig. 10A, lane 4 vs. lane 1). In contrast, transfection with full-length pNL-Bal full-length HIV-1 did not lead to any observable change in BAF protein levels relative to control cells (Fig. 10C, lane 4 vs. lane 1). This discrepancy suggests that the 3-plasmid system, which relies on separate plasmids encoding HIV-1 Gag-Pol, Rev, and vector genome components, may induce cellular stress or activate host responses differently from the full-length provirus. Alternatively, the lack of certain regulatory elements or the non-replicative nature of the 3-plasmid system could contribute to altered BAF protein stability or expression. These

findings highlight the importance of the viral context in modulating host factor expression and suggest that only specific forms or stages of HIV-1 expression are capable of downregulating BAF.

To gain more insight into the role of BAF in the HIV-1 replication cycle, I tested whether BAF is packaged into HIV-1 virions. I aimed to determine if BAF protein is incorporated into HIV-1 viral particles when both BAF and HIV-1 plasmids are co-transfected. 48 hrs post-transfection, the lentiviral vector particles were collected and analyzed by immunoblots using an anti-BAF antibody. Viral particles were detected by an anti-P24 antibody that detects the viral capsid protein. The results showed that BAF protein was incorporated into the HIV-1 viral particles during co-transfection (Fig. 10B and 10D).

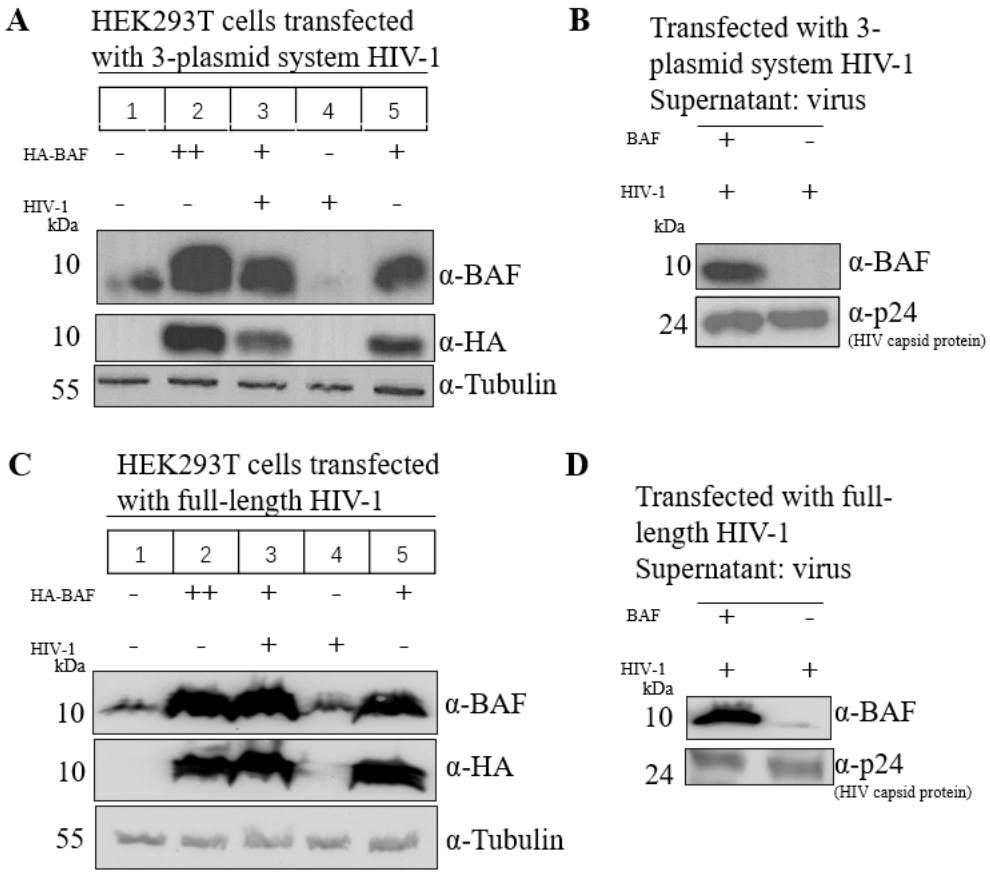

Fig. 10: Differential effects of 3-plasmid system and pNL-Bal full-length HIV-1 on endogenous BAF protein levels in HEK293T cells, and BAF was incorporated into the HIV-1 viral particles. (A) Control lane 1: Untreated HEK293T cells were used as a baseline for BAF protein expression levels. Lane 2: HEK293T cells were only transfected with the HA-BAF (BAF with HA tag) plasmid. Group 3: HA-BAF and HIV-1 3-plasmid system were co-transfected into

HEK293T cells. Lane 4: 293T cells were only transfected with the HIV-1 3-plasmid system to assess the impact on BAF protein expression. Lane 5: Transfected less HA-BAF plasmid than lane 2. Cell lysates were collected to measure protein concentration after 48h of transfection and evaluate the impact of HIV-1 transfection. Western blot analysis was performed to quantify BAF and HA tag protein levels in both control and HIV-1-transfected cells. (B) Control Group: Transfected with HIV-1 3-plasmid system only. Experimental Group: Co-transfected with HIV-1 3-plasmid system and BAF plasmid. Cells were incubated for 48 hours post-transfection. After 48 hours, the supernatant was collected to isolate viral particles. (C) Control lane 1: Untreated HEK293T cells. Lane 2: HEK293T cells were only transfected with HA-BAF plasmid. Group 3: HA-BAF and full-length HIV-1 (pNL-Bal) were co-transfected into HEK293T cells. Lane 4: 293T cells were only transfected with the full-length HIV-1 to assess the impact on BAF protein expression. Lane 5: Transfected less HA-BAF plasmid than lane 2. Cell lysates were collected to measure protein concentration after 48 h transfection and evaluate the impact of HIV-1 transfection. Western blot analysis was performed to quantify BAF and HA tag protein levels in both control and HIV-1-transfected cells. (D) Control Group: Transfected with full-length HIV-1 only. Experimental Group: Co-transfected with full-length HIV-1 and BAF plasmid. Cells were incubated for 48 hours post-transfection. After 48 hours, the supernatant was collected to isolate viral particles. Western Blot detected BAF and p24 (HIV capsid protein) protein in the viral particles. Shown is a typical result. The experiment was repeated five times.

3.2 BAF knockout (KO) in HEK293T and THP-1 cells

To further investigate the effects of BAF on HIV-1 replication across different cellular models, including non-immune cells such as HEK293T and undifferentiated THP-1 cells and immune-like cells such as differentiated THP-1, I performed BAF knockout experiments to assess its role in viral replication. Undifferentiated THP-1 cells are a monocytic leukemia cell line. After PMA-induced differentiation, THP-1 cells exhibit functions similar to macrophages.

BAF-deficient HEK293T and THP-1 cells were generated by using the CRISPR-Cas9 method using lentiviral vectors expressing Cas9 and sgRNA against BAF (Fig. 11A and

11B).

To determine whether BAF knockout affects the normal function of HEK293T and THP-1 cells, I evaluated the cell growth rate between vector-control HEK293T (pLV2 HEK293T) and BAF knockout (KO) HEK293T cells (Fig. 11C), as well as between pLV2 THP-1 and BAF KO THP-1 cells (Fig. 11D). Measuring cell proliferation in vector-control, and KO cells is essential to assess whether the knocked-out protein plays a role in cell growth regulation, to exclude potential non-specific effects of the knockout, and to ensure that any observed biological changes in subsequent experiments are not due to impaired cell viability or proliferation.

Specifically, I measured cell proliferation by counting the number of cells on day 1 and day 3. On day 1, I seeded 3×10^5 pLV2 HEK293T cells and BAF KO HEK293T cells, as well as 4×10^5 pLV2 THP-1 cells and BAF KO THP-1 cells, into separate wells of a 6-well plate. On day 3, I quantified the cell numbers in both groups. The results showed no significant difference in cell numbers between pLV2 HEK293T and BAF KO HEK293T cells (Fig. 11C) or between pLV2 THP-1 and BAF KO THP-1 cells (Fig. 11D) by day 3, suggesting that BAF knockout does not impair the normal proliferation of either HEK293T or THP-1 cells.

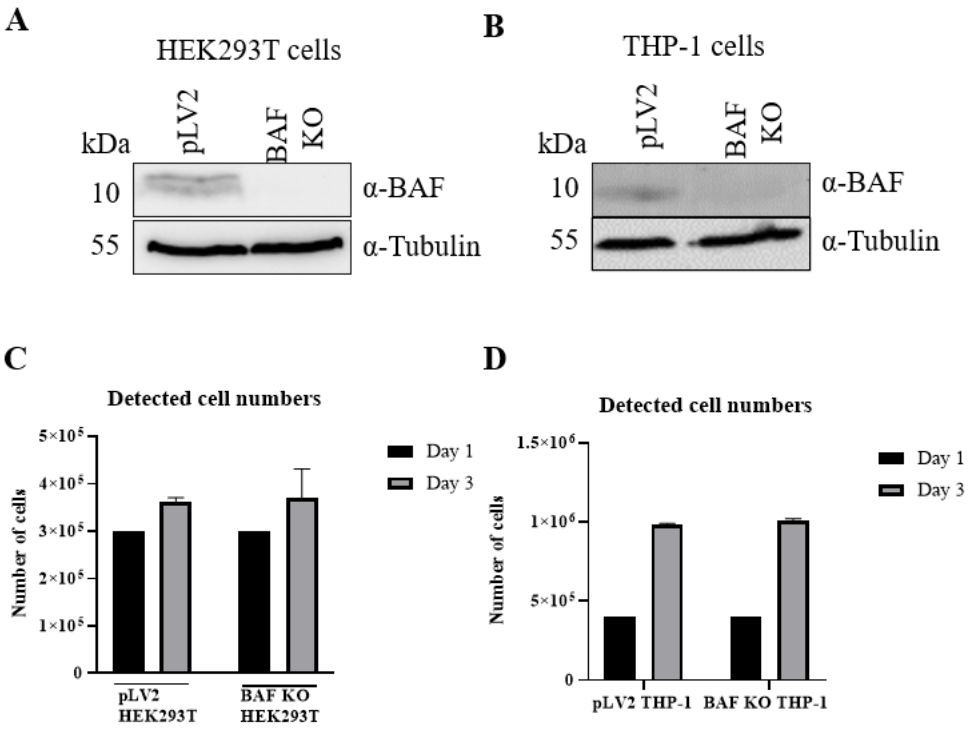

Fig. 11: Verification of BAF knockout and its effect on cell proliferation in HEK293T and THP-1 cells. (A, B) Western blot analysis confirming BAF knockout in HEK293T (A) and THP-1 (B) cells. Whole-cell lysates from vector control (pLV2) and BAF knockout (KO) cells were subjected to immunoblotting with an anti-BAF antibody. α-Tubulin served as a loading control. BAF protein expression was absent in BAF KO cells, confirming successful knockout. (C, D) Cell proliferation analysis of HEK293T (C) and THP-1 (D) cells. The number of cells was counted on day 1 (black bars) and day 3 (gray bars) after seeding pLV2 and BAF KO cells into a 6-well plate. Cell counts for both groups were determined using a hemocytometer. This allowed for comparing cell growth rates between the two cell lines. Data are presented as mean ± standard deviation (SD).

3.3 Effect of BAF KO in producer or target cells on HIV-1 replication

3.3.1 The absence of BAF in producer cells does not affect HIV-1 infectivity

To test the relevance of BAF in the virus producer cell, I produced two types of HIV-1 reporter viral particles. First, I transfected a three-plasmid HIV-1 system into pLV2 HEK293T cells. Second, I transfected the same HIV-1 system into BAF KO HEK293T cells. Then I harvested the two different HIV-1 reporter viral particles. The final step

involved infecting the target cells: pLV2 HEK293T, BAF KO HEK293T, and pLV2 THP-1, BAF KO THP-1 cells. Viral particles were normalized for RT activity. Luciferase activity was measured 48 hr post transduction.

Figure 12 panels (A–D) show the HIV-1 luciferase activity (cps) in different target cells infected with HIV-1 reporter viral particles produced by either wild-type (pLV2 HEK293T) or BAF knockout (BAF KO HEK293T) producer cells. Results show that when pLV2 HEK293T cells were used as target cells, comparable luciferase signals were observed for viruses produced by either wild-type or BAF KO HEK293T producer cells, with no statistically significant difference (Figure 12A). Similarly, in BAF KO HEK293T target cells, infection efficiency remained unchanged between the two virus sources (Figure 12B). When THP-1 cells were used as target cells, a slight decrease in luciferase activity was observed for viruses produced by BAF KO cells compared to those from wild-type HEK293T cells; however, this difference was not statistically significant in either pLV2 THP-1 (Figure 12C) or BAF KO THP-1 target cells (Figure 12D). Together, these results indicate that knockout of BAF in HEK293T producer cells does not significantly affect the infectivity of HIV-1 reporter viral particles, regardless of the target cell type.

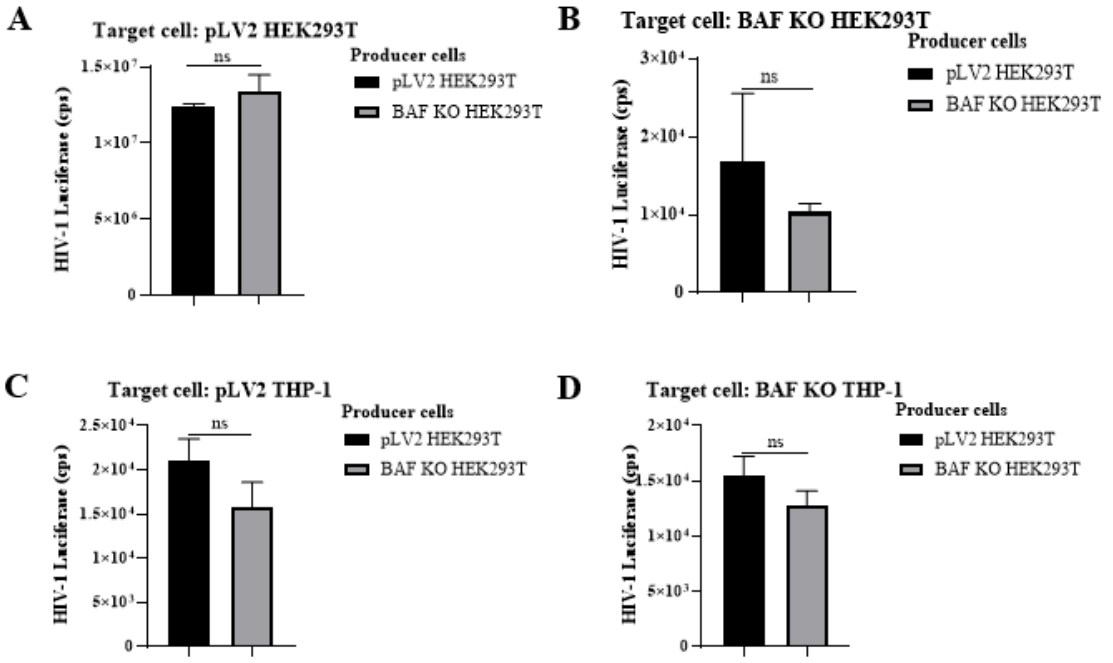

Fig. 12: The absence of BAF in producer cells does not affect the infectivity of HIV-1. (A-D) pLV2 and BAF KO HEK293T, pLV2, and BAF KO THP-1 cells were infected by two types of HIV-1 reporter viral particles, which produced either in pLV2 HEK293T or BAF KO HEK293T cells for 72 hours, followed by luciferase activity analysis. Significance was determined using a two-tailed Student's t-test (Fig. 10) (*P < 0.05, **P < 0.01, ***P < 0.001, and ****P < 0.0001). Data are representative of three independent experiments (graphs show mean ±SD).

To further validate this conclusion, I generated HIV-1 reporter viral particles in the presence of overexpressed BAF. I co-transfected a three-plasmid HIV-1 system with a BAF plasmid into pLV2 HEK293T cells to produce a virus in which BAF was overexpressed in HEK293T cells.

For further infections, I used CRFK cells, derived from a feline kidney. These cells can effectively support the replication of various viruses, including HIV-1, making them an ideal model for studying viral biology and antiviral drug development. HIV-1 infection of CRFK cells with three different viruses (produced in pLV2 293T, BAF KO 293T, and BAF-overexpressing pLV2 293T cells) was performed. The infection was performed with two different viral input amounts: 1 IU and 5 IU of RT-activity. “IU” refers to infectious units based on reverse transcriptase (RT) activity, which serves as a surrogate measure for viral particle quantity. RT activity was quantified using a standard reverse transcriptase assay, and viral input was normalized to ensure equal amounts of virus were used across conditions. Specifically, 1 IU and 5 IU represent two different doses of virus, corresponding to the RT activity equivalent to 1 and 5 units of infectious virus, respectively.

The results show that infection with 1 IU show no significant differences in luciferase activity among viruses produced from the three different producer cell types (Fig. 13). At 5 IU, the luciferase activity significantly increases compared to 1 IU but remains similar across all three producer cell conditions (Fig. 13). No statistically significant differences (ns) were observed between the groups at either viral input level. I conclude that these data suggest that BAF knockout or overexpression in HEK293T producer cells does not significantly affect HIV-1 infectivity in CRFK target cells. Increasing the viral input from

1 IU to 5 IU RT activity leads to a higher infection level, as expected, but the source of virus production does not influence infection efficiency in this setting. These findings indicate that CRFK cells are equally susceptible to HIV-1 regardless of whether the virus was produced in control, BAF KO, or BAF-overexpressing HEK293T cells.

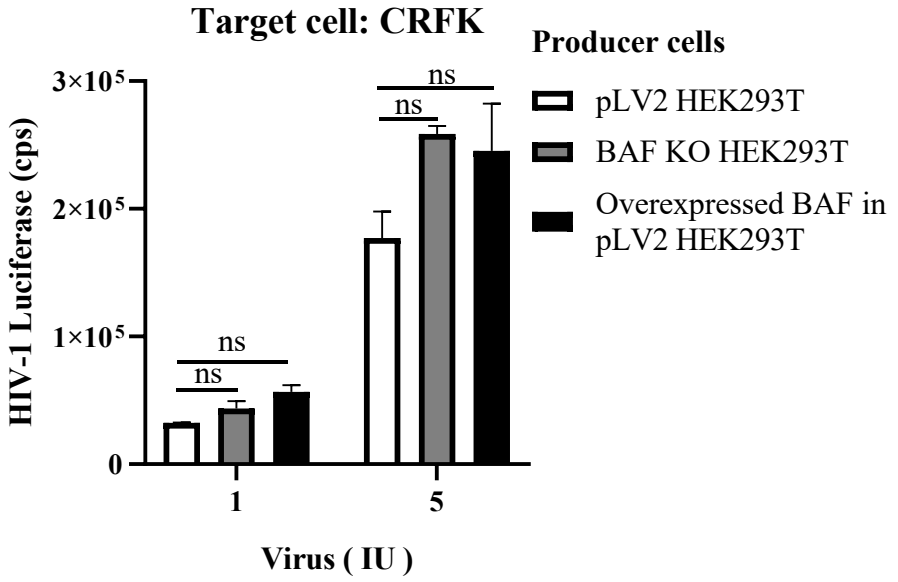

Fig. 13: The absence of BAF in producer cells does not affect the infectivity of HIV-1. CRFK was infected by three different HIV-1 reporter viral particles for 72 hours, followed by luciferase activity analysis. Significance was determined using a two-way analysis of variance (ANOVA) (*P < 0.05, **P < 0.01, ***P < 0.001, and ****P < 0.0001). Data are representative of three independent experiments (graphs show mean ±SD).

3.3.2 The absence of BAF in target cells decreased HIV-1 infection

3.3.2.1 The absence of BAF in target HEK293T cells decreased HIV-1 infection

I found that BAF is not imported for virus-producer cells (section 3.3.1). Next, I tried to figure out if BAF is important for HIV-1 infection in target cells. I employed a virus 3-plasmid system to generate the HIV-1 Luc reporter viral particles in WT HEK293T cells.

Subsequently, I used different viral input amounts for infections: 1, 5, 10, and 20 IU RT activity. I infected pLV2 HEK293T or BAF KO HEK293T cells.

The graph (Fig. 14) illustrates the infection efficiency of HIV-1. In all tested viral doses (1, 5, 10, and 20 IU RT activity), the luciferase signal in pLV2 HEK293T cells (black bars) was significantly higher than that in BAF KO HEK293T cells (gray bars). The luciferase signals increased with the viral input in both cell lines, demonstrating a dose-dependent infection pattern. Statistical analysis indicates highly significant differences ($p < 0.001$ or $*p < 0.0001$) between the two cell lines across all viral doses. These findings suggest that BAF KO HEK293T cells exhibit a significantly reduced susceptibility to HIV-1 infection compared to pLV2 HEK293T cells. This implies that the BAF protein may play a critical role in facilitating HIV-1 infection.

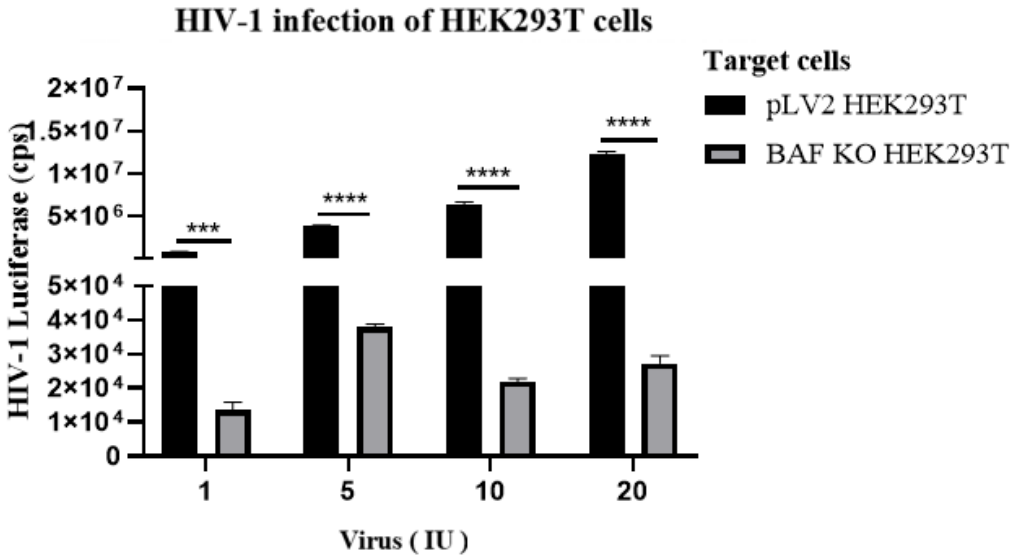

Fig. 14: **The absence of BAF expression in target HEK293T cells decreased HIV-1 infection.** pLV2 HEK293T and BAF KO HEK293T cells were transduced with HIV-1 luciferase reporter viral particles for 72 h, followed by luciferase activity analysis. Significance was determined using two-way ANOVA. ($*P < 0.05$, $**P < 0.01$, $***P < 0.001$, and $****P < 0.0001$). Data are representative of three independent experiments (graphs show mean ±SD).

3.3.2.2 The absence of BAF in target THP-1 cells decreased HIV-1 infection

To further investigate that BAF is important for early HIV-1 infection steps post-entry, I infected PMA-differentiated and undifferentiated THP-1 cells. Viral particles were generated using a 4-plasmid system (HIV-1 with VPX plasmid) to produce the HIV-1 Luc reporter viral particles. VPX promotes viral replication by suppressing the function of sterile alpha motif and HD domain 1 (SAMHD1). SAMHD1 is an intracellular antiviral factor that hydrolyzes deoxynucleotide triphosphates (dNTPs) within the cell, limiting the availability of nucleotides necessary for viral replication, particularly for retroviruses like HIV[221,222]. Antiviral SAMHD1 is expressed in differentiated THP-1 cells. In addition, I used full-length HIV-1 Luc reporter virus generated using the NL-luc and VSV-G plasmids.

The figure 15 presents the infection efficiency of HIV-1 in PMA-differentiated (Fig.15A and Fig.15C) and undifferentiated (Fig.15B and Fig.15D) THP-1 cells, comparing pLV2 THP-1 cells (black bars) and BAF KO THP-1 cells (gray bars). HIV-1 infection was measured by its luciferase activity. HIV-1 (VPX) infection in PMA-differentiated THP-1 cells resulted in significantly higher luciferase activity in pLV2 THP-1 cells compared to BAF KO THP-1 cells ($p < 0.01$) (Fig. 15A). Similarly, in undifferentiated THP-1 cells, HIV-1 (VPX) infection showed a significantly higher luciferase signal in pLV2 THP-1 cells than in BAF KO THP-1 cells ($p < 0.001$) (Fig. 15B). NL-luc HIV-1 infection in PMA-differentiated THP-1 cells followed the same trend, with pLV2 THP-1 cells exhibiting significantly greater luciferase activity than BAF KO THP-1 cells ($p < 0.01$) (Fig. 15C). NL-luc HIV-1 infection in undifferentiated THP-1 cells also demonstrated a significant reduction in luciferase signal in BAF KO THP-1 cells compared to pLV2 THP-1 cells ($p < 0.001$) (Fig. 15D). These results indicate that BAF KO THP-1 cells exhibit significantly reduced susceptibility to HIV-1 infection compared to pLV2 THP-1 cells, regardless of cell differentiation status. This trend is consistent across both VPX-containing and NL-luc HIV-1 infections, suggesting that BAF plays a crucial role in facilitating HIV-1 infection in THP-1 cells.

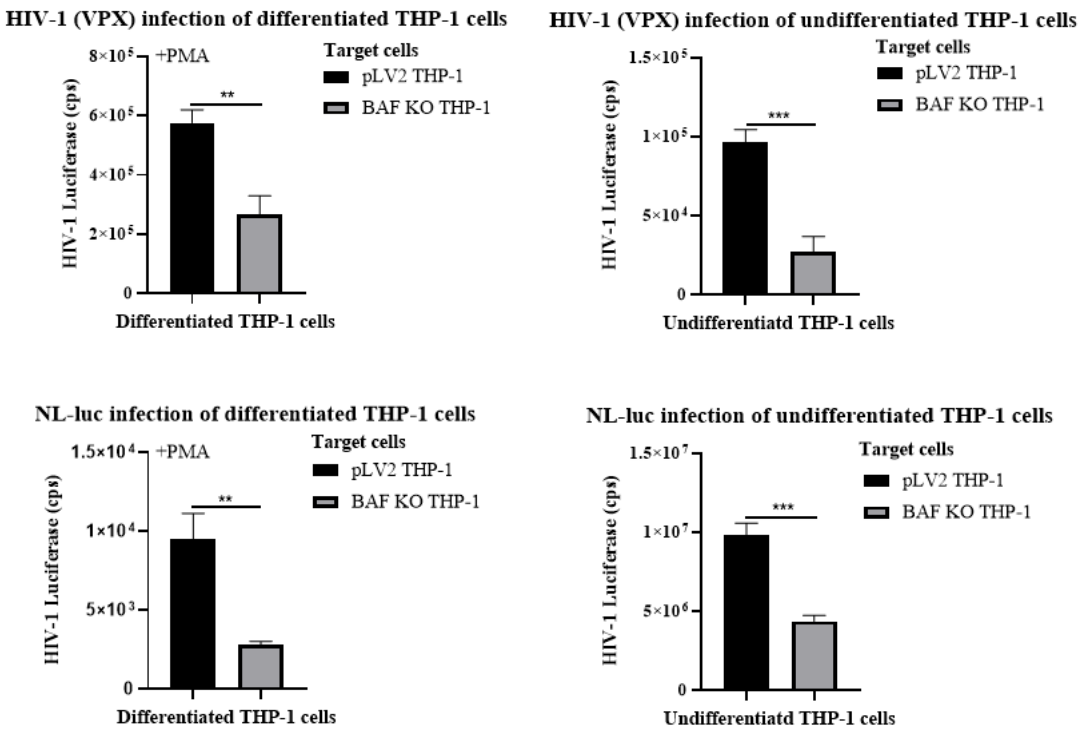

Fig. 15: The absence of BAF expression decreased HIV-1 infection in THP-1 cells. (A) PMA-differentiated pLV2 THP-1 and BAF KO THP-1 cells were transduced with HIV-1/VPX luciferase reporter viral particles for 72 h, followed by luciferase activity analysis. (B) Undifferentiated pLV2 THP-1 and BAF KO THP-1 cells were transduced with HIV-1/VPX luciferase reporter viral particles for 72 h, followed by luciferase activity analysis. (C) PMA-differentiated pLV2 THP-1 and BAF KO THP-1 cells were transduced with full-length HIV-1 luciferase reporter virus for 72 h, followed by luciferase activity analysis. (D) Undifferentiated pLV2 THP-1 and BAF KO THP-1 cells were transduced with full-length HIV-1 luciferase reporter virus for 72 h, followed by luciferase activity analysis. Significance was determined using a two-tailed Student's t-test (*P < 0.05, **P < 0.01, ***P < 0.001, and ****P < 0.0001). Data are representative of three independent experiments (graphs show mean ±SD).

3.4 Restoration of BAF in THP-1 cells to verify its effect on HIV-1 replication

After knocking out the expression of the BAF protein in THP-1 cells using the CRISPR-Cas9 system and observing a decrease in HIV-1 replication, I aimed to confirm that this reduction was specifically due to the absence of BAF. To achieve this, I constructed an MLV-based retroviral vector encoding the BAF protein with mutations in the PAM

sequence in the cDNA, preventing further targeting by the CRISPR-Cas9 system. This vector was then transduced into BAF KO THP-1 cells, allowing stable re-expression of BAF (Fig. 16). This approach assessed whether restoring BAF expression would rescue HIV-1 replication, thereby confirming its essential role in the viral replication process.

The Western blot analysis shown in Figure 16 evaluates the expression levels of BAF protein in different THP-1 cell conditions. α-Tubulin serves as a loading control to ensure equal protein loading across samples. In pLV2 THP-1 cells (wild-type control), a detectable BAF protein band is present. In BAF KO THP-1 cells, the BAF protein band is absent, confirming the successful knockout of BAF via the CRISPR-Cas9 system. In BAF KO + pLNCX2 cells, no visible BAF band is detected, indicating that the empty vector does not restore BAF expression. In BAF KO + BAF reconstituted cells, BAF expression is restored, demonstrating the successful reintroduction of BAF using the MLV-based retroviral vector carrying a PAM-mutated BAF gene. These results confirm the successful knockout of BAF in THP-1 cells and demonstrate that its expression can be effectively restored using a retroviral vector carrying a PAM-mutated BAF construct. This provides a reliable model for investigating the functional role of BAF in HIV-1 replication and other cellular processes.

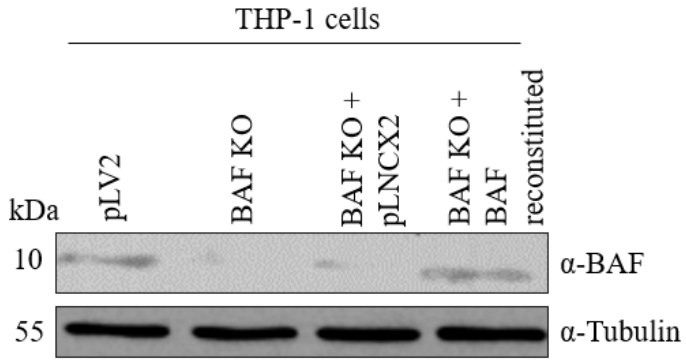

Fig. 16: BAF restoration in BAF KO THP-1 cells. Protein lysates from THP-1 cells. pLV2 THP-1, BAF KO THP-1, pLNCX2 THP-1 and BAF restored THP-1 cells were immunoblotted with the indicated antibodies.

In the next experiment, I investigated the effect of BAF restoration in BAF knockout cells on HIV-1 replication (Fig. 17). HIV-1 infection was measured in THP-1 cells with either

wild-type BAF (pLV2 THP-1) or BAF knockout (BAF KO THP-1) (Fig. 17A). BAF expression was restored in BAF KO THP-1 cells (BAF restores THP-1), and the impact on HIV-1 replication was assessed in these cells (Fig. 17B).

HIV-1 replication, measured by luciferase activity, was significantly reduced in BAF KO THP-1 cells compared to pLV2 THP-1 cells ($p < 0.05$), as seen before. However, reintroducing BAF in the BAF KO THP-1 (BAF KO THP-1 + BAF) cells significantly enhanced HIV-1 replication compared to the control group lacking BAF (BAF KO THP-1 + pLNCX2) ($p < 0.001$) (Fig. 17B). These results further support that BAF promotes early HIV-1 replication in THP-1 cells.

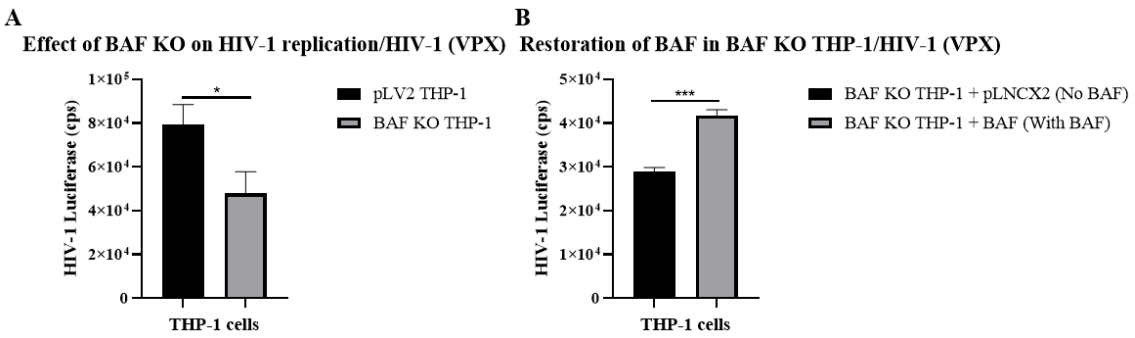

Fig. 17: BAF restoration leads to enhanced HIV-1 replication. (A) pLV2 THP-1 and BAF KO THP-1 were transduced with HIV-1 luciferase reporter viral particles for 72 h, followed by luciferase activity analysis. (B) pLNCX2 THP-1 (empty MLV vector transfected in BAF KO THP-1 cell), and BAF restored THP-1 cells (BAF KO THP-1 +BAF) were transduced with HIV-1 luciferase reporter viral particles for 72 h, followed by luciferase activity analysis. Significance was determined using a two-tailed Student's t-test (*$P < 0.05$, **$P < 0.01$, ***$P < 0.001$, and ****$P < 0.0001$). Data are representative of three independent experiments (graphs show mean ±SD).

3.5 BAF KO regulates STING-mediated signaling activation

3.5.1 BAF KO increased STING-mediated signaling activation upon HIV-1 infection

Since I have established that the presence of BAF in target cells is crucial for HIV-1 infection, it is essential to understand the underlying mechanisms driving this effect. HIV-1 infection triggers an innate immune response[99,223], and I aim to investigate whether there is a relationship between BAF and the innate immune response to HIV-1 infection. The sensing of HIV-1 cDNA by the cGAS–STING signaling pathway has emerged as a major mechanism in mounting the antiviral immune response against the infection[224–226].

This experiment uses Western blot analysis to investigate the effect of STING agonist SR-717 treatment on the expression of key immune-related proteins in THP-1 WT and BAF KO cells. When a STING agonist is added to the cells, it activates the STING (Stimulator of Interferon Genes) pathway. The STING agonist SR-717 acts as a cGAMP mimetic that induces the same "closed" conformation of STING, thus enhancing STING-dependent antitumor immunity and diverse STING-dependent biological processes[227]. First, I treated WT THP-1 cells as a baseline control with 3.6 μM of the STING agonist SR-717 (Fig. 18A). Panel A (Fig. 18A) compares protein expression in WT THP-1 cells treated with either DMSO (control) or SR-717. Panel B (Fig. 18B) shows the effects of SR-717 in BAF KO cells on protein expression.

SR-717 treatment significantly upregulated ISG15 and USP18 expression in WT THP-1 cells compared to the DMSO control. STING expression was reduced, while the A3A, IRF3, and TBK1 levels remained relatively unchanged (Fig. 18A). In BAF KO cells was an altered protein expression pattern detectable in both DMSO- and SR-717-treated cells. Notably, ISG15 and USP18 levels were increased in BAF KO THP-1 cells. BAF KO reduced A3A expression compared to pLV2 control cells, while STING, IRF3, and TBK1 showed no significant changes (Fig. 18B). These findings suggest that BAF KO induces the expression of ISG15 and USP18, key interferon-stimulated genes.

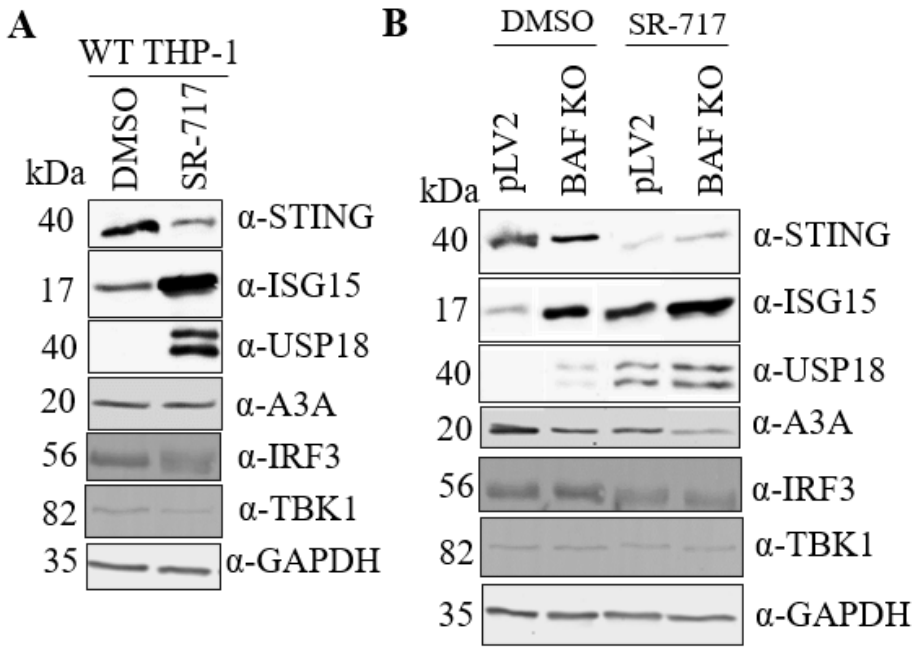

Fig. 18: BAF KO upregulates STING-mediated signaling activation. (A) Protein lysates from WT THP- cells were stimulated with DMSO as a control or 3.6 μM STING agonist SR-717 for 1 hour, followed by immunoblotting analysis with the indicated antibodies. (B) Protein lysates from pLV2 and BAF KO THP-cells were stimulated with DMSO as a control or 3.6 μM STING agonist SR-717 for 1 hour, followed by immunoblotting analysis with the indicated antibodies.

3.5.2 BAF regulates interferon production and *ISGs* at the mRNA level upon HIV-1 infection

This experiment evaluates the production of type I interferon (IFN) in THP-1 cells following HIV-1 infection. After measuring luciferase activity, the supernatants were collected to stimulate HEK-Blue cells, which detect type I IFN signaling[228]. These cells are engineered to report IFN-α/β activity, allowing us to measure IFN-α/β levels in our experiments. The resulting IFN production was quantified. Type I IFN production was measured in pLV2 THP-1 cells treated with either medium only (control) or HIV-1 (Fig. 19A). The effect of BAF knockout (KO) on type I IFN production was examined by comparing pLV2 THP-1 and BAF KO THP-1 cells after HIV-1 infection (Fig. 19B). HIV-1 infection significantly increased type I IFN production in pLV2 THP-1 cells compared to the control group (treated only with medium) ($p < 0.001$). There was no significant

difference in type I IFN production between pLV2 THP-1 and BAF KO THP-1 cells following HIV-1 infection (ns, insignificant). I conclude that HIV-1 infection strongly induces type I IFN production in THP-1 cells. However, BAF KO does not significantly affect HIV–1–induced IFN production, suggesting that BAF may not play a major role in regulating the type I IFN response upon HIV-1 infection.

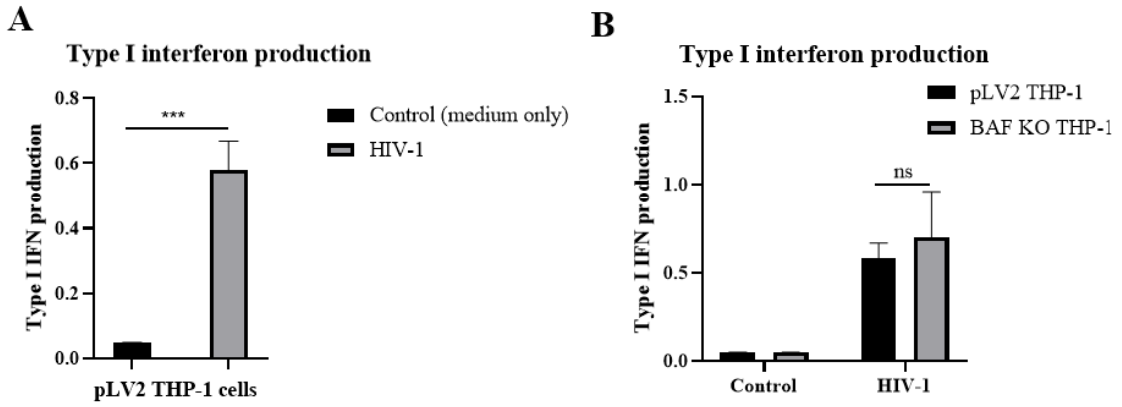

Fig. 19: BAF KO did not change IFN-α/β production upon HIV-1 infection. (A) Type I IFN production was significantly increased in pLV2 THP-1 cells after HIV-1 infection compared to the control group (medium only) ($\boldsymbol{p} < 0.001$). (B) There was no significant difference in type I IFN production between pLV2 THP-1 and BAF KO THP-1 cells following HIV-1 infection (ns, insignificant). Significance was determined using a two-tailed Student's t-test (*P < 0.05, **P < 0.01, ***P < 0.001, and ****P < 0.0001). Data represent mean ± SD of at least three independent experiments.

The next experiment investigates the role of BAF in HIV-1 infection by analyzing the expression of key interferon-stimulated genes (*ISGs*) and type I interferon (IFN) response genes. RT-qPCR was performed to quantify the mRNA levels of *IFNB1* (encoding IFN-β), *ISG15*, and *ISG54* in BAF KO and vector control (pLV2) THP-1 cells after 48 hours of HIV-1 (VPX) infection. Results showed, HIV-1 infection increased IFNB1 expression in both pLV2 and BAF KO THP-1 cells compared to the control condition (medium only), but no significant difference was observed between the two cell types (Fig. 20A). In contrast, HIV-1 infection significantly upregulated *ISG15* expression, and its induction

was significantly higher in BAF KO THP-1 cells compared to pLV2 control cells ($p < 0.01$) (Fig. 20B). Similar to *ISG15*, *ISG54* expression was strongly induced by HIV-1, with a significantly higher increase in BAF KO THP-1 cells compared to pLV2 THP-1 cells (control cells) ($p < 0.0001$) (Fig. 20C). These findings suggest that BAF depletion enhances the expression of *ISG15* and *ISG54* upon HIV-1 infection, indicating that BAF may act as a negative regulator of certain interferon-stimulated genes. However, *IFNB1* expression was not significantly affected by BAF KO, suggesting that the upstream induction of type I IFNs remains intact in the absence of BAF.

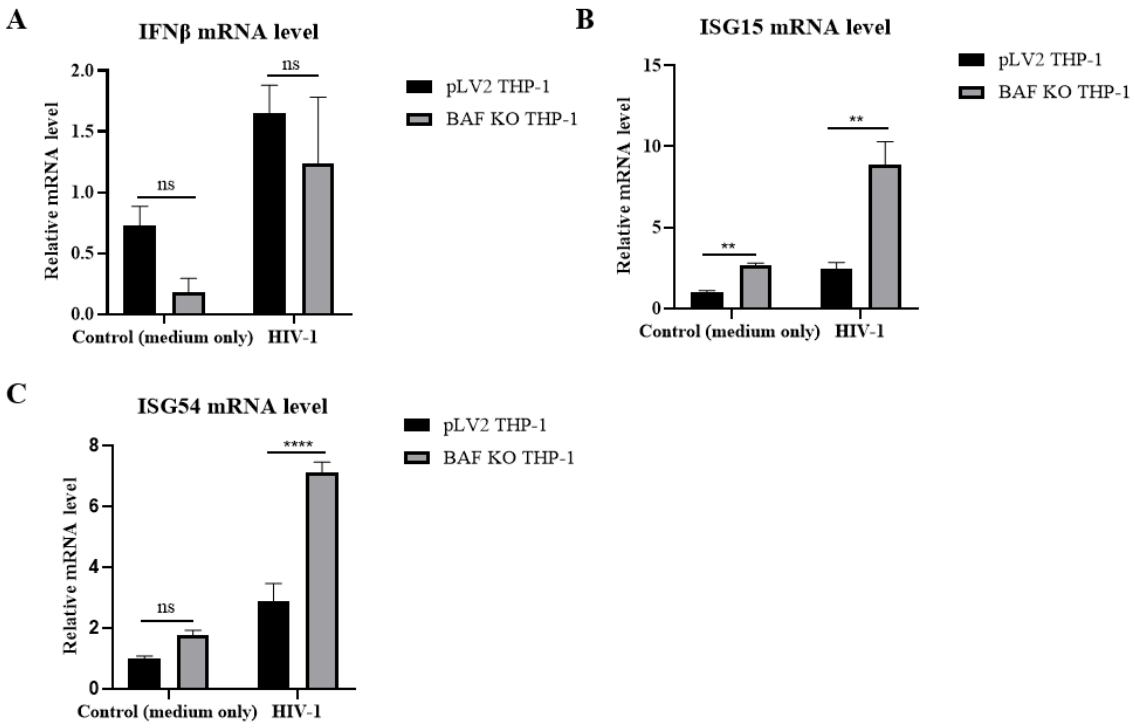

Fig. 20: BAF KO did not change IFNβ mRNA level, but *ISG15* and *ISG54* mRNA was increased upon HIV-1 infection. RT-qPCR analysis of *ISG54*, IFNB1, and *ISG15* mRNA in BAF KO THP-1 and pLV2 THP-1 (vector control) cells infected with HIV-1 (VPX) for 48 hr. (A) *IFNB1* expression was induced by HIV-1 but showed no significant difference between BAF KO THP-1 and pLV2 THP-1 (vector control) cells. (B) HIV-1 infection significantly increased *ISG15* expression, with a higher induction in BAF KO THP-1 cells ($p < 0.01$). (C) *ISG54* expression was strongly upregulated by HIV-1, with a significantly greater increase in BAF KO THP-1 and pLV2 THP-1 (vector control) cells ($p < 0.0001$). Significance was determined using a two-tailed Student's t-test (Figs.11A-11C) (*$P < 0.05$, **$P < 0.01$, ***$P < 0.001$, and ****$P < 0.0001$). Data

are representative of three independent experiments (graphs show mean ±SD).

3.5.3 Type I IFN-α/β triggered from Modified Vaccinia Virus Ankara (MVA), Sendai virus (SeV), or SR-717 in BAF KO THP-1

To further investigate the effect of BAF knockout (KO) on type I interferon (IFN-α/β) responses response to non-HIV pathogens, I examined type I IFN production in BAF KO, STING KO, and vector control (pLV2) THP-1 cells following stimulation with Modified Vaccinia Virus Ankara (MVA), Sendai virus (SeV), or the STING agonist SR-717. These stimuli were selected to activate distinct innate immune pathways: SeV, an RNA virus, primarily triggers the RIG-I/MAVS signaling pathway[229], whereas MVA is a vaccinia virus that can trigger cGAS/STING sensing pathways[230]; in contrast, SR-717 directly activates STING-dependent pathways[231]. By comparing IFN-α/β responses across different stimuli, we aimed to determine whether BAF plays a broader role in regulating innate immune activation beyond HIV-1 infection. IFN-α/β production was quantified using a reporter assay.

MVA stimulation led to a robust induction of type I IFNs in both pLV2 THP-1 (black bar) and BAF KO THP-1 (gray bar) cells, with no significant difference between the two groups (Fig. 21A). STING KO cells (white bar) exhibited no significant difference between control (medium only) in IFN production (Fig. 21B), consistent with the relevance of the cGAS/STING pathway for sensing of MVA. SeV triggered a strong IFN response in all three groups (Fig. 21B). No significant difference was observed between BAF KO THP-1 and pLV2 THP-1 control cells. In contrast, STING KO cells exhibited a slight but significant reduction in IFN production ($p < 0.01$), suggesting a potential minor role for STING in SeV-triggered IFN responses. SR-717 led to a potent IFN response in both pLV2 and BAF KO THP-1 cells, with no significant difference between them (Fig. 21C). STING KO cells exhibited almost no IFN production, confirming that SR-717 specifically activates the STING pathway. These findings demonstrate that BAF knockout does not influence type I IFN responses to MVA, SeV, SR-717, or HIV-1, suggesting that

BAF is not a general regulator of IFN-β induction in response to these stimuli. The complete abolition of IFN responses in STING KO cells upon MVA or SR-717 stimulation further validates the STING dependency of these stimuli, while the slight reduction in SeV-induced IFNs in STING KO cells suggests potential crosstalk between STING and RIG-I/MAVS pathways.

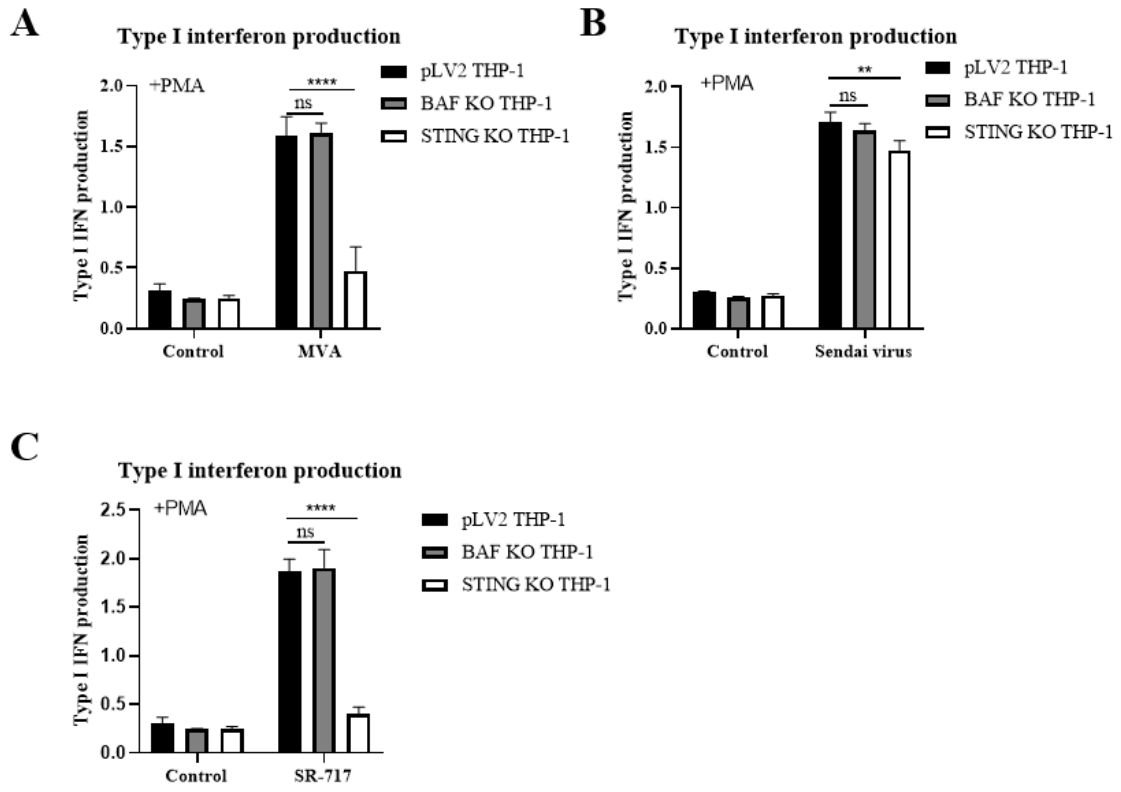

Fig. 21: Type I IFN-α/β production in BAF KO, STING KO, and pLV2 (vector control) THP-1 cells upon stimulation with MVA, SeV, or SR-717. (A) MVA stimulation induced significant IFN production in pLV2 and BAF KO THP-1 cells, but STING KO cells showed a drastic reduction, confirming STING dependence. (B) SeV triggered strong IFN responses across all groups, with a slight but significant reduction in STING KO cells ($p < 0.01$). (C) SR-717 induced robust IFN production in both pLV2 and BAF KO cells, while STING KO cells exhibited nearly no response, confirming the specificity of SR-717 for STING activation. Data represent mean ± SD from at least three independent experiments.

3.5.4 *IFNB1* and *ISG15*, *ISG54* in mRNA level in BAF KO THP-1 cells upon Herring-Sperm (HS)-DNA transfection

To further investigate the effect of BAF knockout (KO) in THP-1 cells on the immune response to non-HIV pathogens, we examined *IFNB1, ISG15*, and *ISG54* mRNA levels in BAF KO and vector control (pLV2) THP-1 cells following transfection with Herring-Sperm (HS)-DNA with 24 hr. Quantitative RT-PCR analysis revealed that, upon HS-DNA stimulation, *IFNB1* expression was significantly upregulated in both cell lines. Specifically, in pLV2 THP-1 cells, *IFNB1* mRNA levels increased by approximately 1012-fold (from an average of 1.03 to 1012.13), while in BAF KO THP-1 cells, the increase was even more pronounced, approximately 1906-fold (from an average of 0.81 to 1525.45). In addition, BAF KO THP-1 cells compared to pLV2 controls showed a further significant increase (****, $p < 0.0001$) (Fig. 22). These results indicate that BAF deficiency further enhances IFNB1 transcriptional activation in response to HS-DNA transfection.

Our findings demonstrate that BAF KO THP-1 cells exhibit a heightened IFNB1 mRNA response to HS-DNA stimulation, suggesting that BAF may function as a negative regulator of *IFNB1* induction in the context of cytosolic DNA sensing. This highlights a potential role for BAF in modulating innate immune signaling pathways activated by non-HIV DNA.

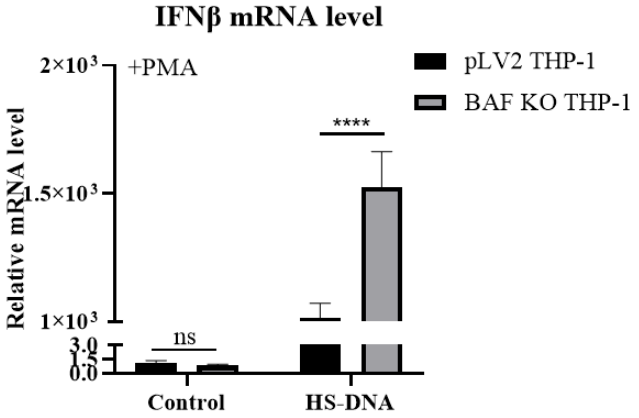

Fig. 22: IFNB1 mRNA expression in BAF KO and vector control (pLV2) THP-1 cells after HS-DNA transfection. Cells were treated with PMA before transfection. Relative *IFNB1* mRNA

levels were measured by qRT-PCR and normalized to housekeeping gene expression. Statistical significance was determined using an unpaired t-test (ns = insignificant; ****, $p < 0.0001$). Data are presented as mean ± SEM from biological replicates.

3.5.5 *ISG15, ISG54*, and *IFNB1* in mRNA level in BAF Knockout Cells upon MVA infection

I used qPCR to measure *ISG15, ISG54*, and *IFNB1* mRNA levels in BAF KO cells upon MVA infection in PMA-differentiated and undifferentiated THP-1 cells. Quantitative RT-PCR analysis revealed that upon MVA infection, *IFNB1*, *ISG15*, and *ISG54* expression were significantly upregulated in both pLV2 and BAF KO THP-1 cells. In PMA-differentiated cells, *IFNB1* expression increased by approximately 24-fold in pLV2 cells and 64-fold in BAF KO cells (Fig. 23A), with BAF KO cells showing a further significant increase. Similarly, *ISG15* expression increased by 33-fold in pLV2 and 10-fold in BAF KO cells (Fig. 23B), and *ISG54* increased by 36-fold in pLV2 and 7-fold in BAF KO cells (Fig. 23C), both showing enhanced expression in the BAF KO group. In undifferentiated cells, *ISG15* expression increased by 33-fold in pLV2 and 10-fold in BAF KO cells (Fig. 23D), while *ISG54* increased by 36-fold in pLV2 and 9-fold in BAF KO cells (Fig. 23E), again with significantly higher expression in BAF KO cells.

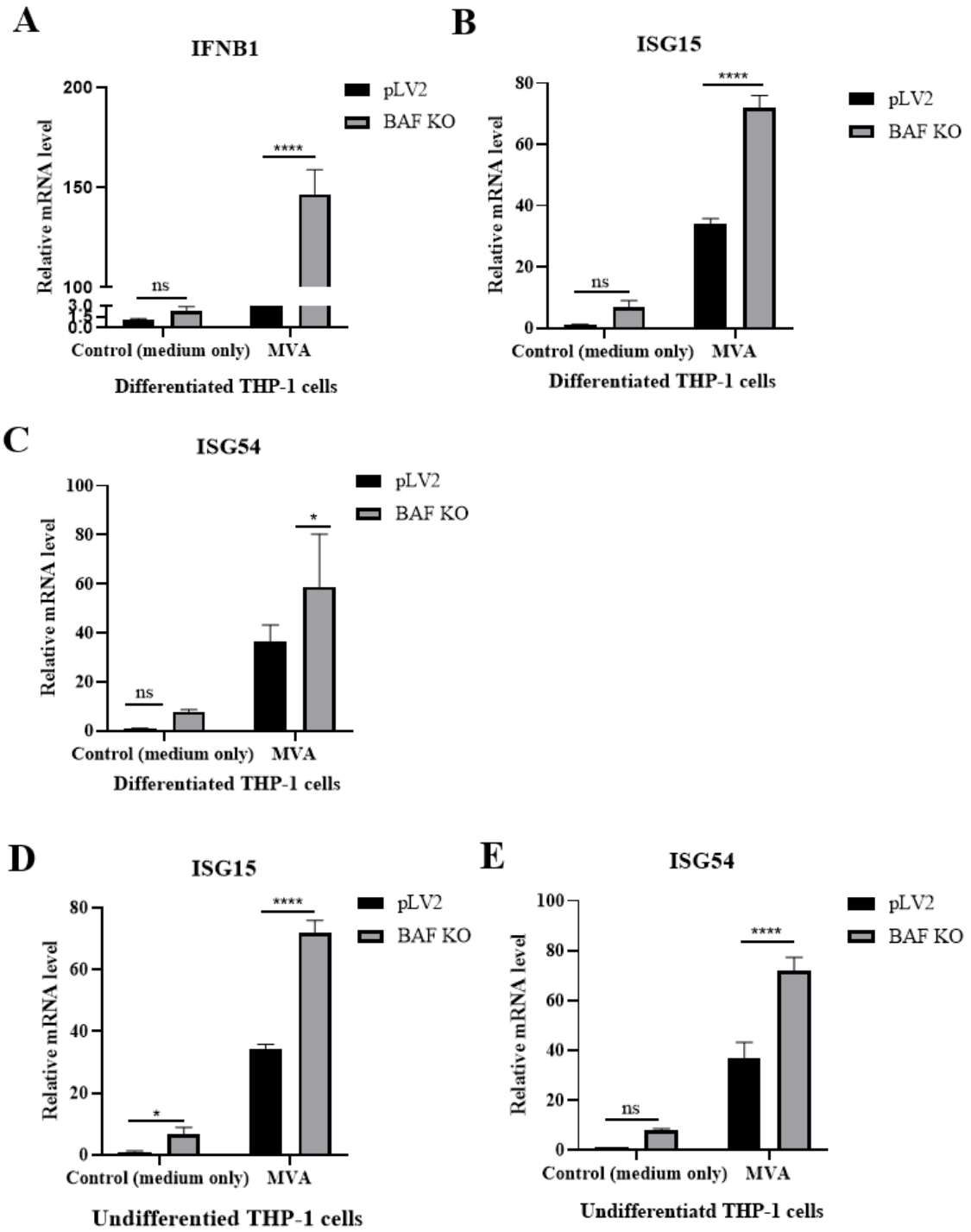

Fig. 23: *IFNβ*, *ISG15*, and *ISG54* mRNA were further increased in BAF KO THP-1 cells upon MVA infection. (A–C) Relative mRNA levels of *IFNB1* (A), *ISG15* (B), and *ISG54* (C) in differentiated THP-1 cells comparing pLV2 control cells and BAF knockout cells following MVA infection. (D–E) Relative mRNA levels of *ISG15* (D) and *ISG54* (E) in undifferentiated THP-1 cells comparing pLV2 and BAF KO cells post-MVA infection. In all panels, 'Control' refers to cells treated with medium only (no MVA infection). RT-qPCR analysis of *ISG54*, *IFNB1*, and

ISG15 mRNA in BAF KO and vector control THP-1 cells with MVA infection for 48h. Significance was determined using a two-tailed Student's t-test (Fig. 20) (*P < 0.05, **P < 0.01, ***P < 0.001, and ****P < 0.0001). Data are representative of three independent experiments (graphs show mean ±SD).

3.6 Quantitative analysis of late RT, 2-LTR circles, and autointegration in HIV-infected THP-1 cells

HIV-1 infection was performed by exposing pLV2 THP-1 cells and BAF KO THP-1 cells to the full-length pNL-Bal virus. After 24 hours of infection, cells were harvested, and genomic DNA was extracted for quantitative PCR (qPCR) analysis. The results revealed distinct differences in viral replication intermediates between the two cell lines. Compared to pLV2 THP-1 cells, BAF KO THP-1 cells exhibited a significant decrease in late RT products, a marked increase in 2-LTR circles, and an elevated level of autointegration. These findings suggest that BAF deficiency impairs late RT, promoting 2-LTR circle formation and autointegration during HIV-1 replication (Fig. 24). In average, over three independent experiments, BAF knockout resulted in a 71% decrease in late RT products compared to control cells (Fig. 24A). In contrast, the level of 2-LTR circles increased by 36% in BAF KO cells (Fig. 24B), indicating enhanced nuclear import or failed integration. Furthermore, autointegration events were elevated by approximately 2.6-fold in BAF KO cells relative to pLV2 controls (Fig. 24C), suggesting that loss of BAF promotes aberrant integration events.

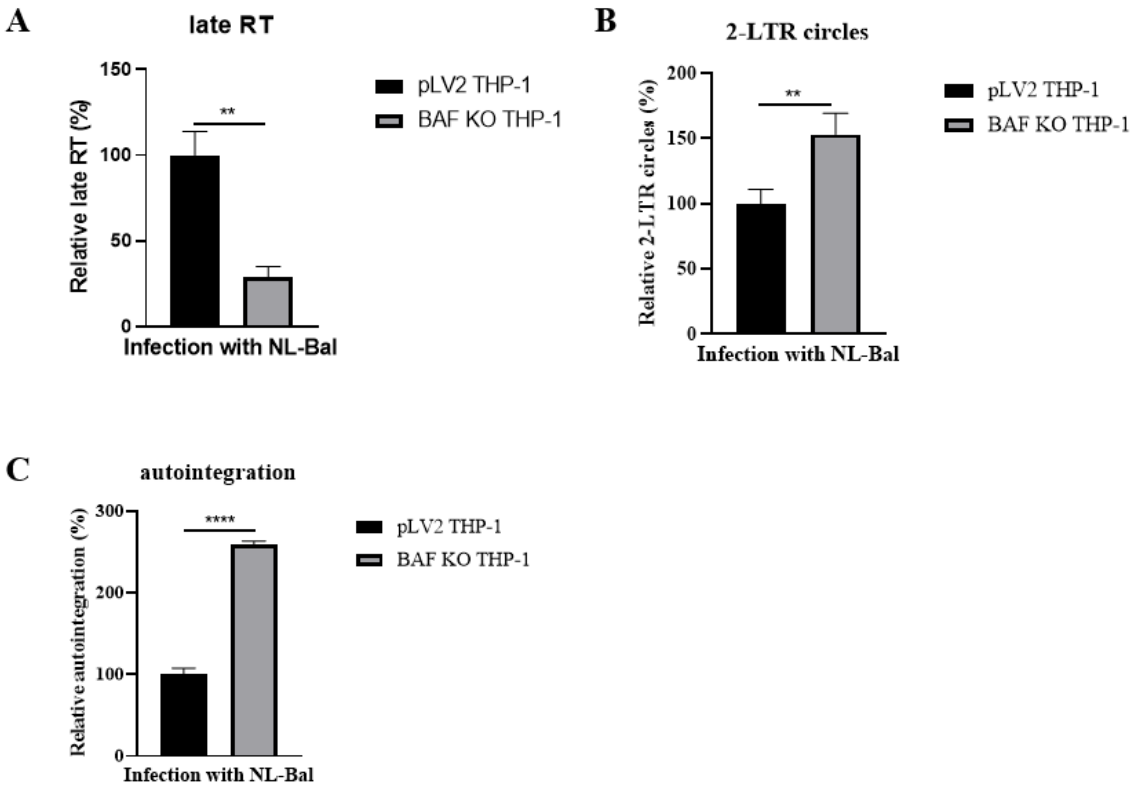

Fig. 24: Analysis of late reverse transcription (RT), 2-LTR circle formation, and autointegration during HIV-1 infection in pLV2 THP-1 and BAF KO THP-1 cells. (A) Late reverse transcription products were quantified in THP-1 cells infected with NL-Bal. A significant reduction in late RT levels was observed in BAF KO THP-1 cells compared to control pLV2 THP-1 cells. (B) The formation of 2-LTR circles, a marker of aborted integration, was assessed. BAF KO THP-1 cells exhibited slightly higher levels of 2-LTR circles than pLV2 THP-1 cells. (C) Relative levels of autointegration were measured. BAF KO THP-1 cells showed a marked increase in autointegration events compared to pLV2 THP-1 cells. Data are presented as the mean ± SEM from three independent experiments, normalized to the control condition.

3.7 DNA-PK inhibitor: KU-57788

Given the mutual regulatory relationship between BAF, DNA-PK, and the cGAS–STING pathway, I next sought to investigate the role of DNA-PK activity in this context. BAF has been reported to inhibit DNA-PK, while DNA-PK negatively regulates cGAS–STING signaling. Since BAF also serves to restrain cGAS–STING activation, I

hypothesized that pharmacological inhibition of DNA-PK might modulate this signaling axis in the absence of BAF.

3.7.1 DNK-PK inhibitor: KU-57788 with 4h treatment

In both undifferentiated and differentiated pLV2 THP-1 cells, as well as BAF KO THP-1 cells, cells were preincubated with the DNA-PK inhibitor KU-57788 for 4 hours. After this preincubation, the inhibitor-containing medium was removed and replaced with fresh medium containing HIV-1(VPX) or NL-luc R-E- full-length virus, without the inhibitor. Under these conditions, HIV-1 luciferase activity was consistently reduced, demonstrating that the inhibitory effect is independent of BAF (Fig. 25).

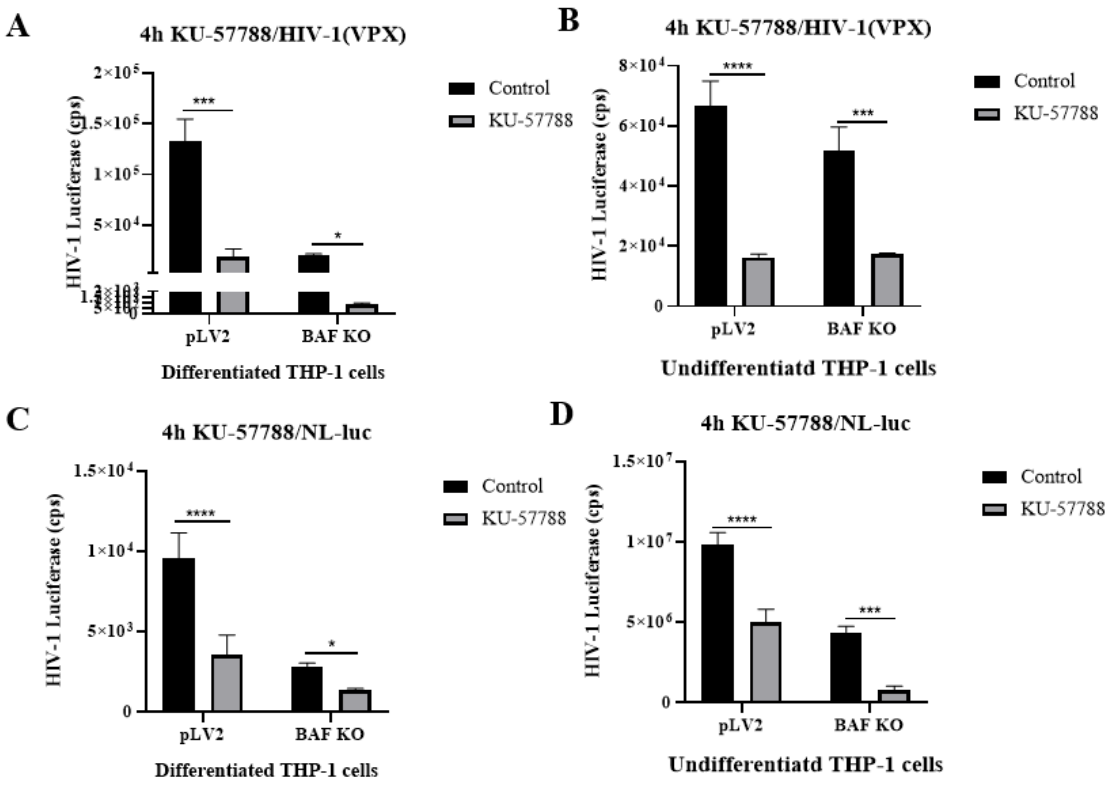

Fig. 25: DNA-PK inhibitor KU-57788 treatment for 4h inhibits HIV-1(VPX) and NL-luc independent of BAF. (A and B) PMA-differentiated and undifferentiated pLV2 THP-1 and BAF KO THP-1 cells were treated with KU-57788 for 4 h, followed by HIV-1(VPX) infection for 48 h. (C and D) PMA-differentiated and undifferentiated pLV2 THP-1 and BAF KO THP-1 cells

were treated with KU-57788 for 4 h, followed by HIV-1(NL-luc) infection for 48 h, and analyzed by luciferase activity assay. Significance was determined using two-way ANOVA (*P < 0.05, **P < 0.01, ***P < 0.001, and****P < 0.0001). Data are representative of three independent experiments (graphs show mean ±SD).

Furthermore, when measuring interferon (IFN) production under the above-described experimental conditions using differentiated THP-1 cells, only one of the two virus systems showed increased IFN in the cell supernatant. An increase in IFN was observed in control cells and much stronger increase in BAF KO THP-1 cells infected with HIV-1(VPX) (Fig. 26A, B). In contrast, there was a noticeable decrease in HIV-1 luciferase activity without any change in IFN levels when infected with NL-Luc (Fig. 26C, D).

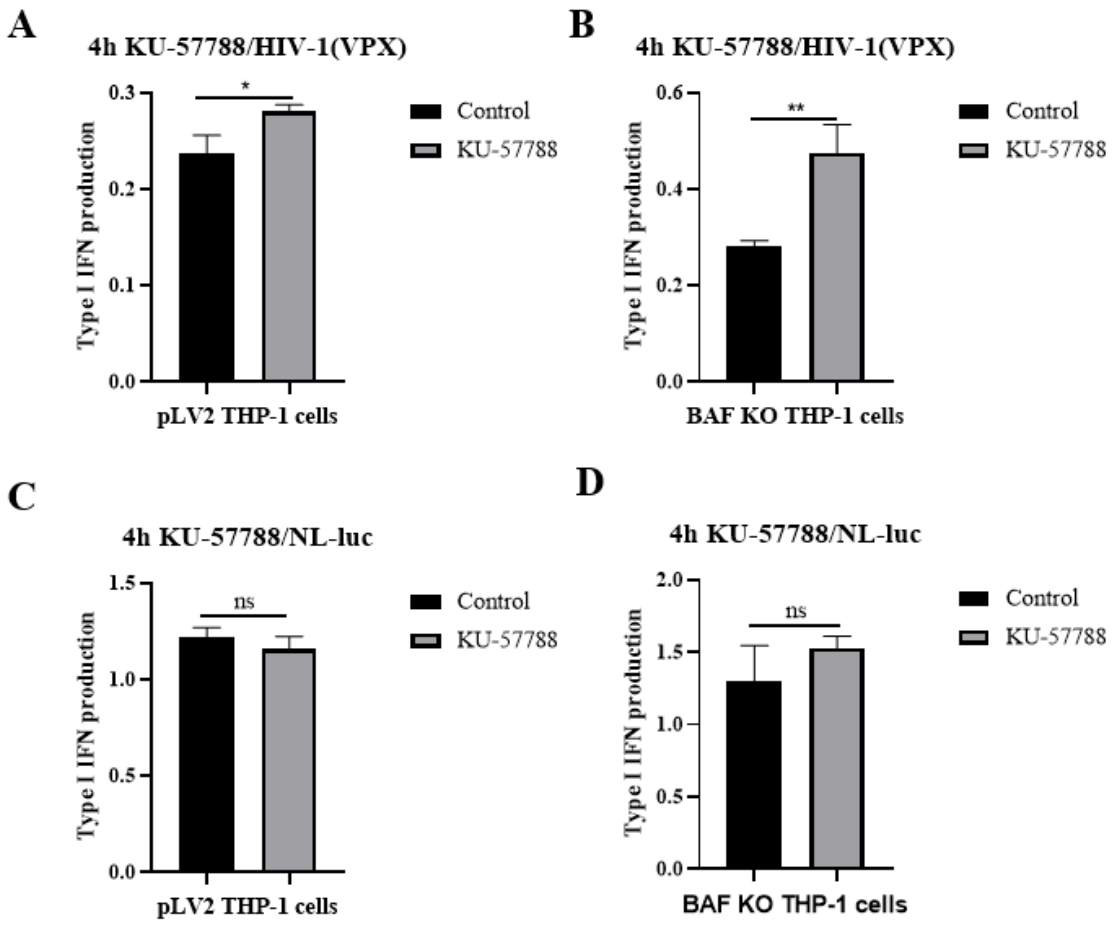

Fig. 26: After DNA-PK inhibitor KU-57788 4h treatment, interferon production was increased in differentiated BAF KO THP-1 cells when infected with HIV-1(VPX). (A) After

analyzing the luciferase activity assay, I measured the interferon production assay in pLV2 THP-1 cells infected with HIV-1(VPX). (B) After analyzing the luciferase activity assay, I measured the interferon production assay in BAF KO THP-1 cells infected with HIV-1(VPX). (C) After analyzing the luciferase activity assay, I measured the interferon production assay in pLV2 THP-1 cells infected with NL-luc. (B) After analyzing the luciferase activity assay, I measured the interferon production assay in BAF KO THP-1 cells infected with NL-luc. Significance was determined using a two-tailed Student's t-test (*P < 0.05, **P < 0.01, ***P < 0.001, and ****P < 0.0001). Data are representative of three independent experiments (graphs show mean ±SD).

3.7.2 DNK-PK inhibitor: KU-57788 with 24h treatment

In the next experiments, both undifferentiated and differentiated pLV2 THP-1 cells, as well as BAF KO THP-1 cells, were preincubated with the DNA-PK inhibitor KU-57788 for 24 hours. After this preincubation, the inhibitor-containing medium was removed and replaced with fresh medium containing HIV-1(VPX) or NL-luc R-E- full-length virus, without the inhibitor. The results showed that HIV-1 inhibition was observed only in the pLV2 THP-1 cells, while no inhibitory effect was detected in the BAF KO group (Fig. 27). This suggests that BAF may be essential for DNA-PK inhibitor-mediated suppression of HIV-1 in THP-1 cells. The lack of inhibition in the BAF KO cells indicates that BAF may play a key role in facilitating this inhibitory pathway.

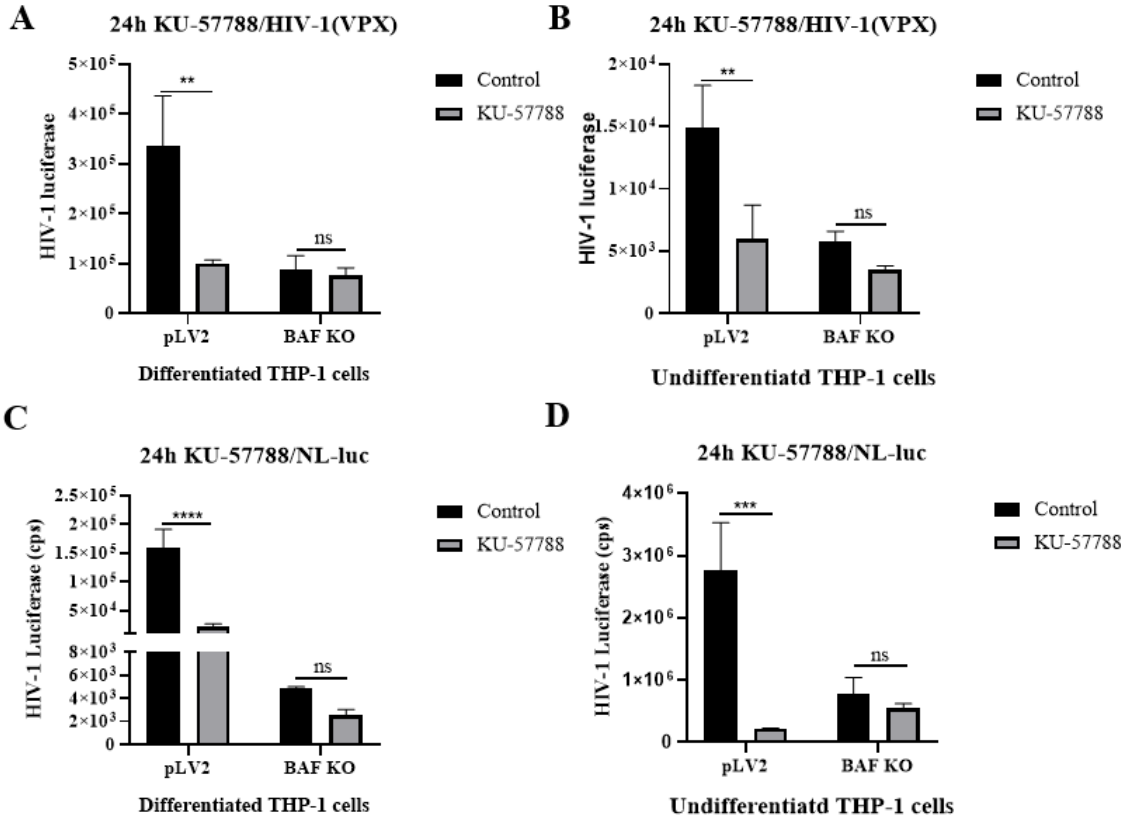

Fig. 27: DNA-PK inhibitor KU-57788 inhibits HIV-1(VPX) and NL-luc for 24h depends on BAF. (A and B) PMA-differentiated and undifferentiated pLV2 THP-1 and BAF KO THP-1 cells were treated with different concentrations of KU-57788 for 24 h and followed by HIV-1(VPX) infected within 48 h. (C and D) PMA-differentiated and undifferentiated pLV2 THP-1 and BAF KO THP-1 cells were treated with different concentrations of KU-57788 for 24 h and followed by HIV-1(NL-luc) infected within 48 h. And analyzed by luciferase activity assay. Significance was determined using two-way ANOVA (*P < 0.05, **P < 0.01, ***P < 0.001, and****P < 0.0001). Data are representative of three independent experiments (graphs show mean ±SD).

Furthermore, when measuring interferon (IFN) production, a decrease was observed in pLV2 THP-1 cells. Without any change in IFN levels in BAF KO THP-1 cells (Fig. 28).

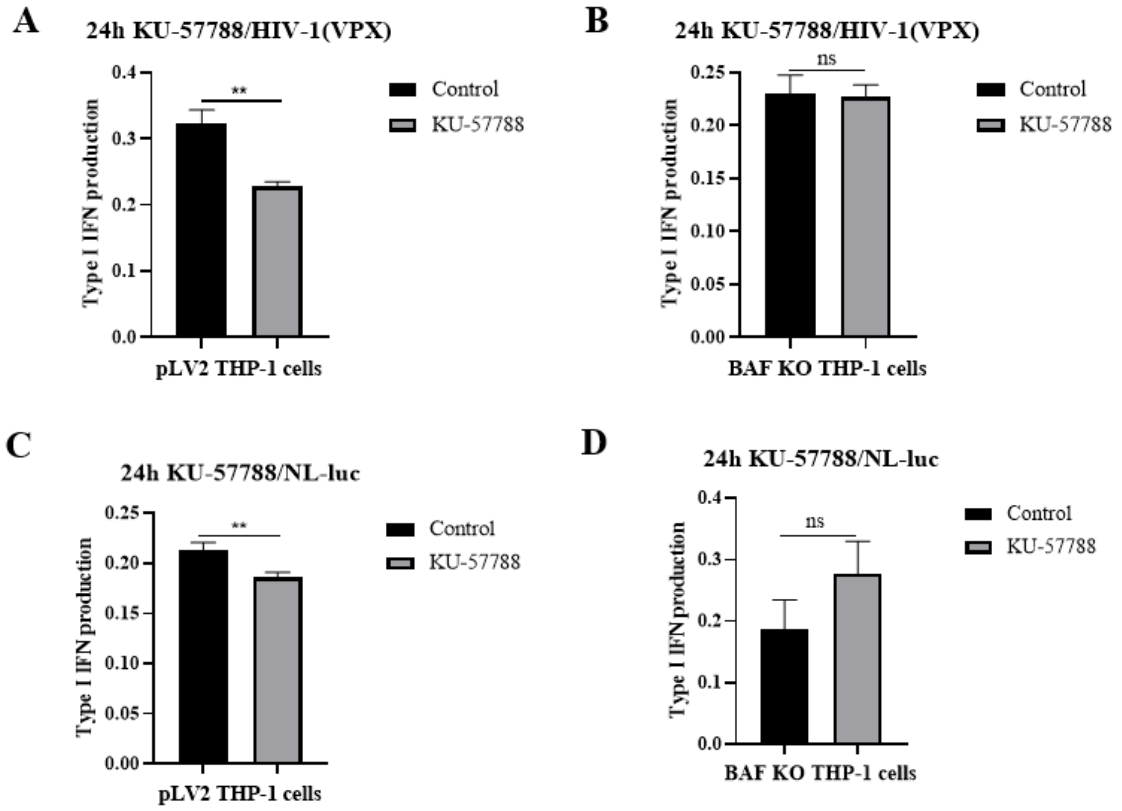

Fig. 28: After DNA-PK inhibitor KU-57788 24h treatment, interferon production was decreased in pLV2 THP-1 cells. (A) After analyzing the luciferase activity assay, I measured the interferon production assay in pLV2 THP-1 cells infected with HIV-1(VPX). (B) After analyzing the luciferase activity assay, I measured the interferon production assay in BAF KO THP-1 cells infected with HIV-1(VPX). (C) After analyzing the luciferase activity assay, I measured the interferon production assay in pLV2 THP-1 cells infected with NL-luc. (B) After analyzing the luciferase activity assay, I measured the interferon production assay in BAF KO THP-1 cells infected with NL-luc. Significance was determined using a two-tailed Student's t-test (*P < 0.05, **P < 0.01, ***P < 0.001, and ****P < 0.0001). Data are representative of three independent experiments (graphs show mean ±SD).

3.7.3 DNK-PK inhibitor: KU-57788 with 24h treatment of STING KO cells

Both differentiated and undifferentiated STING knockout (KO) THP-1 cells were treated with a DNA-PK inhibitor for 24 hours. The results showed that the DNA-PK inhibitor did not exhibit any inhibitory effect on HIV-1 in the STING KO THP-1 cells (Fig. 29).

This lack of response suggests that STING may be required for the DNA-PK inhibitor's suppressive action on HIV-1, highlighting a potential role for STING in mediating or enhancing this inhibitory pathway.

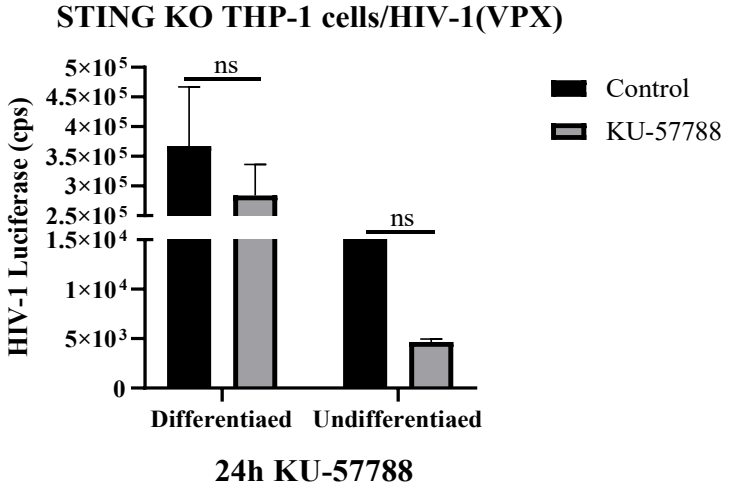

Fig. 29: DNA-PK inhibitor KU-57788 has no inhibition of HIV-1(VPX) in STING KO THP-1. PMA-differentiated and undifferentiated STING KO THP-1 cells were treated with KU-57788 for 24 h and followed by HIV-1(VPX) infection within 48 h. And analyzed by luciferase activity assay. Significance was determined using two-way ANOVA (*P < 0.05, **P < 0.01, ***P < 0.001, and****P < 0.0001). Data are representative of three independent experiments (graphs show mean ±SD).

3.8 The absence of BAF on MLV infection

After investigation of the effects of knocking out the BAF on the infection rates of HIV-1, I wanted to test infections of an unrelated other retrovirus, the Murine Leukemia Virus (MLV) in BAF KO cells. Infection experiments were performed using undifferentiated THP-1 cells. MLV was generated by co-transfecting three plasmids. pMP71 (encoding the MLV genome), pHIT60 (providing the gag-pol proteins), and VSVG (encoding the vesicular stomatitis virus G envelope protein for pseudotyping) into HEK293T cells. The resulting pseudotyped MLV particles were collected from the supernatant and used for infection experiments. HIV-1-based viruses were produced using a three-plasmid system. Virus-containing supernatants were harvested and used to infect THP-1 cells. HIV

infection was done in parallel to the MLV infections (Fig. 30A). As shown above, after knocking out BAF, HIV-1 infection was significantly inhibited (Fig. 30A). In contrast, MLV infection showed an increase following BAF KO (Fig. 30A).

To confirm that the measured luciferase activity was specific to viral infection, medium-only controls were included in a separate experiment (Fig. 30B). Both undifferentiated pLV2 control and BAF KO THP-1 cells showed negligible luciferase signals in the absence of virus, confirming the specificity of MLV-derived luciferase activity.

This may indicate that MLV's integration process is less dependent on BAF, or other cellular factors might compensate for the absence of BAF, facilitating MLV integration and replication. Additionally, the loss of BAF might alter chromatin structure to favor MLV access to the host genome. These results highlight the distinct roles that BAF plays in the life cycles of HIV-1 and MLV. The differential impact suggests that HIV-1 relies on BAF for infection, and its absence disrupts some steps in this process. MLV either does not depend on BAF or benefits from changes in the cellular environment caused by BAF KO, leading to enhanced replication.

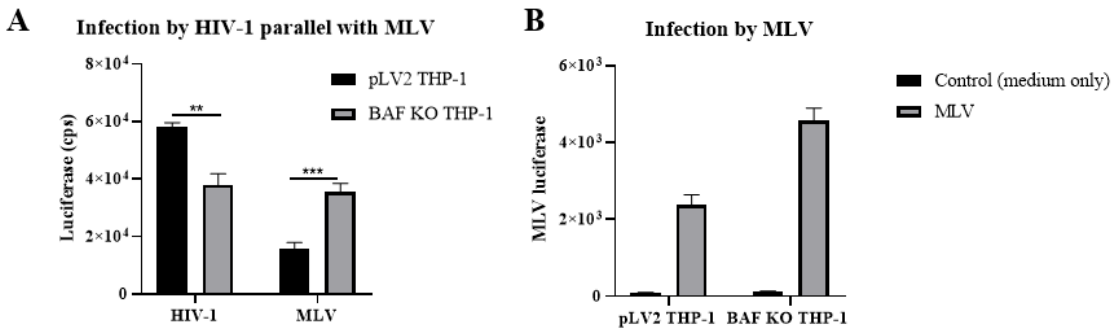

Fig. 30: In the absence of BAF, decreased HIV-1 but increased MLV. (A) pLV2 THP-1 and BAF KO THP-1 cells were infected with HIV-1 paralleled with MLV within 48 h. (B) pLV2 THP-1 and BAF KO THP-1 cells were infected with MLV within 48 h, and analyzed by luciferase activity assay. Significance was determined using a two-tailed Student's t-test (*P < 0.05, **P < 0.01, ***P < 0.001, and ****P < 0.0001). Data are representative of three independent experiments (graphs show mean ±SD).

3.9 BAF phosphorylation

3.9.1 VRK1 inhibitor: Luteolin

3.9.1.1 Luteolin short-term (4 h) effects on HIV-1 replication.

Luteolin is described to be an inhibitor of VRK1, the kinase that phosphorylates BAF[232–234]. To investigate the effect of luteolin on HIV-1 replication, Both undifferentiated and differentiated pLV2 THP-1 cells, as well as BAF KO THP-1 cells, were preincubated with luteolin for 4 hours. After this preincubation, the inhibitor-containing medium was removed and replaced with fresh medium containing HIV-1(VPX) or NL-luc R-E- full-length virus, without the inhibitor.

In the first experiment, short-term treatment with luteolin produced differential effects on HIV-1 replication depending on the cell differentiation state and BAF status (Fig. 31). In differentiated THP-1 cells, luteolin significantly reduced HIV-1(VPX) luciferase expression in control (pLV2) cells ($p < 0.01$, Fig. 31A), but had no significant effect in BAF KO cells. However, luteolin did not significantly alter luciferase expression in cells infected with NL-luc R-E- full-length virus, regardless of BAF status (Fig. 31B). In undifferentiated THP-1 cells, luteolin had no significant effect on HIV-1(VPX) replication in either pLV2 or BAF KO cells (Fig. 31C), while it significantly reduced NL-luc R-E- full-length expression in pLV2 cells ($p < 0.01$) but not in BAF KO cells (Fig. 31D). These findings suggest that luteolin can inhibit HIV-1 replication in a BAF-dependent manner, particularly in differentiated cells, although this effect is context-dependent and not consistent across different viral constructs or cell states. The variability in short-term responses may reflect complex regulatory mechanisms involving VRK1 and BAF, where immediate phosphorylation changes may not directly or uniformly impact HIV-1 replication dynamics.

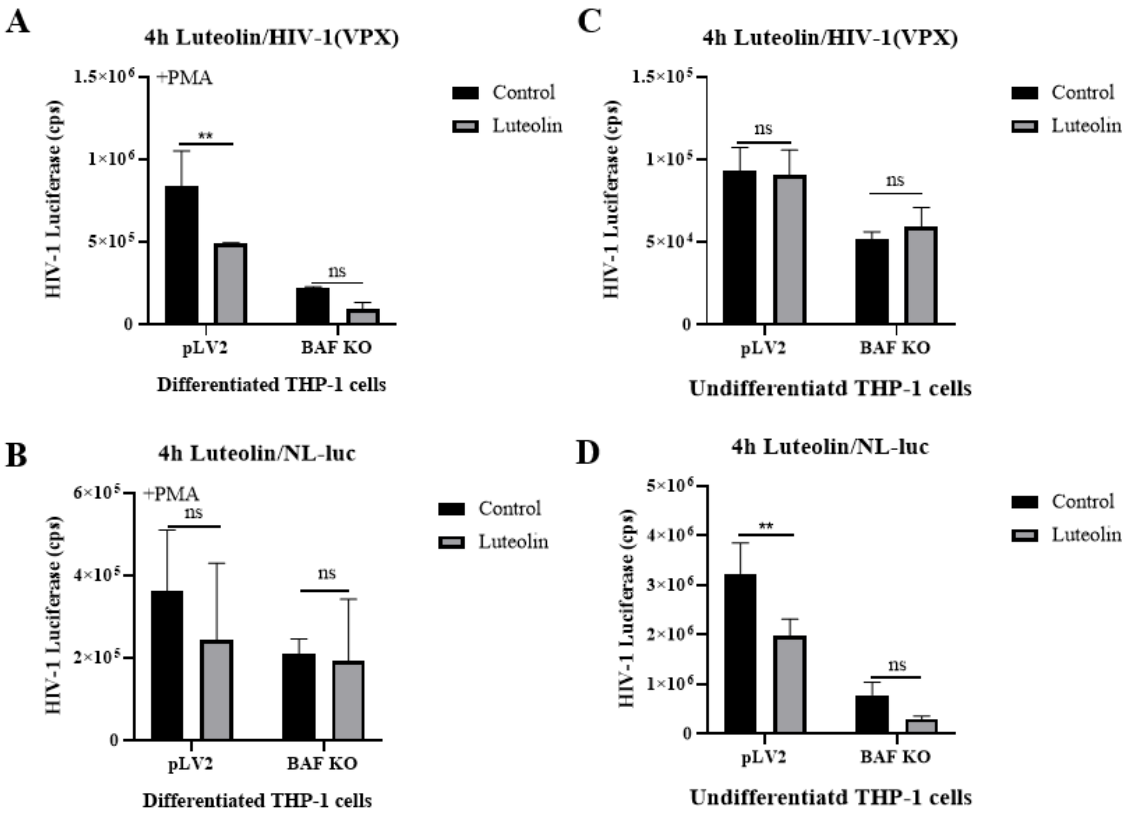

Fig. 31: Short-term effects of luteolin on HIV-1 replication. (A and B) Differentiated and undifferentiated pLV2 THP-1 and BAF KO THP-1 were treated with luteolin for 4 h and then infected with HIV-1(VPX) within 48 h, and analyzed by luciferase activity assay. (C and D) Differentiated and undifferentiated pLV2 THP-1 and BAF KO THP-1 were treated with luteolin for 4 h, infected with NL-luc R-E- full-length within 48 h, and analyzed by luciferase activity assay. Significance was determined using two-way ANOVA (*P < 0.05, **P < 0.01, ***P < 0.001, and****P < 0.0001). Data are representative of three independent experiments (graphs show mean ±SD).

3.9.1.2 Luteolin long-term (24 h) effects on HIV-1 replication

In a second assay, the cells were treated for 24 hours with Luteolin. After 24 hours of luteolin treatment, significant inhibition of HIV-1 replication was consistently observed in pLV2 THP-1 cells but not in BAF KO THP-1 (Fig. 32). The inconsistency in short-term treatments maybe caused by the complexity of immediate phosphorylation events, while the significant reduction in HIV-1 levels at 24 hours suggests that prolonged VRK1

inhibition effectively disrupts critical pathways necessary for HIV-1 replication. These findings underscore the potential of luteolin as a therapeutic agent in targeting HIV-1, especially in strategies aimed at modulating VRK1 and BAF interactions. Importantly, the anti-HIV-1 activity of luteolin depends on the presence of BAF.

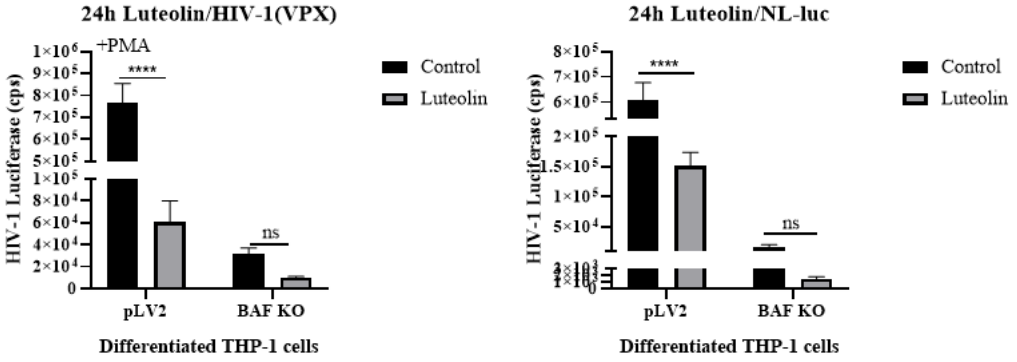

Fig. 32: Long-term effects of luteolin on HIV-1 replication. pLV2 THP-1 and BAF KO THP-1 were treated with luteolin for 24 h and then infected with HIV-1(VPX) or NL-luc within 48 h, and analyzed by luciferase activity assay. Significance was determined using two-way ANOVA (*P < 0.05, **P < 0.01, ***P < 0.001, and **** P < 0.0001). Data are representative of three independent experiments (graphs show mean ±SD).

3.9.1.3 Luteolin enhances type I IFN production in BAF KO compared to pLV2 THP-1 cells upon HIV-1 infection

Since I observed that luteolin can inhibit HIV-1 replication in pLV2 THP-1 cells, I conducted additional tests to assess interferon (IFN) production to determine whether this inhibitory effect is associated with IFN response (Fig. 33). I assessed IFN production using the HEK-Blue IFN-α/β reporter assay. Differentiated pLV2 or BAF KO THP-1 cells were preincubated with luteolin for 4 hours (Fig. 33A) or 24 hours (Fig. 33B). After this preincubation, the inhibitor-containing medium was removed and replaced with fresh medium containing HIV-1(VPX) virus, without the inhibitor. Supernatants were collected and applied to HEK-Blue cells to quantify secreted type I IFNs.

As shown in Fig. 33A, at 4 hours post-treatment, HIV-1 infection alone did not

significantly alter type I IFN production in BAF KO THP-1 compared to pLV2 cells. However, in the presence of luteolin, a significant increase in IFN production was observed in BAF KO cells compared to pLV2 cells. At 24 hours (Fig. 33B), IFN production showed the same trend as 4 hours post-treatment.

These results suggest that luteolin treatment reduced HIV-1 replication in pLV2 THP-1 cells but had no inhibitory effect in BAF KO cells, suggesting that BAF is required for luteolin's antiviral activity. While HIV-1 infection alone did not significantly alter type I IFN production in BAF KO cells compared to pLV2 cells, luteolin treatment led to a markedly higher IFN response in BAF KO cells than in pLV2 cells at both 4 and 24 hours post-treatment.

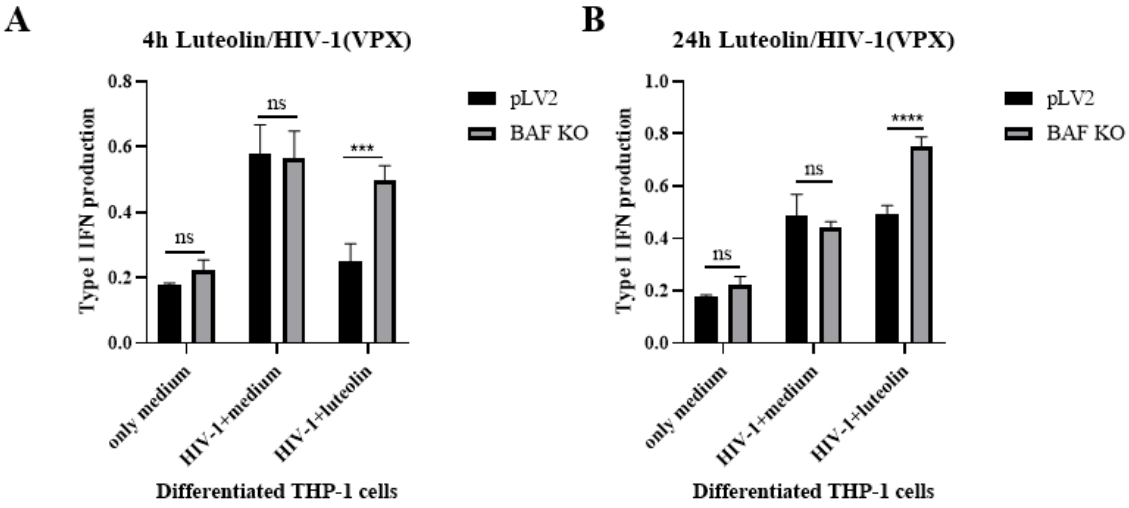

Fig. 33: BAF deficiency enhances luteolin-mediated IFN response in HIV-1-infected THP-1 cells. Differentiated pLV2 or BAF KO THP-1 cells were infected with HIV-1 (VPX) in the presence or absence of luteolin. After analyzing the luciferase activity assay, supernatants were collected at (A) 4 hours and (B) 24 hours post-infection and analyzed for type I IFN production using HEK-Blue IFN-α/β reporter cells. Significance was determined using a two-way ANOVA (*P < 0.05, **P < 0.01, ***P < 0.001, and ****P < 0.0001). Data are representative of three independent experiments (graphs show mean ±SD).

3.9.1.3 Luteolin on BlaER1 cells of HIV-1 replication

BlaER1 cells are a B cell line that can be transdifferentiated into macrophage-like cells. I differentiated the BlaER1 cells and used them to study the effect of luteolin in the early

phase of HIV-1 infection. I used the HIV-1(VPX) virus. Luteolin was given to cells for 24 hours and then replaced with media containing the virus. The virus transferred luciferase expression was measured 48 hours post-infection. Results show that luteolin significantly inhibited HIV-1 infection in BlaER1 cells in a dose-dependent manner (Fig. 34).

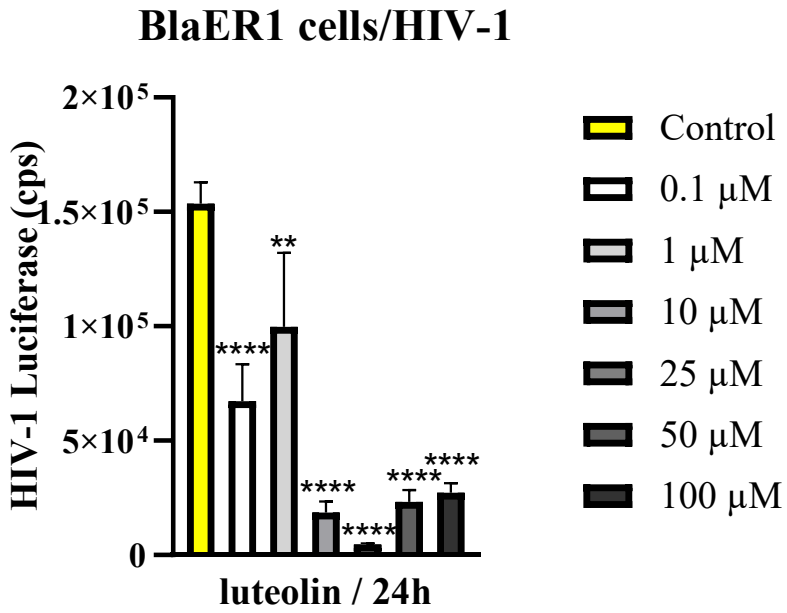

Fig. 34: Luteolin decreased HIV-1 replication in BlaER1. BlaER1 macrophage-like cells were treated with luteolin for 24 h and then infected with HIV-1 within 48 h, and analyzed by luciferase activity assay. Significance was determined using one-way ANOVA (*P < 0.05, **P < 0.01, ***P < 0.001, and **** P < 0.0001). Data are representative of three independent experiments (graphs show mean ±SD).

3.10 NF-κB inhibitor: CAPE

Caffeic acid phenethyl ester (CAPE) is an NF-κB inhibitor[76,235]. NF-κB is activated by several cellular pathways and also downstream of the cGAS-STING cascade[236]. Once STING is activated, it triggers two major pathways. The Interferon Regulatory Factor 3 (IRF3) pathway produces type I interferons, which are crucial for antiviral

defense[237,238]. The NF-κB pathway drives the production of pro-inflammatory cytokines (e.g., IL-6, TNF-α) that are essential for the immune response[237,239]. An NF-κB signaling pathway is involved in the transcription of HIV-1, which can be exploited for HIV-1 cure studies[240].

Our study explored the effects of Caffeic Acid Phenethyl Ester (CAPE) on HIV-1 replication in both pLV2 THP-1 and BAF KO THP-1 cells across multiple time points (Fig. 35 and Fig. 36). Differentiated or undifferentiated pLV2 or BAF KO THP-1 cells were preincubated with CAPE for 4 hours (Fig. 35) or 24 hours (Fig. 36). After this preincubation, the inhibitor-containing medium was removed and replaced with fresh medium containing HIV-1(VPX) or NL-luc R-E- full-length virus, without the inhibitor. HIV replication was measured via luciferase activity after 48 hours post-infection. Supernatants were collected and applied to HEK-Blue cells to quantify secreted type I IFNs (Fig. 37).

In differentiated THP-1 cells infected with HIV-1(VPX), after 4 hours of CAPE treatment, significantly reduced luciferase activity in both pLV2 and BAF KO cells (Fig. 35A). In undifferentiated THP-1 cells, CAPE also significantly suppressed HIV-1(VPX) replication in both cell types (Fig. 35B). Similar inhibitory effects of CAPE were observed when differentiated cells were infected with NL-luc R-E- full-length virus, confirming the antiviral activity of CAPE in both pLV2 and BAF KO cells (Fig. 35C). These data suggest that CAPE effectively inhibits HIV-1 replication in THP-1 cells regardless of BAF expression.

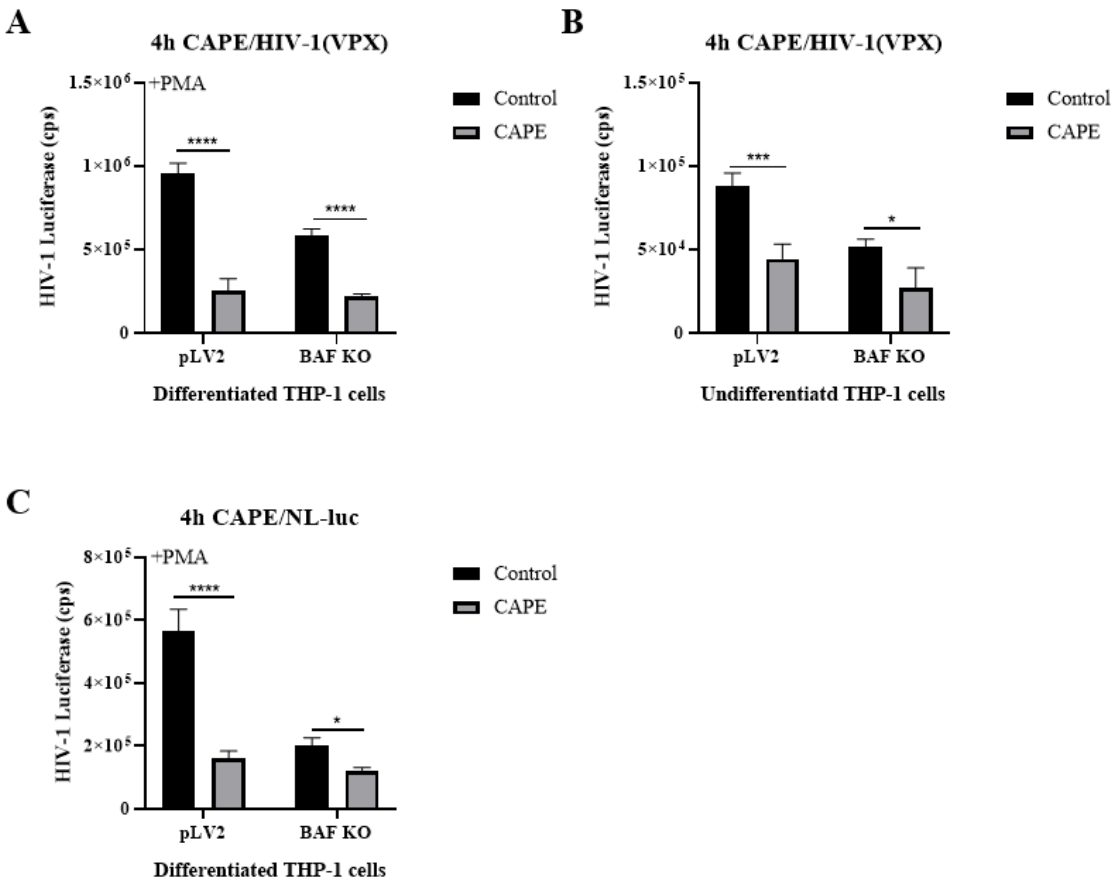

Fig. 35: Four-hour CAPE treatment inhibits HIV-1 in a BAF-independent manner. Differentiated and undifferentiated pLV2 and BAF KO THP-1 cells were treated with CAPE for four hours and then infected with HIV-1(VPX) or NL-luc full-length virus within 48 h. And analyzed by luciferase activity assay. Significance was determined using two-way ANOVA (*P < 0.05, **P < 0.01, ***P < 0.001, and****P < 0.0001). Data are representative of three independent experiments (graphs show mean ±SD).

As shown in Figure 36A, CAPE treatment significantly reduced HIV-1(VPX)-mediated luciferase activity in pLV2 cells, indicating a strong inhibitory effect. In contrast, the BAF KO cells are less susceptible than the pLV2 cells to CAPE on HIV-1(VPX) replication, suggesting that the presence of the BAF is necessary for CAPE-mediated inhibition for 24h treatment (Fig. 36A). Similarly, in Figure B, CAPE treatment significantly suppressed NL-luc R-E- full-length virus replication in pLV2 cells, but this inhibitory effect was abolished in BAF KO cells (Fig. 36B). These results demonstrate that the antiviral effect of 24h treatment CAPE against HIV-1 is dependent on the BAF,

implicating BAF as a potential mediator of NF-κB–regulated antiviral responses.

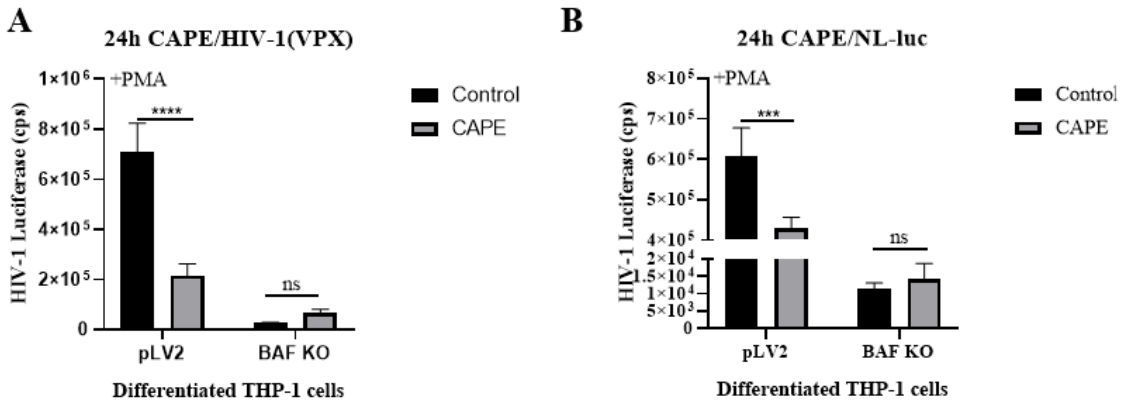

Fig. 36: 24-hour CAPE treatment inhibits HIV-1 in a BAF-dependent manner. pLV2 and BAF KO THP-1 cells were treated with pyrimethamine for 24h and then infected with HIV-1(VPX) or NL-luc R-E- full-length virus within 48 h, and analyzed by luciferase activity assay. Significance was determined using two-way ANOVA (*P < 0.05, **P < 0.01, ***P < 0.001, and****P < 0.0001). Data are representative of three independent experiments (graphs show mean ±SD).

To assess whether CAPE modulates type I interferon (IFN) production following HIV-1 infection, I measured secreted IFN activity in the supernatants of PMA-differentiated THP-1 cells using the HEK-Blue IFN-α/β reporter assay. Cells were treated with CAPE or only medium as a control and infected with HIV-1(VPX) as previously described. Following luciferase measurements, and used to stimulate HEK-Blue cells to detect IFN-dependent reporter activity. CAPE treatment significantly reduced IFN activity in pLV2 and BAF KO cells, indicating suppression of type I IFN responses (Fig. 37). These findings support a model in which CAPE suppresses HIV-1-induced type I IFN production.

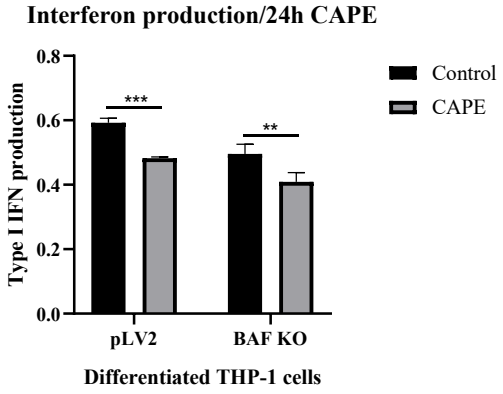

Fig. 37: IFN production reduced by CAPE treatment for 24h during HIV-1 infection. pLV2 and BAF KO THP-1 cells were treated with CAPE for 24 hours and then infected with HIV-1(VPX) within 48 hours, followed by interferon production analysis. Significance was determined using two-way ANOVA (*P < 0.05, **P < 0.01, ***P < 0.001, and****P < 0.0001). Data are representative of three independent experiments (graphs show mean ±SD).

3.11 Pyrimethamine inhibits HIV-1 dependent on BAF

Pyrimethamine (PYR) is an anti-malarial drug[241]. Co-infections of HIV and malaria are two of the leading causes of mortality and morbidity in sub-Saharan Africa and part of Asia[242–245]. Pyrimethamine is a competitive inhibitor of the dihydrofolate reductase (DHFR) enzyme, leading to a deficiency of thymidylate monophosphate (dTMP)[246], thus causing inhibition of DNA biosynthesis and cell growth. Previous reports have suggested that pyrimethamine probably enhanced the pre-transcriptional step and facilitated viral RT reaction in the accumulated S-phase[247,248]during HIV-1 replication. Given this, I hypothesized that pyrimethamine treatment could enhance HIV-1 replication by altering the host cell cycle and facilitating reverse transcription. However, the mechanistic basis for this effect remains poorly understood. Considering the widespread use of pyrimethamine in HIV-1–endemic regions, elucidating how this drug modulates HIV-1 replication could have important implications for co-infection management and may uncover novel host-dependent regulatory pathways exploitable for therapeutic intervention.

To investigate the impact of pyrimethamine on early HIV-1 replication, PMA-differentiated (Fig. 38A) and undifferentiated (Figure 38B) THP-1 cells were preincubated with pyrimethamine for 1 hour (Fig. 38) or 24 hours (Fig. 39). After this preincubation, the inhibitor-containing medium was removed and replaced with fresh medium containing HIV-1(VPX) or NL-luc R-E- full-length virus, without the inhibitor. HIV replication was measured via luciferase activity after 48 hours post-infection. Supernatants were collected and applied to HEK-Blue cells to quantify secreted type I IFNs (Fig. 40). In PMA-differentiated pLV2 cells, PYR treatment significantly reduced HIV-1 luciferase activity (Fig. 38A), indicating an inhibitory effect on early HIV-1 replication. However, this inhibitory effect was abolished in BAF KO cells, where luciferase levels remained low and unchanged by PYR treatment, suggesting that the presence of the BAF is required for PYR-mediated restriction of HIV-1. Similarly, in undifferentiated THP-1 cells (Fig. 38B), PYR treatment also significantly reduced HIV-1 luciferase activity in pLV2 cells, but again had no significant effect in BAF KO cells. These findings indicate that, contrary to previous reports suggesting a potential enhancement of HIV-1 reverse transcription by PYR, in our THP-1 cell model, PYR restricts early HIV-1 replication in a manner dependent on the BAF, possibly through modulation of chromatin remodeling or early antiviral signaling pathways.

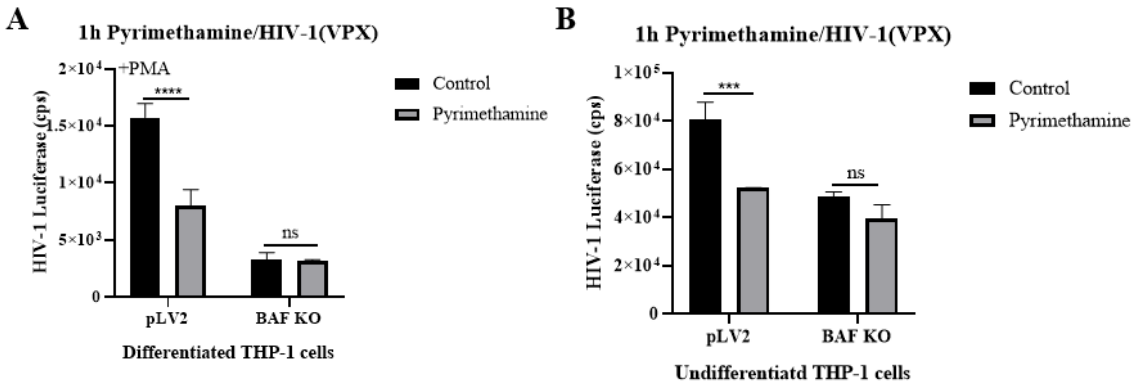

Fig. 38: One-hour pyrimethamine treatment inhibits HIV-1 in a BAF-dependent manner. (A and B) Differentiated and undifferentiated pLV2 and BAF KO THP-1 cells were treated with pyrimethamine for one hour, then infected with HIV-1(VPX) within 48 h, and analyzed by luciferase activity assay. Significance was determined using two-way ANOVA (*P < 0.05, **P <

0.01, ***P < 0.001, and****P < 0.0001). Data are representative of three independent experiments (graphs show mean ±SD).

In the second experiment, differentiated pLV2 and BAF KO THP-1 cells were preincubated with pyrimethamine for 24 hours (Fig. 39). After this preincubation, the inhibitor-containing medium was removed and replaced with fresh medium containing HIV-1(VPX) (Fig. 39A) or NL-luc R-E- full-length virus (Fig. 39B), without the inhibitor. PYR treatment significantly reduced HIV-1(VPX) luciferase activity (Fig. 39A). However, this inhibitory effect was abolished in BAF KO cells, where luciferase levels remained low and unchanged by PYR treatment, suggesting that the presence of the BAF is required for PYR-mediated restriction of HIV-1 during 24h PYR treatment. Similarly, PYR treatment also significantly reduced NL-luc R-E- full-length virus luciferase activity in pLV2 cells, but again had no significant effect in BAF KO cells (Fig. 39B). These findings indicate that PYR restricts early HIV-1 replication in a manner dependent on the BAF either with short-term (1h) (Fig. 38) or longer-term (24h) (Fig. 39) treatment.

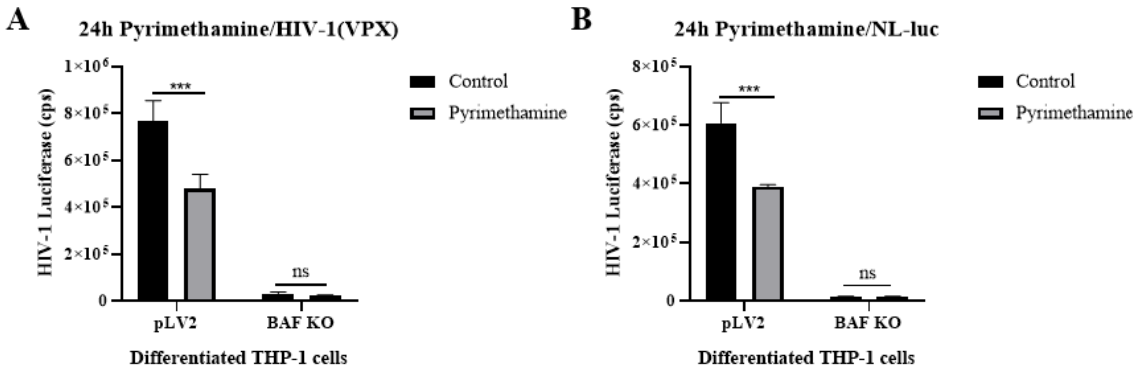

Fig. 39: 24-hour pyrimethamine treatment inhibits HIV-1 in a BAF-dependent manner. (A and B) pLV2 and BAF KO THP-1 cells were treated with pyrimethamine for 24 hours and then infected with HIV-1(VPX) or NL-luc full-length virus within 48 hours and analyzed by luciferase activity assay and followed by interferon production analysis. Significance was determined using two-way ANOVA (*P < 0.05, **P < 0.01, ***P < 0.001, and****P < 0.0001). Data are representative of three independent experiments (graphs show mean ±SD).

To assess whether PYR induces type I interferon (IFN) responses, I measured IFN activity

in the supernatants of infected cells using the HEK-Blue IFN-α/β reporter assay after 24 hours of PYR treatment and HIV-1(VPX) infection. No significant change in IFN activity was detected in either pLV2 or BAF KO cells, indicating that the observed antiviral effect of PYR is independent of type I IFN induction. Together, these findings suggest that PYR restricts HIV-1 replication through a BAF-dependent, IFN-independent mechanism.

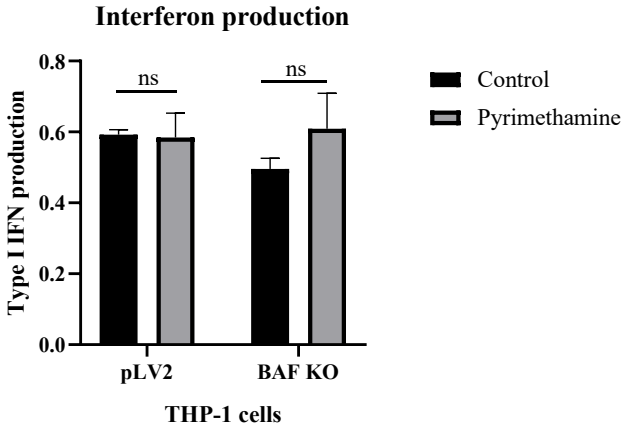

Fig. 40: IFN production unaltered by pyrimethamine treatment during HIV-1 infection. pLV2 and BAF KO THP-1 cells were treated with pyrimethamine for 24 hours and then infected with HIV-1(VPX) within 48 hours, followed by interferon production analysis. Significance was determined using two-way ANOVA (*P < 0.05, **P < 0.01, ***P < 0.001, and****P < 0.0001). Data are representative of three independent experiments (graphs show mean ±SD).

4. Discussion

4.1 Differential effects of HIV-1 construct on BAF protein levels

This study provides significant insights into the interaction between HIV-1 and BAF (Barrier to Autointegration Factor 1). BAF is a highly evolutionarily conserved DNA-binding protein inhibiting retroviral DNA autointegration, promoting retroviral DNA integration into the host chromosome[125,249,250]. BAF is recognized as a natural host co-factor for HIV-1 integration due to its role in facilitating the HIV-1 pre-integration complex (PIC)[160,251]. Previous reports suggested that BAF was expressed in all cell types[175], consistent with its proposed essential roles in cell division[175,198,252].

Consistent with our findings, Western blotting results revealed that HIV-1 infection reduces endogenous BAF protein levels in HEK293T cells when transfected with the 3-plasmid HIV-1 system. In contrast, transfection with full-length pNL-Bal full-length HIV-1 did not lead to any observable change in BAF protein levels.

4.2 BAF incorporation into HIV-1 virions under overexpression conditions

Although previous reports suggested that BAF is excluded from MoMLV[126] and HIV-1[124] particles, my data challenge the previous assumption that when BAF is overexpressed in virus-producing HEK293T cells, BAF can be detected in the HIV-1 virions. This suggests that BAF may be incorporated into HIV-1 under overexpression conditions. Unlike other host restriction factors that may be incorporated into the virion to affect viral infectivity, BAF appears to have a primarily cell-autonomous function. However, its potential low-level presence in viral particles under overexpression conditions warrants further investigation.

4.3 BAF is essential in target cells for efficient HIV-1 replication

Furthermore, even though BAF can be detected in the supernatant, the absence of BAF in virus-producing cells does not affect the virus's infectivity. However, the depletion of BAF in target cells reduces HIV-1 replication. I utilized four distinct THP-1 cell groups. Knockout of BAF significantly reduced HIV-1 infection compared to pLV2 THP-1 cells. The reintroduction of BAF partially restored infection levels. These results are consistent with previous studies suggesting that BAF plays a critical role in maintaining viral genomic integrity by preventing autointegration of retroviral DNA [124,138,178,239]. The finding that BAF does not affect viral infectivity in producer cells further emphasizes its role in the post-entry phase of target cells, where its loss appears to limit HIV-1 replication.

4.4 BAF as a negative regulator of cGAS–STING pathway activation

The cGAS–STING signaling axis, comprising the synthase for the second messenger cyclic GMP–AMP (cGAS) and the cyclic GMP–AMP receptor stimulator of interferon genes (STING), detects pathogenic DNA to trigger an innate immune reaction involving a potent type I interferon response against microbial infections[90]. Type I interferons impede viral propagation[253–255]. The knockout of BAF led to the upregulation of ISG15 and USP18, while APOBEC3A (A3A) protein levels were downregulated. Upon stimulation with SR-717, a STING agonist, similar patterns were observed, with further upregulation of ISG15 and USP18 and a continued decrease in A3A levels. These findings contribute to the growing evidence suggesting that BAF is crucial in regulating the innate immune response. The upregulation of ISG15 and USP18 in the absence of BAF suggests that BAF may generally act as a negative regulator of these pathways. This is consistent with previous studies that have implicated BAF protects against a basal cGAS-STING response[72]. BAF might suppress these pathways under normal conditions, potentially as a means of preventing excessive immune activation. The further increase in these proteins following SR-717 stimulation suggests that the STING pathway remains responsive even in the absence of BAF but is modulated differently when BAF is absent. Mechanistically, upregulated A3A exacerbates cytosolic double-stranded DNA (dsDNA) accumulation, thus stimulating the cGAS-STING pathway[256]. The decrease in A3A might be a specific regulatory mechanism to avoid excessive DNA damage or mutations, which could be detrimental under heightened immune activation conditions.

4.5 BAF knockout differentially affects type I IFN induction and ISG expression

I investigated the impact of BAF knockout on the innate immune response in THP-1 cells, focusing on type I interferons (IFNs) and interferon-stimulated genes (ISGs) following stimulation with HIV-1, MVA, Sendai virus, SR-717, and HS-DNA. Surprisingly, BAF knockout did not significantly alter type I IFN expression compared to control pLV2 THP-1 cells in response to these stimuli, suggesting that BAF is not essential for the initial activation of type I IFN pathways, or that compensatory mechanisms might mask its loss.

However, a marked upregulation of *ISG15* and *ISG54* was observed in BAF KO cells compared to pLV2 THP-1 cells. Although both are interferon-stimulated genes, their regulation differs from *IFN-β*. *IFN-β* is an early response cytokine rapidly induced upon sensing cytosolic DNA or RNA, initiating the antiviral response[257,258]. In contrast, *ISG15* and *ISG54* are downstream ISGs whose expression is driven by IFN-β signaling via the JAK-STAT pathway[259–262]. ISG15 encodes a ubiquitin-like protein involved in ISGylation, modulating protein stability and antiviral signaling, while ISG54 inhibits viral replication by suppressing translation of viral RNA. Both are typically considered early to intermediate ISGs, activated soon after IFN signaling begins, but their sustained expression may be influenced by additional regulatory layers, including mRNA stability, chromatin accessibility, or repressor release, potentially modulated by BAF. Thus, the elevation of ISG15 and ISG54 without a corresponding increase in IFN-β suggests that BAF may regulate ISG expression independently or downstream of IFN production, possibly at the transcriptional or post-transcriptional level.

In summary, while BAF appears dispensable for the initial induction of IFN-β, it plays a role in fine-tuning ISG expression, particularly ISG15 and ISG54. These findings point to a broader immunoregulatory function of BAF beyond its known role in viral DNA integration. Further research should focus on dissecting how BAF modulates ISG transcription or stability and whether this impacts antiviral outcomes.

4.6 BAF differentially regulates HIV-1 and MLV replication

My results showed that BAF knockout reduced HIV-1 replication but significantly increased MLV (Murine Leukemia Virus) replication in THP-1 cells. There is limited literature addressing the relationship between MLV and BAF. However, despite both MLV and HIV-1 being retroviruses, they belong to different classes; HIV-1 is a lentivirus, while MLV is a *γ*-retrovirus[263,264]. These significant differences may account for the distinct ways these viruses[263,264]interact with host cellular factors like BAF. MLV integrations were equally distributed inside (49.4%) and outside (50.6%) genes, whereas 75.7% of the HIV-1 integrations were within genes[265]. Whereas MLV integration sites

clustered around transcription start sites, HIV-1 insertions were significantly reduced in the same region and equally distributed to the other areas of the targeted genes[266]. HIV-1 did not share the preference of MLV for regulatory elements. Although similarly clustered, HIV-1 integrations avoid promoters and regulatory elements and prefer transcribed regions marked by H3K36me3 and H2BK5me1 instead. These differences have interesting implications in terms of viral evolution. γ-Retroviruses may have evolved a mechanism coupling target site selection to gene regulation to activate or maintain their proviral expression[265,266]. Fine mapping of MLV sites around the TSS of > 8000 genes showed a bimodal distribution. There were virtually no insertions in the -38 to +34 region, where the general transcription factors contact the core promoter and recruit Pol II[267]. In particular, no integration was detected in the -35 to -25 and +5 to +10 regions, corresponding to the TATA box and the first component of the tripartite downstream core promoter element. This indicates that basal transcription factors, most likely TFIID, occupy the promoter of all targeted genes, making it physically inaccessible to retroviral PICs[265]. Furthermore, the increase in MLV replication may indicate that BAF may affect other stages of the retroviral life cycle, such as reverse transcription or nuclear import of viral DNA. The exact mechanism by which BAF exerts its inhibitory effects on MLV and potentially other retroviruses remains to be fully elucidated.

4.7 Time-dependent effects of DNA-PK inhibition on HIV-1 infection and IFN responses

There is a complex relationship between BAF, DNA-PK, and cGAS-STING. BAF can inhibit DNA-PK[207]. DNA-PK phosphorylates cGAS and suppresses its enzymatic activity[210]. DNA-PK deficiency reduces cGAS phosphorylation and promotes antiviral innate immune responses, thereby potently restricting viral replication[120,210,268,269]. Although previous studies have demonstrated the therapeutic potential of KU-57788 in enhancing cancer treatment efficacy[270,271], such as improving survival in glioblastoma models through DNA-PK inhibition[270], no prior research has reported its

use in suppressing HIV replication. My study provides novel evidence that KU-57788 activates antiviral innate immune responses and restricts HIV-1 infection, revealing a previously unrecognized role for this inhibitor in the context of retroviral immunity. My study investigated the impact of the DNA-PK inhibitor KU-57788 on HIV infection and associated interferon (IFN) production. These findings reveal the relationship between DNA-PK signaling, HIV-1 replication, and innate immune responses. Short-term treatment with KU-57788 (4 hours) significantly decreased HIV-1 infection in both pLV2 THP-1 cells and BAF KO THP-1 cells. This effect was accompanied by a concurrent increase in IFN production in both cell lines. These results suggest that DNA-PK plays a pivotal role in facilitating HIV-1 infection, and its inhibition activates innate immune signaling, potentially enhancing antiviral responses. The observed elevation in IFN production aligns with previous reports linking DNA-PK inhibition to the activation of IFN-stimulatory DNA pathways or other innate immune sensors (e.g., cGAS-STING). Importantly, this increase in IFN production occurred independently of BAF, highlighting a broader mechanism of action that is not solely reliant on the BAF-mediated restriction pathway.

In contrast, the long-term treatment (24 hours) with KU-57788 demonstrated differential effects based on the presence of BAF. While HIV-1 infection was significantly decreased in pLV2 THP-1 cells following prolonged exposure to the inhibitor, this reduction was not observed in BAF KO THP-1 cells. This finding indicates that the long-term antiviral effect of KU-57788 is BAF-dependent, implicating a potential crosstalk between DNA-PK inhibition and the BAF-mediated restriction pathway in the context of prolonged inhibition. Interestingly, IFN production showed an opposite trend, decreasing after long-term treatment in pLV2 THP-1 cells, while remaining unaffected in BAF KO THP-1 cells. This suggests that the sustained IFN response elicited by short-term DNA-PK inhibition may be transient or subject to negative feedback regulation, possibly mediated by DNA-PK-independent pathways or cellular homeostatic mechanisms.

Taken together, my results highlight the dual role of DNA-PK in regulating HIV-1 replication and modulating innate immune responses. The short-term effects appear to reflect the direct inhibition of DNA-PK's pro-viral functions and subsequent activation of

IFN signaling. In contrast, the long-term effects reveal a more complex interplay involving BAF-dependent restriction of HIV and temporal modulation of the IFN response. These findings underscore the importance of considering treatment duration and cellular context when evaluating the therapeutic potential of DNA-PK inhibitors. Future studies should further dissect the molecular mechanisms underpinning the differential effects of short- and long-term DNA-PK inhibition, focusing on the downstream pathways that govern IFN production and BAF-mediated restriction. Additionally, the potential for negative feedback mechanisms or compensatory pathways to dampen the antiviral and immunostimulatory effects of DNA-PK inhibition over time warrants further investigation. Elucidating these pathways may aid in the optimization of therapeutic strategies targeting DNA-PK for HIV-1 and other viral infections.

4.8 BAF as a mediator of luteolin's antiviral activity against HIV-1 via VRK1 inhibition

BAF can bind DNA, thereby facilitating HIV-1 replication[160,175,180]. However, when BAF is phosphorylated by the kinase VRK1, its DNA-binding capacity is inhibited. Luteolin functions as an inhibitor of VRK1[272]. Luteolin has demonstrated antiviral activity against a range of viruses, including PEDV, PRV, hPIV-2, HSV-1, and HBV[273–278], through mechanisms such as inhibiting viral replication and modulating host immune responses. However, its effects on HIV-1 remain unclear. I investigated the effects of luteolin on HIV-1 infection and innate immune responses, focusing on the role of BAF and IFN production.

My findings demonstrate that luteolin treatment selectively decreases HIV-1 infection in pLV2 THP-1 cells, but this effect is absent in BAF KO THP-1 cells. Moreover, luteolin treatment did not alter IFN production in pLV2 THP-1 or BAF KO THP-1 cells, suggesting that its antiviral activity is independent of innate immune activation. Without BAF, the VRK1 inhibition induced by luteolin does not impact HIV-1 replication, further confirming that the antiviral activity of luteolin is mediated through BAF-dependent mechanisms. My findings highlight the specificity of luteolin as a VRK1 inhibitor and its

capacity to modulate BAF activity, providing a novel avenue for restricting HIV-1 replication. These results further emphasize the importance of BAF as a key restriction factor.

4.9 BAF-dependent modulation of CAPE's antiviral efficacy against HIV-1 over time

NF-κB plays a pivotal role in regulating IFN production, while IFN, in turn, can modulate NF-κB activity through feedback mechanisms[236,279,280]. Both factors are intricately involved in multiple aspects of immune regulation and are essential components of antiviral immunity and inflammatory responses[281]. Caffeic acid phenethyl ester (CAPE) is an NF-κB inhibitor[282]. CAPE exhibits broad antiviral activity against viruses including SARS-CoV-2, PRRSV, FCV, and HIV-1[283–288]. Previous studies have shown that CAPE selectively inhibits HIV-1 integrase activity, indicating a direct mechanism of action against viral replication. Previous findings support CAPE's potential as a natural antiviral compound with relevance to HIV-1 infection. My study integrates the roles of BAF and the NF-κB inhibitor CAPE in the context of HIV-1 infection, with a particular focus on the temporal dynamics of antiviral responses across different treatment durations.

My study demonstrates that 4 hours of CAPE (Caffeic Acid Phenethyl Ester) treatment effectively inhibits HIV-1 replication and decreases IFN (Interferon) production in both of pLV2 and BAF KO THP-1 cells. This indicates that CAPE has a significant antiviral effect. Interestingly, a different trend was observed when CAPE was administered for longer durations of 24 hours. The antiviral efficacy of CAPE was notably reduced in BAF knockout cells after 24 hours of treatment. This suggests that the absence of BAF alters the cellular response to CAPE. Under these conditions, CAPE retained its ability to inhibit HIV-1 replication in pLV2 cells. This temporal effect implies that the initial stages of CAPE interaction with cellular targets are still effective in the absence of BAF. Still, longer exposure times may lead to compensatory mechanisms or the depletion of factors necessary for CAPE's antiviral activity.

4.10 Pyrimethamine suppresses HIV-1 replication via a BAF-dependent mechanism

Previous studies have shown that pyrimethamine, used as an antimalarial and antiparasitic agent, also exhibits inhibitory effects against HIV-1, particularly through mechanisms involving immune modulation and potential synergy with antiretroviral drugs[289–292]. However, these studies have largely focused on its effects in combination therapies or its indirect immunological roles. My findings provide direct evidence that pyrimethamine alone effectively suppresses HIV-1 replication in pLV2 THP-1 cells at both early (1 hour) and late (24 hours) time points post-treatment. This temporal analysis reveals the compound's rapid and sustained antiviral activity, offering novel insights into its potential as a direct-acting antiviral agent against HIV-1. However, this inhibitory effect was not observed in BAF KO THP-1 cells. This suggests that the mechanism by which pyrimethamine inhibits HIV-1 replication is likely dependent on the presence of BAF. BAF may be required to activate or stabilize antiviral pathways triggered by pyrimethamine, and its absence might impair these pathways, leading to the loss of pyrimethamine efficacy.

In conclusion, my study identifies BAF as a key factor in HIV-1 replication and immune regulation and highlights the potential of Luteolin, CAPE, and pyrimethamine as therapeutic agents against HIV-1. The differential effects of these compounds in BAF KO cells underscore the complexity of their mechanisms of action and suggest potential avenues for combination therapies that target multiple stages of the HIV-1 life cycle.

1 Freed EO. **HIV-1 Replication**. *Somat Cell Mol Genet* 2001; **26**:13–33.

2 Barré-Sinoussi F, Ross AL, Delfraissy J-F. **Past, present and future: 30 years of HIV research**. *Nat Rev Microbiol* 2013; **11**:877–883.

3 Frankel AD, Young JAT. **HIV-1: Fifteen Proteins and an RNA**. *Annual Review of Biochemistry* 1998; **67**:1–25.

4 Smyth RP, Davenport MP, Mak J. **The origin of genetic diversity in HIV-1**. *Virus Research* 2012; **169**:415–429.

5 Burdick RC, Li C, Munshi M, Rawson JMO, Nagashima K, Hu W-S, *et al.* **HIV-1 uncoats in the nucleus near sites of integration**. *Proceedings of the National Academy of Sciences* 2020; **117**:5486–5493.

6 Li C, Burdick RC, Nagashima K, Hu W-S, Pathak VK. **HIV-1 cores retain their integrity until minutes before uncoating in the nucleus**. *Proceedings of the National Academy of Sciences* 2021; **118**:e2019467118.

7 Dharan A, Bachmann N, Talley S, Zwikelmaier V, Campbell EM. **Nuclear pore blockade reveals that HIV-1 completes reverse transcription and uncoating in the nucleus**. *Nat Microbiol* 2020; **5**:1088–1095.

8 Müller TG, Zila V, Müller B, Kräusslich H-G. **Nuclear Capsid Uncoating and Reverse Transcription of HIV-1**. *Annual Review of Virology* 2022; **9**:261–284.

9 Lucas S, Nelson AM. **HIV and the spectrum of human disease**. *The Journal of Pathology* 2015; **235**:229–241.

10 Dull T, Zufferey R, Kelly M, Mandel RJ, Nguyen M, Trono D, *et al.* **A Third-Generation Lentivirus Vector with a Conditional Packaging System**. *Journal of Virology* 1998; **72**:8463–8471.

11 Louten J. **Virus Replication**. *Essential Human Virology* 2016; :49–70.

12 Lai Y-T. **Small Molecule HIV-1 Attachment Inhibitors: Discovery, Mode of Action and Structural Basis of Inhibition**. *Viruses* 2021; **13**:843.

13 Burdick RC, Li C, Munshi M, Rawson JMO, Nagashima K, Hu W-S, *et al.* **HIV-1 uncoats in the nucleus near sites of integration**. *Proc Natl Acad Sci USA* 2020; **117**:5486–5493.

14 Harrison SC. **Viral membrane fusion**. *Virology* 2015; **479–480**:498–507.

15 Xiao T, Cai Y, Chen B. **HIV-1 Entry and Membrane Fusion Inhibitors**. *Viruses* 2021; **13**:735.

16 Zhu P, Chertova E, Bess J, Lifson JD, Arthur LO, Liu J, *et al.* **Electron tomography analysis of envelope glycoprotein trimers on HIV and simian immunodeficiency virus virions**. *Proceedings of the National Academy of Sciences* 2003; **100**:15812–15817.

17 Checkley MA, Luttge BG, Freed EO. **HIV-1 Envelope Glycoprotein Biosynthesis, Trafficking, and Incorporation**. *Journal of Molecular Biology* 2011; **410**:582–608.

18 Pezeshkian N, Groves NS, van Engelenburg SB. **Single-molecule imaging of HIV-1 envelope glycoprotein dynamics and Gag lattice association exposes determinants responsible for virus incorporation**. *Proceedings of the National*

Academy of Sciences 2019; **116**:25269–25277.

19 Weissenhorn W. **Atomic structure of the ectodomain from HIV-1 gp4**. 1997.

20 Liu Q, Acharya P, Dolan MA, Zhang P, Guzzo C, Lu J, *et al.* **Quaternary contact in the initial interaction of CD4 with the HIV-1 envelope trimer**. *Nat Struct Mol Biol* 2017; **24**:370–378.

21 Yang Z, Wang H, Liu AZ, Gristick HB, Bjorkman PJ. **Asymmetric opening of HIV-1 Env bound to CD4 and a coreceptor-mimicking antibody**. *Nat Struct Mol Biol* 2019; **26**:1167–1175.

22 Tan Q, Zhu Y, Li J, Chen Z, Han GW, Kufareva I, *et al.* **Structure of the CCR5 Chemokine Receptor–HIV Entry Inhibitor Maraviroc Complex**. *Science* 2013; **341**:1387–1390.

23 Hütter G, Bodor J, Ledger S, Boyd M, Millington M, Tsie M, *et al.* **CCR5 Targeted Cell Therapy for HIV and Prevention of Viral Escape**. *Viruses* 2015; **7**:4186–4203.

24 Sarker MdS. **Prevalence of R5 and X4-Tropic strains in HIV-1 Infected bangladeshi population**. *Indian Journal of Medical Microbiology* 2023; **45**:100377.

25 Bieniasz PD, Fridell RA, Anthony K, Cullen BR. **Murine CXCR-4 is a functional coreceptor for T-cell-tropic and dual-tropic strains of human immunodeficiency virus type 1**. *Journal of Virology* 1997; **71**:7097–7100.

26 Caillat C, Guilligay D, Sulbaran G, Weissenhorn W. **Neutralizing Antibodies Targeting HIV-1 gp41**. *Viruses* 2020; **12**:1210.

27 Garg H, Viard M, Jacobs A, Blumenthal R. **Targeting HIV-1 gp41-induced Fusion and Pathogenesis for Anti-viral Therapy**. *Current Topics in Medicinal Chemistry*; **11**:2947–2958.

28 Chen B. **Molecular Mechanism of HIV-1 Entry**. *Trends in Microbiology* 2019; **27**:878–891.

29 Burdick RC, Morse M, Rouzina I, Williams MC, Hu W-S, Pathak VK. **HIV-1 uncoating requires long double-stranded reverse transcription products**. *Sci Adv* 2024; **10**:eadn7033.

30 Li C, Burdick RC, Nagashima K, Hu W-S, Pathak VK. **HIV-1 cores retain their integrity until minutes before uncoating in the nucleus**. *Proc Natl Acad Sci U S A* 2021; **118**:e2019467118.

31 Dharan A, Bachmann N, Talley S, Zwikelmaier V, Campbell EM. **Nuclear pore blockade reveals that HIV-1 completes reverse transcription and uncoating in**

the nucleus. *Nat Microbiol* 2020; **5**:1088–1095.

32 Goff SP. **Host factors exploited by retroviruses**. *Nat Rev Microbiol* 2007; **5**:253–263.

33 Yan N, Cherepanov P, Daigle JE, Engelman A, Lieberman J. **The SET Complex Acts as a Barrier to Autointegration of HIV-1**. *PLoS Pathog* 2009; **5**:e1000327.

34 Suzuki Y, Craigie R. **The road to chromatin — nuclear entry of retroviruses**. *Nat Rev Microbiol* 2007; **5**:187–196.

35 Yoder K, Sarasin A, Kraemer K, McIlhatton M, Bushman F, Fishel R. **The DNA repair genes XPB and XPD defend cells from retroviral infection**. *Proc Natl Acad Sci USA* 2006; **103**:4622–4627.

36 Takaoka A, Wang Z, Choi MK, Yanai H, Negishi H, Ban T, *et al.* **DAI (DLM-1/ZBP1) is a cytosolic DNA sensor and an activator of innate immune response**. *Nature* 2007; **448**:501–505.

37 Medzhitov R. **Recognition of microorganisms and activation of the immune response**. *Nature* 2007; **449**:819–826.

38 Stetson DB, Ko JS, Heidmann T, Medzhitov R. **Trex1 Prevents Cell-Intrinsic Initiation of Autoimmunity**. *Cell* 2008; **134**:587–598.

39 Bukrinskaya AG. **HIV-1 assembly and maturation**. *Arch Virol* 2004; **149**:1067–1082.

40 Ganser-Pornillos BK, Yeager M, Sundquist WI. **The structural biology of HIV assembly**. *Curr Opin Struct Biol* 2008; **18**:203–217.

41 Pornillos O, Ganser-Pornillos BK, Yeager M. **Atomic-level modelling of the HIV capsid**. *Nature* 2011; **469**:424–427.

42 Guo X, Yu D, Liu M, Li H, Chen M, Wang X, *et al.* **A unified classification system for HIV-1 5' long terminal repeats**. *PLOS ONE* 2024; **19**:e0301809.

43 Farnet CM, Haseltine WA. **Integration of human immunodeficiency virus type 1 DNA in vitro**. *Proc Natl Acad Sci U S A* 1990; **87**:4164–4168.

44 Sloan RD, Wainberg MA. **The role of unintegrated DNA in HIV infection**. *Retrovirology* 2011; **8**:52.

45 Interaction between Reverse Transcriptase and Integrase Is Required for Reverse Transcription during HIV-1 Replication. doi:10.1128/jvi.01471-15

46 Engelman A, Cherepanov P. **Retroviral Integrase Structure and DNA Recombination Mechanism**. *Microbiol Spectr* 2014; **2**:1–22.

47 Engelman A, Mizuuchi K, Craigie R. **HIV-1 DNA integration: Mechanism of viral DNA cleavage and DNA strand transfer**. *Cell* 1991; **67**:1211–1221.

48 Bar-Magen T, Sloan RD, Faltenbacher VH, Donahue DA, Kuhl BD, Oliveira M, *et al.* **Comparative biochemical analysis of HIV-1 subtype B and C integrase enzymes**. *Retrovirology* 2009; **6**:103.

49 Weitzman MD, Fradet-Turcotte A. **Virus DNA Replication and the Host DNA Damage Response**. *Annu Rev Virol* 2018; **5**:141–164.

50 Yoder KE, Bushman FD. **Repair of gaps in retroviral DNA integration intermediates**. *J Virol* 2000; **74**:11191–11200.

51 Scherdin U, Rhodes K, Breindl M. **Transcriptionally active genome regions are preferred targets for retrovirus integration**. *Journal of Virology* 1990; **64**:907–912.

52 Schröder ARW, Shinn P, Chen H, Berry C, Ecker JR, Bushman F. **HIV-1 Integration in the Human Genome Favors Active Genes and Local Hotspots**. *Cell* 2002; **110**:521–529.

53 Wang GP, Ciuffi A, Leipzig J, Berry CC, Bushman FD. **HIV integration site selection: Analysis by massively parallel pyrosequencing reveals association with epigenetic modifications**. *Genome Res* 2007; **17**:1186–1194.

54 Col E, Gilquin B, Caron C, Khochbin S. **Tat-controlled Protein Acetylation***. *Journal of Biological Chemistry* 2002; **277**:37955–37960.

55 Kao S, Miyagi E, Mallorson R, Saito H, Sukegawa S, Mukherji A, *et al.* **The Myeloid-Specific Transcription Factor PU.1 Upregulates Mannose Receptor Expression but Represses Basal Activity of the HIV-LTR Promoter**. *J Virol* 2022; **96**:e0065222.

56 Chun T-W, Carruth L, Finzi D, Shen X, DiGiuseppe JA, Taylor H, *et al.* **Quantification of latent tissue reservoirs and total body viral load in HIV-1 infection**. *Nature* 1997; **387**:183–188.

57 Sharkey ME, Teo I, Greenough T, Sharova N, Luzuriaga K, Sullivan JL, *et al.* **Persistence of episomal HIV-1 infection intermediates in patients on highly active anti-retroviral therapy**. *Nat Med* 2000; **6**:76–81.

58 Pang S, Koyanagi Y, Miles S, Wiley C, Vinters HV, Chen ISY. **High levels of unintegrated HIV-1 DNA in brain tissue of AIDS dementia patients**. *Nature* 1990; **343**:85–89.

59 Teo I, Veryard C, Barnes H, An SF, Jones M, Lantos PL, *et al.* **Circular forms of unintegrated human immunodeficiency virus type 1 DNA and high levels of**

viral protein expression: association with dementia and multinucleated giant cells in the brains of patients with AIDS. *J Virol* 1997; **71**:2928–2933.

60 Shank PR, Hughes SH, Kung H-J, Majors JE, Quintrell N, Guntaka RV, *et al.* **Mapping unintegrated avian sarcoma virus DNA: Termini of linear DNA bear 300 nucleotides present once or twice in two species of circular DNA**. *Cell* 1978; **15**:1383–1395.

61 Brown PO, Bowerman B, Varmus HE, Bishop JM. **Retroviral integration: structure of the initial covalent product and its precursor, and a role for the viral IN protein**. *Proc Natl Acad Sci U S A* 1989; **86**:2525–2529.

62 Fujiwara T, Mizuuchi K. **Retroviral DNA integration: Structure of an integration intermediate**. *Cell* 1988; **54**:497–504.

63 Brown PO, Bowerman B, Varmus HE, Bishop JM. **Correct integration of retroviral DNA in vitro**. *Cell* 1987; **49**:347–356.

64 Yan N, O'Day E, Wheeler LA, Engelman A, Lieberman J. **HIV DNA is heavily uracilated, which protects it from autointegration**. *Proc Natl Acad Sci USA* 2011; **108**:9244–9249.

65 De Iaco A, Santoni F, Vannier A, Guipponi M, Antonarakis S, Luban J. **TNPO3 protects HIV-1 replication from CPSF6-mediated capsid stabilization in the host cell cytoplasm**. *Retrovirology* 2013; **10**:20.

66 Lee YM, Coffin JM. **Efficient autointegration of avian retrovirus DNA in vitro**. *J Virol* 1990; **64**:5958–5965.

67 Shoemaker C, Hoffman J, Goff SP, Baltimore D. **Intramolecular integration within Moloney murine leukemia virus DNA**. *J Virol* 1981; **40**:164–172.

68 Jolicoeur P, Rassart E. **Effect of Fv-1 gene product on synthesis of linear and supercoiled viral DNA in cells infected with murine leukemia virus**. *Journal of Virology* 1980; **33**:183–195.

69 Yoshimura FK, Weinberg RA. **Restriction endonuclease cleavage of linear and closed circular murine leukemia viral DNAS: Discovery of a smaller circular form**. *Cell* 1979; **16**:323–332.

70 Olivares I, Pernas M, Casado C, López-Galindez C. **Human Immunodeficiency Virus Type 1 Two-Long Terminal Repeat Circles: A Subject for Debate**. *AIDS Reviews*

71 Hamid FB, Kim J, Shin C-G. **Distribution and fate of HIV-1 unintegrated DNA species: a comprehensive update**. *AIDS Research and Therapy* 2017; **14**:9.

72 Ma H, Qian W, Bambouskova M, Collins PL, Porter SI, Byrum AK, *et al.* **Barrier-to-Autointegration Factor 1 Protects against a Basal cGAS-STING Response**. *mBio* 2020; **11**:e00136-20.

73 Kvarnhammar AM, Tengroth L, Adner M, Cardell L-O. **Innate Immune Receptors in Human Airway Smooth Muscle Cells: Activation by TLR1/2, TLR3, TLR4, TLR7 and NOD1 Agonists**. *PLOS ONE* 2013; **8**:e68701.

74 Colonna M. **TLR pathways and IFN-regulatory factors: To each its own**. *European Journal of Immunology* 2007; **37**:306–309.

75 Onoguchi K, Yoneyama M, Fujita T. **Retinoic Acid-Inducible Gene-I-Like Receptors**. *Journal of Interferon & Cytokine Research* 2011; **31**:27–31.

76 Lawrence T. **The Nuclear Factor NF-κB Pathway in Inflammation**. *Cold Spring Harb Perspect Biol* 2009; **1**:a001651.

77 Akbar AN, Lord JM, Salmon M. **IFN-α and IFN-β: a link between immune memory and chronic inflammation**. *Immunology Today* 2000; **21**:337–342.

78 Li H, Gade P, Xiao W, Kalvakolanu DV. **The interferon signaling network and transcription factor C/EBP-beta**. *Cell Mol Immunol* 2007; **4**:407–418.

79 Schoggins JW. **Interferon-stimulated genes: roles in viral pathogenesis**. *Curr Opin Virol* 2014; **6**:40–46.

80 Aguirre S, Luthra P, Sanchez-Aparicio MT, Maestre AM, Patel J, Lamothe F, *et al.* **Dengue virus NS2B protein targets cGAS for degradation and prevents mitochondrial DNA sensing during infection**. *Nat Microbiol* 2017; **2**:17037.

81 Dong L, Hou Y, Xu N, Gao X, Sun Z, Yang Q, *et al.* **Cyclic GMP-AMP synthase recognizes the physical features of DNA**. *Acta Pharmacol Sin* 2024; :1–7.

82 Quicke KM, Diamond MS, Suthar MS. **Negative regulators of the RIG-I-like receptor signaling pathway**. *Eur J Immunol* 2017; **47**:615–628.

83 Wu J, Chen ZJ. **Innate immune sensing and signaling of cytosolic nucleic acids**. *Annu Rev Immunol* 2014; **32**:461–488.

84 Li T, Chen ZJ. **The cGAS-cGAMP-STING pathway connects DNA damage to inflammation, senescence, and cancer**. *J Exp Med* 2018; **215**:1287–1299.

85 Chen Q, Sun L, Chen ZJ. **Regulation and function of the cGAS-STING pathway of cytosolic DNA sensing**. *Nat Immunol* 2016; **17**:1142–1149.

86 Tao J, Zhou X, Jiang Z. **cGAS-cGAMP-STING: The three musketeers of cytosolic DNA sensing and signaling**. *IUBMB Life* 2016; **68**:858–870.

87 Ablasser A, Chen ZJ. **cGAS in action: Expanding roles in immunity and inflammation**. *Science* 2019; **363**:eaat8657.

88 Motwani M, Pesiridis S, Fitzgerald KA. **DNA sensing by the cGAS-STING pathway in health and disease**. *Nat Rev Genet* 2019; **20**:657–674.

89 Ablasser A, Schmid-Burgk JL, Hemmerling I, Horvath GL, Schmidt T, Latz E, *et al.* **Cell intrinsic immunity spreads to bystander cells via the intercellular transfer of cGAMP**. *Nature* 2013; **503**:530–534.

90 Sun L, Wu J, Du F, Chen X, Chen ZJ. **Cyclic GMP-AMP synthase is a cytosolic DNA sensor that activates the type I interferon pathway**. *Science* 2013; **339**:786–791.

91 Yin Q, Tian Y, Kabaleeswaran V, Jiang X, Tu D, Eck MJ, *et al.* **Cyclic di-GMP sensing via the innate immune signaling protein STING**. *Mol Cell* 2012; **46**:735–745.

92 Ishikawa H, Barber GN. **STING is an endoplasmic reticulum adaptor that facilitates innate immune signalling**. *Nature* 2008; **455**:674–678.

93 Zhong B, Yang Y, Li S, Wang Y-Y, Li Y, Diao F, *et al.* **The adaptor protein MITA links virus-sensing receptors to IRF3 transcription factor activation**. *Immunity* 2008; **29**:538–550.

94 Ishikawa H, Ma Z, Barber GN. **STING regulates intracellular DNA-mediated, type I interferon-dependent innate immunity**. *Nature* 2009; **461**:788–792.

95 Saitoh T, Fujita N, Hayashi T, Takahara K, Satoh T, Lee H, *et al.* **Atg9a controls dsDNA-driven dynamic translocation of STING and the innate immune response**. *Proc Natl Acad Sci U S A* 2009; **106**:20842–20846.

96 Shang G, Zhang C, Chen ZJ, Bai X-C, Zhang X. **Cryo-EM structures of STING reveal its mechanism of activation by cyclic GMP-AMP**. *Nature* 2019; **567**:389–393.

97 Zhang C, Shang G, Gui X, Zhang X, Bai X-C, Chen ZJ. **Structural basis of STING binding with and phosphorylation by TBK1**. *Nature* 2019; **567**:394–398.

98 Tanaka Y, Chen ZJ. **STING specifies IRF3 phosphorylation by TBK1 in the cytosolic DNA signaling pathway**. *Sci Signal* 2012; **5**:ra20.

99 Cai X, Chiu Y-H, Chen ZJ. **The cGAS-cGAMP-STING pathway of cytosolic DNA sensing and signaling**. *Mol Cell* 2014; **54**:289–296.

100 Schoggins JW, MacDuff DA, Imanaka N, Gainey MD, Shrestha B, Eitson JL, *et al.* **Pan-viral specificity of IFN-induced genes reveals new roles for cGAS in innate**

immunity. *Nature* 2014; **505**:691–695.

101 Ma Z, Damania B. **The cGAS-STING Defense Pathway and Its Counteraction by Viruses**. *Cell Host & Microbe* 2016; **19**:150–158.

102 Kopitar-Jerala N. **The Role of Interferons in Inflammation and Inflammasome Activation**. *Front Immunol* 2017; **8**:873.

103 Li H, Gade P, Xiao W, Kalvakolanu DV. **The Interferon Signaling Network and Transcription Factor C/EBP-β**. *Cell Mol Immunol* 2007; **4**:407–418.

104 Kalvakolanu D, Borden E. **Interferons: Cellular and Molecular Biology of Their Actions**. *Encyclopedia of Cancer* 2002; **2**:511–521.

105 Stark GR, Kerr IM, Williams BR, Silverman RH, Schreiber RD. **How cells respond to interferons**. *Annu Rev Biochem* 1998; **67**:227–264.

106 A Biron C. **Initial and innate responses to viral infections — pattern setting in immunity or disease**. *Current Opinion in Microbiology* 1999; **2**:374–381.

107 Williams BRG. **Signal Integration via PKR**. *Science's STKE* 2001; **2001**:re2–re2.

108 2-5A-Dependent RNase L: A Regulated Endoribonuclease in the Interferon System - ScienceDirect. https://www.sciencedirect.com/science/article/abs/pii/B9780125889452500170 (accessed 16 Jul2024).

109 Proteome analysis reveals ubiquitin-conjugating enzymes to be a new family of interferon-α-regulated genes - Nyman - 2000 - European Journal of Biochemistry - Wiley Online Library. https://febs.onlinelibrary.wiley.com/doi/10.1046/j.1432-1327.2000.01433.x (accessed 16 Jul2024).

110 Taniguchi T, Ogasawara K, Takaoka A, Tanaka N. **IRF Family of Transcription Factors as Regulators of Host Defense**. *Annu Rev Immunol* 2001; **19**:623–655.

111 Enninga J, Levy DE, Blobel G, Fontoura BMA. **Role of Nucleoporin Induction in Releasing an mRNA Nuclear Export Block**. *Science* 2002; **295**:1523–1525.

112 Takayanagi H, Kim S, Matsuo K, Suzuki H, Suzuki T, Sato K, *et al.* **RANKL maintains bone homeostasis through c-Fos-dependent induction of interferon-β**. *Nature* 2002; **416**:744–749.

113 Horiuchi M, Hayashida W, Akishita M, Yamada S, Lehtonen JYA, Tamura K, *et al.* **Interferon-γ Induces AT2 Receptor Expression in Fibroblasts by Jak/STAT Pathway and Interferon Regulatory Factor-1**. *Circulation Research* 2000; **86**:233–240.

114 Kalvakolanu DV. **The GRIMs: a new interface between cell death regulation**

and interferon/retinoid induced growth suppression. *Cytokine Growth Factor Rev* 2004; **15**:169–194.

115 Levy-Strumpf N, Kimchi A. **Death associated proteins (DAPs): from gene identification to the analysis of their apoptotic and tumor suppressive functions**. *Oncogene* 1998; **17**:3331–3340.

116 Pestka S, Krause CD, Walter MR. **Interferons, interferon-like cytokines, and their receptors**. *Immunological Reviews* 2004; **202**:8–32.

117 Davis AJ, Chen BPC, Chen DJ. **DNA-PK: a dynamic enzyme in a versatile DSB repair pathway**. *DNA Repair (Amst)* 2014; **17**:21–29.

118 Ferguson BJ, Mansur DS, Peters NE, Ren H, Smith GL. **DNA-PK is a DNA sensor for IRF-3-dependent innate immunity**. *Elife* 2012; **1**:e00047.

119 Kotula E, Faigle W, Berthault N, Dingli F, Loew D, Sun J-S, *et al.* **DNA-PK target identification reveals novel links between DNA repair signaling and cytoskeletal regulation**. *PLoS One* 2013; **8**:e80313.

120 Burleigh K, Maltbaek JH, Cambier S, Green R, Gale M, James RC, *et al.* **Human DNA-PK activates a STING-independent DNA sensing pathway**. *Science Immunology* 2020; **5**:eaba4219.

121 Peters NE, Ferguson BJ, Mazzon M, Fahy AS, Krysztofinska E, Arribas-Bosacoma R, *et al.* **A Mechanism for the Inhibition of DNA-PK-Mediated DNA Sensing by a Virus**. *PLoS Pathog* 2013; **9**:e1003649.

122 Scutts SR, Ember SW, Ren H, Ye C, Lovejoy CA, Mazzon M, *et al.* **DNA-PK Is Targeted by Multiple Vaccinia Virus Proteins to Inhibit DNA Sensing**. *Cell Reports* 2018; **25**:1953-1965.e4.

123 Jamin A, Wiebe MS. **Barrier to Autointegration Factor (BANF1): interwoven roles in nuclear structure, genome integrity, innate immunity, stress responses and progeria**. *Current Opinion in Cell Biology* 2015; **34**:61–68.

124 Lee MS, Craigie R. **A previously unidentified host protein protects retroviral DNA from autointegration**. *Proc Natl Acad Sci USA* 1998; **95**:1528–1533.

125 Cai M, Huang Y, Zheng R, Wei S-Q, Ghirlando R, Lee MS, *et al.* **Solution structure of the cellular factor BAF responsible for protecting retroviral DNA from autointegration**. *Nat Struct Mol Biol* 1998; **5**:903–909.

126 Lee MS, Craigie R. **Protection of retroviral DNA from autointegration: involvement of a cellular factor**. *Proc Natl Acad Sci U S A* 1994; **91**:9823–9827.

127 Chen H, Engelman A. **The barrier-to-autointegration protein is a host factor for**

HIV type 1 integration. *Proc Natl Acad Sci U S A* 1998; **95**:15270–15274.

128 Suzuki Y, Craigie R. **Regulatory mechanisms by which barrier-to-autointegration factor blocks autointegration and stimulates intermolecular integration of Moloney murine leukemia virus preintegration complexes**. *J Virol* 2002; **76**:12376–12380.

129 De Sandre-Giovannoli A, Bernard R, Cau P, Navarro C, Amiel J, Boccaccio I, *et al.* **Lamin A Truncation in Hutchinson-Gilford Progeria**. *Science* 2003; **300**:2055–2055.

130 Bonne G, Levy N. ***LMNA* mutations in atypical Werner's syndrome**. *The Lancet* 2003; **362**:1585–1586.

131 Eriksson M, Brown WT, Gordon LB, Glynn MW, Singer J, Scott L, *et al.* **Recurrent de novo point mutations in lamin A cause Hutchinson–Gilford progeria syndrome**. *Nature* 2003; **423**:293–298.

132 Kobayashi S, Koujin T, Kojidani T, Osakada H, Mori C, Hiraoka Y, *et al.* **BAF is a cytosolic DNA sensor that leads to exogenous DNA avoiding autophagy**. *Proc Natl Acad Sci U S A* 2015; **112**:7027–7032.

133 Jamin A, Wiebe MS. **Barrier to Autointegration Factor (BANF1): interwoven roles in nuclear structure, genome integrity, innate immunity, stress responses and progeria**. *Curr Opin Cell Biol* 2015; **34**:61–68.

134 Halfmann CT, Roux KJ. **Barrier-to-autointegration factor: a first responder for repair of nuclear ruptures**. *Cell Cycle* 2021; **20**:647–660.

135 Sears RM, Roux KJ. **Diverse cellular functions of barrier-to-autointegration factor and its roles in disease**. *J Cell Sci* 2020; **133**:jcs246546.

136 Haraguchi T, Koujin T, Osakada H, Kojidani T, Mori C, Masuda H, *et al.* **Nuclear localization of barrier-to-autointegration factor is correlated with progression of S phase in human cells**. *Journal of Cell Science* 2007; **120**:1967–1977.

137 Rose M, Bai B, Tang M, Cheong CM, Beard S, Burgess JT, *et al.* **The Impact of Rare Human Variants on Barrier-To-Auto-Integration Factor 1 (Banf1) Structure and Function**. *Front Cell Dev Biol* 2021; **9**:775441.

138 Segura-Totten M, Wilson KL. **BAF: roles in chromatin, nuclear structure and retrovirus integration**. *Trends in Cell Biology* 2004; **14**:261–266.

139 Sears RM, Roux KJ. **Diverse cellular functions of barrier-to-autointegration factor and its roles in disease**. *Journal of Cell Science* 2020; **133**:jcs246546.

140 Haraguchi T, Koujin T, Osakada H, Kojidani T, Mori C, Masuda H, *et al.* **Nuclear**

localization of barrier-to-autointegration factor is correlated with progression of S phase in human cells. *Journal of Cell Science* 2007; **120**:1967–1977.

141 Katz RA, Merkel G, Kulkosky J, Leis J, Skalka AM. **The avian retroviral IN protein is both necessary and sufficient for integrative recombination in vitro**. *Cell* 1990; **63**:87–95.

142 Lin C-W, Engelman A. **The Barrier-to-Autointegration Factor Is a Component of Functional Human Immunodeficiency Virus Type 1 Preintegration Complexes**. *Journal of Virology* 2003; **77**:5030–5036.

143 Craigie R, Fujiwara T, Bushman F. **The IN protein of Moloney murine leukemia virus processes the viral DNA ends and accomplishes their integration in vitro**. *Cell* 1990; **62**:829–837.

144 Wei S, Mizuuchi K, Craigie R. **A large nucleoprotein assembly at the ends of the viral DNA mediates retroviral DNA integration**. *The EMBO Journal* 1997; **16**:7511–7520.

145 Brown PO, Bowerman B, Varmus HE, Bishop JM. **Correct integration of retroviral DNA in vitro**. *Cell* 1987; **49**:347–356.

146 Ellison V, Abrams H, Roe T, Lifson J, Brown P. **Human immunodeficiency virus integration in a cell-free system**. *Journal of Virology* 1990; **64**:2711–2715.

147 Farnet CM, Haseltine WA. **Integration of human immunodeficiency virus type 1 DNA in vitro.** *Proceedings of the National Academy of Sciences* 1990; **87**:4164–4168.

148 Lee YMH, Coffin JM. **Relationship of Avian Retrovirus DNA Synthesis to Integration In Vitro**. *Molecular and Cellular Biology* 1991; **11**:1419–1430.

149 Miller MD, Farnet CM, Bushman FD. **Human immunodeficiency virus type 1 preintegration complexes: studies of organization and composition**. *Journal of Virology* 1997; **71**:5382–5390.

150 Li L, Yoder K, Hansen MST, Olvera J, Miller MD, Bushman FD. **Retroviral cDNA Integration: Stimulation by HMG I Family Proteins**. *Journal of Virology* 2000; **74**:10965–10974.

151 Li L, Olvera JM, Yoder KE, Mitchell RS, Butler SL, Lieber M, *et al.* **Role of the non-homologous DNA end joining pathway in the early steps of retroviral infection**. *The EMBO Journal* 2001; **20**:3272–3281.

152 Heinzinger NK, Bukinsky MI, Haggerty SA, Ragland AM, Kewalramani V, Lee MA, *et al.* **The Vpr protein of human immunodeficiency virus type 1 influences nuclear localization of viral nucleic acids in nondividing host cells.** *Proceedings*

of the National Academy of Sciences 1994; **91**:7311–7315.

153 Farnet CM, Haseltine WA. **Determination of viral proteins present in the human immunodeficiency virus type 1 preintegration complex**. *Journal of Virology* 1991; **65**:1910–1915.

154 Bukrinsky MI, Sharova N, McDonald TL, Pushkarskaya T, Tarpley WG, Stevenson M. **Association of integrase, matrix, and reverse transcriptase antigens of human immunodeficiency virus type 1 with viral nucleic acids following acute infection.** *Proceedings of the National Academy of Sciences* 1993; **90**:6125–6129.

155 Lee MS, Craigie R. **Protection of retroviral DNA from autointegration: involvement of a cellular factor**. *Proc Natl Acad Sci U S A* 1994; **91**:9823–9827.

156 Lin C-W, Engelman A. **The barrier-to-autointegration factor is a component of functional human immunodeficiency virus type 1 preintegration complexes**. *J Virol* 2003; **77**:5030–5036.

157 Mansharamani M, Graham DRM, Monie D, Lee KK, Hildreth JEK, Siliciano RF, *et al.* **Barrier-to-autointegration factor BAF binds p55 Gag and matrix and is a host component of human immunodeficiency virus type 1 virions**. *J Virol* 2003; **77**:13084–13092.

158 Greene WC, Peterlin BM. **Charting HIV's remarkable voyage through the cell: Basic science as a passport to future therapy**. *Nat Med* 2002; **8**:673–680.

159 Gallay P, Swingler S, Song J, Bushman F, Trono D. **HIV nuclear import is governed by the phosphotyrosine-mediated binding of matrix to the core domain of integrase**. *Cell* 1995; **83**:569–576.

160 Chen H, Engelman A. **The barrier-to-autointegration protein is a host factor for HIV type 1 integration**. *Proc Natl Acad Sci U S A* 1998; **95**:15270–15274.

161 Carteau S, Gorelick RJ, Bushman FD. **Coupled integration of human immunodeficiency virus type 1 cDNA ends by purified integrase in vitro: stimulation by the viral nucleocapsid protein**. *J Virol* 1999; **73**:6670–6679.

162 Chen H, Engelman A. **The barrier-to-autointegration protein is a host factor for HIV type 1 integration**. *Proc Natl Acad Sci USA* 1998; **95**:15270–15274.

163 Dwivedi R, Prakash P, Kumbhar BV, Balasubramaniam M, Dash C. **HIV-1 capsid and viral DNA integration**. *mBio* 2024; **15**:e00212-22.

164 Freed EO. **HIV-1 assembly, release and maturation**. *Nat Rev Microbiol* 2015; **13**:484–496.

165 Scoca V, Di Nunzio F. **The HIV-1 Capsid: From Structural Component to Key**

Factor for Host Nuclear Invasion. *Viruses* 2021; **13**:273.

166 Menéndez-Arias L, Sebastián-Martín A, Álvarez M. **Viral reverse transcriptases**. *Virus Research* 2017; **234**:153–176.

167 Lin F, Blake DL, Callebaut I, Skerjanc IS, Holmer L, McBurney MW, *et al.* **MAN1, an inner nuclear membrane protein that shares the LEM domain with lamina-associated polypeptide 2 and emerin**. *J Biol Chem* 2000; **275**:4840–4847.

168 Cai M, Huang Y, Ghirlando R, Wilson KL, Craigie R, Clore GM. **Solution structure of the constant region of nuclear envelope protein LAP2 reveals two LEM-domain structures: one binds BAF and the other binds DNA**. *The EMBO Journal* 2001; **20**:4399–4407.

169 Wolff N, Gilquin B, Courchay K, Callebaut I, Worman HJ, Zinn-Justin S. **Structural analysis of emerin, an inner nuclear membrane protein mutated in X-linked Emery–Dreifuss muscular dystrophy**. *FEBS Letters* 2001; **501**:171–176.

170 Dechat T, Korbei B, Vaughan OA, Vlcek S, Hutchison CJ, Foisner R. **Lamina-associated polypeptide 2α binds intranuclear A-type lamins**. *Journal of Cell Science* 2000; **113**:3473–3484.

171 Gant TM, Harris CA, Wilson KL. **Roles of LAP2 Proteins in Nuclear Assembly and DNA Replication: Truncated LAP2β Proteins Alter Lamina Assembly, Envelope Formation, Nuclear Size, and DNA Replication Efficiency in Xenopus laevis Extracts**. *Journal of Cell Biology* 1999; **144**:1083–1096.

172 Martins S, Eikvar S, Furukawa K, Collas P. **HA95 and LAP2 beta mediate a novel chromatin-nuclear envelope interaction implicated in initiation of DNA replication**. *J Cell Biol* 2003; **160**:177–188.

173 Liu J, Lee KK, Segura-Totten M, Neufeld E, Wilson KL, Gruenbaum Y. **MAN1 and emerin have overlapping function(s) essential for chromosome segregation and cell division in Caenorhabditis elegans**. *Proc Natl Acad Sci U S A* 2003; **100**:4598–4603.

174 Shumaker DK, Lee KK, Tanhehco YC, Craigie R, Wilson KL. **LAP2 binds to BAF.DNA complexes: requirement for the LEM domain and modulation by variable regions**. *EMBO J* 2001; **20**:1754–1764.

175 Zheng R, Ghirlando R, Lee MS, Mizuuchi K, Krause M, Craigie R. **Barrier-to-autointegration factor (BAF) bridges DNA in a discrete, higher-order nucleoprotein complex**. *Proc Natl Acad Sci U S A* 2000; **97**:8997–9002.

176 Furukawa K. **LAP2 binding protein 1 (L2BP1/BAF) is a candidate mediator of LAP2-chromatin interaction**. *J Cell Sci* 1999; **112 (Pt 15)**:2485–2492.

177 Furukawa K, Sugiyama S, Osouda S, Goto H, Inagaki M, Horigome T, *et al.* **Barrier-to-autointegration factor plays crucial roles in cell cycle progression and nuclear organization in Drosophila**. *J Cell Sci* 2003; **116**:3811–3823.

178 Harris D, Engelman A. **Both the Structure and DNA Binding Function of the Barrier-to-Autointegration Factor Contribute to Reconstitution of HIV Type 1 Integration *in Vitro* ***. *Journal of Biological Chemistry* 2000; **275**:39671–39677.

179 Skoko D, Li M, Huang Y, Mizuuchi M, Cai M, Bradley CM, *et al.* **Barrier-to-autointegration factor (BAF) condenses DNA by looping**. *Proceedings of the National Academy of Sciences* 2009; **106**:16610–16615.

180 Bradley CM, Ronning DR, Ghirlando R, Craigie R, Dyda F. **Structural basis for DNA bridging by barrier-to-autointegration factor**. *Nat Struct Mol Biol* 2005; **12**:935–936.

181 Wang X, Xu S, Rivolta C, Li LY, Peng G-H, Swain PK, *et al.* **Barrier to autointegration factor interacts with the cone-rod homeobox and represses its transactivation function**. *J Biol Chem* 2002; **277**:43288–43300.

182 Bickel D, Vranken W. **Effects of Phosphorylation on Protein Backbone Dynamics and Conformational Preferences**. *J Chem Theory Comput* 2024; **20**:4998–5011.

183 Marcelot A, Petitalot A, Ropars V, Le Du M-H, Samson C, Dubois S, *et al.* **Di-phosphorylated BAF shows altered structural dynamics and binding to DNA, but interacts with its nuclear envelope partners**. *Nucleic Acids Research* 2021; **49**:3841–3855.

184 Gorjánácz M, Klerkx EPF, Galy V, Santarella R, López-Iglesias C, Askjaer P, *et al.* **Caenorhabditis elegans BAF-1 and its kinase VRK-1 participate directly in post-mitotic nuclear envelope assembly**. *EMBO J* 2007; **26**:132–143.

185 Nichols RJ, Wiebe MS, Traktman P. **The Vaccinia-related Kinases Phosphorylate the N′ Terminus of BAF, Regulating Its Interaction with DNA and Its Retention in the Nucleus**. *MBoC* 2006; **17**:2451–2464.

186 Bengtsson L, Wilson KL. **Barrier-to-autointegration factor phosphorylation on Ser-4 regulates emerin binding to lamin A in vitro and emerin localization in vivo**. *Mol Biol Cell* 2006; **17**:1154–1163.

187 Molitor TP, Traktman P. **Depletion of the protein kinase VRK1 disrupts nuclear envelope morphology and leads to BAF retention on mitotic chromosomes**. *MBoC* 2014; **25**:891–903.

188 Valbuena A, Sanz-García M, López-Sánchez I, Vega FM, Lazo PA. **Roles of VRK1 as a new player in the control of biological processes required for cell division**.

Cellular Signalling 2011; **23**:1267–1272.

189 Santos CR, Rodríguez-Pinilla M, Vega FM, Rodríguez-Peralto JL, Blanco S, Sevilla A, *et al.* **VRK1 Signaling Pathway in the Context of the Proliferation Phenotype in Head and Neck Squamous Cell Carcinoma**. *Molecular Cancer Research* 2006; **4**:177–185.

190 Cartwright TN, Harris RJ, Meyer SK, Mon AM, Watson NA, Tan C, *et al.* **Dissecting the roles of Haspin and VRK1 in histone H3 phosphorylation during mitosis**. *Sci Rep* 2022; **12**:11210.

191 Valbuena A, Castro-Obregón S, Lazo PA. **Downregulation of VRK1 by p53 in Response to DNA Damage Is Mediated by the Autophagic Pathway**. *PLOS ONE* 2011; **6**:e17320.

192 Sevilla A, Santos CR, Vega FM, Lazo PA. **Human Vaccinia-related Kinase 1 (VRK1) Activates the ATF2 Transcriptional Activity by Novel Phosphorylation on Thr-73 and Ser-62 and Cooperates with JNK ***. *Journal of Biological Chemistry* 2004; **279**:27458–27465.

193 Martín-Doncel E, Rojas AM, Cantarero L, Lazo PA. **VRK1 functional insufficiency due to alterations in protein stability or kinase activity of human VRK1 pathogenic variants implicated in neuromotor syndromes**. *Sci Rep* 2019; **9**:13381.

194 Lee KK, Haraguchi T, Lee RS, Koujin T, Hiraoka Y, Wilson KL. **Distinct functional domains in emerin bind lamin A and DNA-bridging protein BAF**. *Journal of Cell Science* 2001; **114**:4567–4573.

195 Holaska JM, Lee KK, Kowalski AK, Wilson KL. **Transcriptional Repressor Germ Cell-less (GCL) and Barrier to Autointegration Factor (BAF) Compete for Binding to Emerin *in Vitro* ***. *Journal of Biological Chemistry* 2003; **278**:6969–6975.

196 Mansharamani M, Wilson KL. **Direct Binding of Nuclear Membrane Protein MAN1 to Emerin *in Vitro* and Two Modes of Binding to Barrier-to-Autointegration Factor***. *Journal of Biological Chemistry* 2005; **280**:13863–13870.

197 Samwer M, Schneider MWG, Hoefler R, Schmalhorst PS, Jude JG, Zuber J, *et al.* **DNA Cross-Bridging Shapes a Single Nucleus from a Set of Mitotic Chromosomes**. *Cell* 2017; **170**:956-972.e23.

198 Segura-Totten M, Kowalski AK, Craigie R, Wilson KL. **Barrier-to-autointegration factor : major roles in chromatin decondensation and nuclear assembly**. *Journal of Cell Biology* 2002; **158**:475–485.

199 Haraguchi T, Kojidani T, Koujin T, Shimi T, Osakada H, Mori C, *et al.* **Live cell imaging and electron microscopy reveal dynamic processes of BAF-directed nuclear envelope assembly**. *Journal of Cell Science* 2008; **121**:2540–2554.

200 Mehla R, Bivalkar-Mehla S, Chauhan A. **A Flavonoid, Luteolin, Cripples HIV-1 by Abrogation of Tat Function**. *PLOS ONE* 2011; **6**:e27915.

201 Lopez-Lazaro M. **Distribution and Biological Activities of the Flavonoid Luteolin**. *Mini-Reviews in Medicinal Chemistry*; **9**:31–59.

202 Lin Y-S, Tsai P-H, Kandaswami CC, Cheng C-H, Ke F-C, Lee P-P, *et al.* **Effects of dietary flavonoids, luteolin, and quercetin on the reversal of epithelial–mesenchymal transition in A431 epidermal cancer cells**. *Cancer Science* 2011; **102**:1829–1839.

203 Lin Y, Shi R, Wang X, Shen H-M. **Luteolin, a Flavonoid with Potential for Cancer Prevention and Therapy**. *Current Cancer Drug Targets*; **8**:634–646.

204 Seelinger G, Merfort I, Wölfle U, Schempp CM. **Anti-carcinogenic Effects of the Flavonoid Luteolin**. *Molecules* 2008; **13**:2628–2651.

205 Seelinger G, Merfort I, Schempp CM. **Anti-oxidant, anti-inflammatory and anti-allergic activities of luteolin**. *Planta Med* 2008; **74**:1667–1677.

206 Kim YS, Kim S-H, Shin J, Harikishore A, Lim J-K, Jung Y, *et al.* **Luteolin Suppresses Cancer Cell Proliferation by Targeting Vaccinia-Related Kinase 1**. *PLOS ONE* 2014; **9**:e109655.

207 Burgess JT, Cheong CM, Suraweera A, Sobanski T, Beard S, Dave K, *et al.* **Barrier-to-autointegration-factor (Banf1) modulates DNA double-strand break repair pathway choice via regulation of DNA-dependent kinase (DNA-PK) activity**. *Nucleic Acids Research* 2021; **49**:3294–3307.

208 Oca RM de, Shoemaker CJ, Gucek M, Cole RN, Wilson KL. **Barrier-to-Autointegration Factor Proteome Reveals Chromatin-Regulatory Partners**. *PLOS ONE* 2009; **4**:e7050.

209 Ku80: Product of the XRCC5 Gene and Its Role in DNA Repair and V(D)J Recombination | Science. https://www.science.org/doi/10.1126/science.8073286 (accessed 23 Aug2024).

210 Sun X, Liu T, Zhao J, Xia H, Xie J, Guo Y, *et al.* **DNA-PK deficiency potentiates cGAS-mediated antiviral innate immunity**. *Nat Commun* 2020; **11**:6182.

211 Taffoni C, Vila IK, Jardine J, Schussler M, McKellar J, Chemarin M, *et al.* DNA-PK controls cyclic dinucleotide-associated type I Interferon responses. 2024. doi:10.1101/2024.09.17.613246

212 Hubel P, Urban C, Bergant V, Schneider WM, Knauer B, Stukalov A, *et al.* **A protein-interaction network of interferon-stimulated genes extends the innate immune system landscape**. *Nat Immunol* 2019; **20**:493–502.

213 Decout A, Katz JD, Venkatraman S, Ablasser A. **The cGAS–STING pathway as a therapeutic target in inflammatory diseases**. *Nat Rev Immunol* 2021; **21**:548–569.

214 Dull T, Zufferey R, Kelly M, Mandel RJ, Nguyen M, Trono D, *et al.* **A Third-Generation Lentivirus Vector with a Conditional Packaging System**. *Journal of Virology* 1998; **72**:8463–8471.

215 Bähr A, Singer A, Hain A, Vasudevan AAJ, Schilling M, Reh J, *et al.* **Interferon but not MxB inhibits foamy retroviruses**. *Virology* 2016; **488**:51–60.

216 Sunseri N, O'Brien M, Bhardwaj N, Landau NR. **Human Immunodeficiency Virus Type 1 Modified To Package Simian Immunodeficiency Virus Vpx Efficiently Infects Macrophages and Dendritic Cells**. *Journal of Virology* 2011; **85**:6263–6274.

217 Edmonds TG, Ding H, Yuan X, Wei Q, Smith KS, Conway JA, *et al.* **Replication competent molecular clones of HIV-1 expressing Renilla luciferase facilitate the analysis of antibody inhibition in PBMC**. *Virology* 2010; **408**:1–13.

218 He J, Choe S, Walker R, Di Marzio P, Morgan DO, Landau NR. **Human immunodeficiency virus type 1 viral protein R (Vpr) arrests cells in the G2 phase of the cell cycle by inhibiting p34cdc2 activity**. *J Virol* 1995; **69**:6705–6711.

219 Bock M, Bishop KN, Towers G, Stoye JP. **Use of a Transient Assay for Studying the Genetic Determinants of Fv1 Restriction**. *Journal of Virology* 2000; **74**:7422–7430.

220 Pizzato M, Erlwein O, Bonsall D, Kaye S, Muir D, McClure MO. **A one-step SYBR Green I-based product-enhanced reverse transcriptase assay for the quantitation of retroviruses in cell culture supernatants**. *Journal of Virological Methods* 2009; **156**:1–7.

221 Mohamed A, Bakir T, Al-Hawel H, Al-Sharif I, Bakheet R, Kouser L, *et al.* **HIV-2 Vpx neutralizes host restriction factor SAMHD1 to promote viral pathogenesis**. *Sci Rep* 2021; **11**:20984.

222 Bakir TM. **The role of SAMHD1 expression and its relation to HIV-2 (Vpx) gene production**. *Saudi Pharmaceutical Journal : SPJ* 2018; **26**:903.

223 Altfeld M, Gale M. **Innate immunity against HIV-1 infection**. *Nat Immunol* 2015; **16**:554–562.

224 Eschbach JE, Puray-Chavez M, Mohammed S, Wang Q, Xia M, Huang L-C, *et al.* **HIV-1 capsid stability and reverse transcription are finely balanced to minimize sensing of reverse transcription products via the cGAS-STING pathway**. *mBio* 2024; **15**:e0034824.

225 Wang Y, Qian G, Zhu L, Zhao Z, Liu Y, Han W, *et al.* **HIV-1 Vif suppresses antiviral immunity by targeting STING**. *Cell Mol Immunol* 2022; **19**:108–121.

226 Lin C, Kuffour EO, Fuchs NV, Gertzen CGW, Kaiser J, Hirschenberger M, *et al.* **Regulation of STING activity in DNA sensing by ISG15 modification**. *Cell Rep* 2023; **42**:113277.

227 Chin EN, Yu C, Vartabedian VF, Jia Y, Kumar M, Gamo AM, *et al.* **Antitumor activity of a systemic STING-activating non-nucleotide cGAMP mimetic**. *Science* 2020; **369**:993–999.

228 Mejía-Calvo I, Muñoz-García L, Jiménez-Uribe A, Camacho-Sandoval R, González-González E, Mellado-Sánchez G, *et al.* **Validation of a cell-based colorimetric reporter gene assay for the evaluation of Type I Interferons**. *Biotechnol Rep (Amst)* 2019; **22**:e00331.

229 Zheng Y, Deng J, Han L, Zhuang M-W, Xu Y, Zhang J, *et al.* **SARS-CoV-2 NSP5 and N protein counteract the RIG-I signaling pathway by suppressing the formation of stress granules**. *Signal Transduct Target Ther* 2022; **7**:22.

230 Döring M, De Azevedo K, Blanco-Rodriguez G, Nadalin F, Satoh T, Gentili M, *et al.* **Single-cell analysis reveals divergent responses of human dendritic cells to the MVA vaccine**. *Sci Signal* 2021; **14**:eabd9720.

231 Shan B, Hou H, Zhang K, Li R, Shen C, Chen Z, *et al.* **Design, Synthesis, and Biological Evaluation of Bipyridazine Derivatives as Stimulator of Interferon Genes (STING) Receptor Agonists**. *J Med Chem* 2023; **66**:3327–3347.

232 Kim YS, Kim S-H, Shin J, Harikishore A, Lim J-K, Jung Y, *et al.* **Luteolin suppresses cancer cell proliferation by targeting vaccinia-related kinase 1**. *PLoS One* 2014; **9**:e109655.

233 Lee N, Kwon J-H, Kim YB, Kim S-H, Park SJ, Xu W, *et al.* **Vaccinia-related kinase 1 promotes hepatocellular carcinoma by controlling the levels of cell cycle regulators associated with G1/S transition**. *Oncotarget* 2015; **6**:30130–30148.

234 Liu Z-C, Cao K, Xiao Z-H, Qiao L, Wang X-Q, Shang B, *et al.* **VRK1 promotes cisplatin resistance by up-regulating c-MYC via c-Jun activation and serves as a therapeutic target in esophageal squamous cell carcinoma**. *Oncotarget* 2017; **8**:65642–65658.

235 Olgierd B, Kamila Ż, Anna B, Emilia M. **The Pluripotent Activities of Caffeic Acid Phenethyl Ester**. *Molecules* 2021; **26**:1335.

236 Zhong S, Zhou Q, Yang J, Zhang Z, Zhang X, Liu J, *et al.* **Relationship between the cGAS−STING and NF-κB pathways-role in neurotoxicity**. *Biomedicine & Pharmacotherapy* 2024; **175**:116698.

237 Yum S, Li M, Fang Y, Chen ZJ. **TBK1 recruitment to STING activates both IRF3 and NF-κB that mediate immune defense against tumors and viral infections**. *Proc Natl Acad Sci U S A* 2021; **118**:e2100225118.

238 AL Hamrashdi M, Brady G. **Regulation of IRF3 activation in human antiviral signaling pathways**. *Biochemical Pharmacology* 2022; **200**:115026.

239 Yu H, Lin L, Zhang Z, Zhang H, Hu H. **Targeting NF-κB pathway for the therapy of diseases: mechanism and clinical study**. *Sig Transduct Target Ther* 2020; **5**:209.

240 Wong LM, Jiang G. **NF-κB sub-pathways and HIV cure: A revisit**. *EBioMedicine* 2020; **63**:103159.

241 Oguariri RM, Adelsberger JW, Baseler MW, Imamichi T. **Evaluation of the effect of pyrimethamine, an anti-malarial drug, on HIV-1 replication**. *Virus Research* 2010; **153**:269–276.

242 Redmond AM, Skinner-Adams T, Andrews KT, Gardiner DL, Ray J, Kelly M, *et al.* **Antimalarial activity of sera from subjects taking HIV protease inhibitors**. *AIDS* 2007; **21**:763.

243 Hewitt K, Steketee R, Mwapasa V, Whitworth J, French N. **Interactions between HIV and malaria in non-pregnant adults: evidence and implications**. *AIDS* 2006; **20**:1993–2004.

244 Karp CL, Auwaerter PG. **Coinfection with HIV and tropical infectious diseases. I. Protozoal pathogens**. *Clin Infect Dis* 2007; **45**:1208–1213.

245 Van geertruyden J-P, D'Alessandro U. **Malaria and HIV: a silent alliance**. *Trends in Parasitology* 2007; **23**:465–467.

246 Gangjee A, Kurup S, Namjoshi O. **Dihydrofolate Reductase as a Target for Chemotherapy in Parasites**. *Current Pharmaceutical Design*; **13**:609–639.

247 Patki AH, Zielske SP, Sieg SF, Lederman MM. **Preferential S Phase Entry and Apoptosis of CD4+ T Lymphocytes of HIV-1-Infected Patients after *in Vitro* Cultivation**. *Clinical Immunology* 2000; **97**:241–247.

248 Harel J, Rassart E, Jolicoeur P. **Cell cycle dependence of synthesis of unintegrated viral DNA in mouse cells newly infected with murine leukemia virus**. *Virology*

1981; **110**:202–207.

249 Brown PO, Bowerman B, Varmus HE, Bishop JM. **Correct integration of retroviral DNA in vitro**. *Cell* 1987; **49**:347–356.

250 Ellison V, Abrams H, Roe T, Lifson J, Brown P. **Human immunodeficiency virus integration in a cell-free system**. *Journal of Virology* 1990; **64**:2711–2715.

251 Bedwell GJ, Engelman AN. **Factors that mold the nuclear landscape of HIV-1 integration**. *Nucleic Acids Research* 2021; **49**:621–635.

252 Haraguchi T, Koujin T, Segura-Totten M, Lee KK, Matsuoka Y, Yoneda Y, *et al.* **BAF is required for emerin assembly into the reforming nuclear envelope**. *Journal of Cell Science* 2001; **114**:4575–4585.

253 Hopfner K-P, Hornung V. **Molecular mechanisms and cellular functions of cGAS–STING signalling**. *Nat Rev Mol Cell Biol* 2020; **21**:501–521.

254 Gan Y, Li X, Han S, Liang Q, Ma X, Rong P, *et al.* **The cGAS/STING Pathway: A Novel Target for Cancer Therapy**. *Front Immunol* 2022; **12**. doi:10.3389/fimmu.2021.795401

255 Chen Q, Sun L, Chen ZJ. **Regulation and function of the cGAS–STING pathway of cytosolic DNA sensing**. *Nat Immunol* 2016; **17**:1142–1149.

256 Yang J, Xiang T, Zhu S, Lao Y, Wang Y, Liu T, *et al.* **Comprehensive Analyses Reveal Effects on Tumor Immune Infiltration and Immunotherapy Response of APOBEC Mutagenesis and Its Molecular Mechanisms in Esophageal Squamous Cell Carcinoma**. *International Journal of Biological Sciences* 2023; **19**:2551–2571.

257 Nagarajan UM. **Induction and Function of IFNβ During Viral and Bacterial Infection**. *Crit Rev Immunol* 2011; **31**:459–474.

258 Cheng Y, Schorey JS. **Mycobacterium tuberculosis-induced IFN-β production requires cytosolic DNA and RNA sensing pathways**. *J Exp Med* 2018; **215**:2919–2935.

259 Ashley CL, Abendroth A, McSharry BP, Slobedman B. **Interferon-Independent Upregulation of Interferon-Stimulated Genes during Human Cytomegalovirus Infection is Dependent on IRF3 Expression**. *Viruses* 2019; **11**:246.

260 Imaizumi T, Yoshida H, Hayakari R, Xing F, Wang L, Matsumiya T, *et al.* **Interferon-stimulated gene (ISG) 60, as well as ISG56 and ISG54, positively regulates TLR3/IFN-β/STAT1 axis in U373MG human astrocytoma cells**. *Neurosci Res* 2016; **105**:35–41.

261 Albert M, Bécares M, Falqui M, Fernández-Lozano C, Guerra S. **ISG15, a Small Molecule with Huge Implications: Regulation of Mitochondrial Homeostasis**. *Viruses* 2018; **10**:629.

262 Kang JA, Kim YJ, Jeon YJ. **The diverse repertoire of ISG15: more intricate than initially thought**. *Exp Mol Med* 2022; **54**:1779–1792.

263 Tsuruyama T, Hiratsuka T, Yamada N. **Hotspots of MLV integration in the hematopoietic tumor genome**. *Oncogene* 2017; **36**:1169–1175.

264 Wei Y, Chen S, Wang M, Cheng A. **Tripartite motif-containing proteins precisely and positively affect host antiviral immune response**. *Scandinavian Journal of Immunology* 2018; **87**:e12669.

265 Cattoglio C, Pellin D, Rizzi E, Maruggi G, Corti G, Miselli F, *et al.* **High-definition mapping of retroviral integration sites identifies active regulatory elements in human multipotent hematopoietic progenitors**. *Blood* 2010; **116**:5507–5517.

266 Wolff JH, Mikkelsen JG. **Delivering genes with human immunodeficiency virus-derived vehicles: still state-of-the-art after 25 years**. *J Biomed Sci* 2022; **29**:79.

267 Thomas MC, Chiang C-M. **The General Transcription Machinery and General Cofactors**. *Critical Reviews in Biochemistry and Molecular Biology* 2006; **41**:105–178.

268 Li X-D, Wu J, Gao D, Wang H, Sun L, Chen ZJ. **Pivotal Roles of cGAS-cGAMP Signaling in Antiviral Defense and Immune Adjuvant Effects**. *Science* 2013; **341**:1390–1394.

269 Burg M van der, IJspeert H, Verkaik NS, Turul T, Wiegant WW, Morotomi-Yano K, *et al.* **A *DNA-PKcs* mutation in a radiosensitive T^-B^- SCID patient inhibits Artemis activation and nonhomologous end-joining**. *J Clin Invest* 2009; **119**:91–98.

270 Budhiraja S, McManus G, Baisiwala S, Perrault EN, Cho S, Saathoff M, *et al.* **ARF4-mediated retrograde trafficking as a driver of chemoresistance in glioblastoma**. *Neuro Oncol* 2024; **26**:1421–1437.

271 Ovejero-Sánchez M, Rubio-Heras J, Vicente de la Peña MDC, San-Segundo L, Pérez-Losada J, González-Sarmiento R, *et al.* **Chloroquine-Induced DNA Damage Synergizes with Nonhomologous End Joining Inhibition to Cause Ovarian Cancer Cell Cytotoxicity**. *Int J Mol Sci* 2022; **23**:7518.

272 Liu Z-C, Cao K, Xiao Z-H, Qiao L, Wang X-Q, Shang B, *et al.* **VRK1 promotes cisplatin resistance by up-regulating c-MYC via c-Jun activation and serves as a therapeutic target in esophageal squamous cell carcinoma**. *Oncotarget* 2017; **8**:65642–65658.

273 Wang J, Zeng X, Gou J, Zhu X, Yin D, Yin L, *et al.* **Antiviral activity of luteolin against porcine epidemic diarrhea virus in silico and in vitro**. *BMC Vet Res* 2024; **20**:288.

274 Men X, Li S, Cai X, Fu L, Shao Y, Zhu Y. **Antiviral Activity of Luteolin against Pseudorabies Virus In Vitro and In Vivo**. *Animals (Basel)* 2023; **13**:761.

275 Sakai-Sugino K, Uematsu J, Yamamoto H, Kihira S, Kawano M, Nishio M, *et al.* **Inhibitory effects of kaempferol, quercetin and luteolin on the replication of human parainfluenza virus type 2 in vitro**. *Drug Discov Ther* 2024; **18**:16–23.

276 Wang Y, Li F, Wang Z, Song X, Ren Z, Wang X, *et al.* **Luteolin inhibits herpes simplex virus 1 infection by activating cyclic guanosine monophosphate-adenosine monophosphate synthase-mediated antiviral innate immunity**. *Phytomedicine* 2023; **120**:155020.

277 Fu L, Li S, Men X, Cai X, Wang Z, Xu Y, *et al.* **Optimizing the Extraction and Enrichment of Luteolin from Patrinia villosa and Its Anti-Pseudorabies Virus Activity**. *Molecules* 2023; **28**:5005.

278 Wu Z, Zhao X, Li R, Wen X, Xiu Y, Long M, *et al.* **The combination of Schisandrin C and Luteolin synergistically attenuates hepatitis B virus infection via repressing HBV replication and promoting cGAS-STING pathway activation in macrophages**. *Chin Med* 2024; **19**:48.

279 Guo Q, Jin Y, Chen X, Ye X, Shen X, Lin M, *et al.* **NF-κB in biology and targeted therapy: new insights and translational implications**. *Sig Transduct Target Ther* 2024; **9**:1–37.

280 Liu T, Zhang L, Joo D, Sun S-C. **NF-κB signaling in inflammation**. *Signal Transduct Target Ther* 2017; **2**:17023-.

281 Yang Y, Wang L, Peugnet-González I, Parada-Venegas D, Dijkstra G, Faber KN. **cGAS-STING signaling pathway in intestinal homeostasis and diseases**. *Front Immunol* 2023; **14**. doi:10.3389/fimmu.2023.1239142

282 Pérez R, Burgos V, Marín V, Camins A, Olloquequi J, González-Chavarría I, *et al.* **Caffeic Acid Phenethyl Ester (CAPE): Biosynthesis, Derivatives and Formulations with Neuroprotective Activities**. *Antioxidants* 2023; **12**:1500.

283 Kumar V, Sari AN, Gupta D, Ishida Y, Terao K, Kaul SC, *et al.* **Anti-COVID-19 Potential of Withaferin-A and Caffeic Acid Phenethyl Ester**. *Curr Top Med Chem* 2024; **24**:830–842.

284 Taysi S, Algburi FS, Taysi ME, Caglayan C. **Caffeic acid phenethyl ester: A review on its pharmacological importance, and its association with free radicals, COVID-19, and radiotherapy**. *Phytother Res* 2023; **37**:1115–1135.

285 Cui Z, Zhang J, Wang J, Liu J, Sun P, Li J, *et al.* **Caffeic acid phenethyl ester: an effective antiviral agent against porcine reproductive and Respiratory Syndrome Virus**. *Antiviral Res* 2024; **225**:105868.

286 Cui Z, Wang Q, Li D, Zhao S, Zhang Q, Tan Y, *et al.* **Icariin, Formononetin and Caffeic Acid Phenethyl Ester Inhibit Feline Calicivirus Replication In Vitro**. *Arch Virol* 2021; **166**:2443–2450.

287 Fesen MR, Pommier Y, Leteurtre F, Hiroguchi S, Yung J, Kohn KW. **Inhibition of HIV-1 integrase by flavones, caffeic acid phenethyl ester (CAPE) and related compounds**. *Biochem Pharmacol* 1994; **48**:595–608.

288 Olgierd B, Kamila Ż, Anna B, Emilia M. **The Pluripotent Activities of Caffeic Acid Phenethyl Ester**. *Molecules* 2021; **26**:1335.

289 Semrau K, Kuhn L, Kasonde P, Sinkala M, Kankasa C, Shutes E, *et al.* **Impact of chloroquine on viral load in breast milk**. *Tropical Medicine & International Health* 2006; **11**:800–803.

290 Pyrimethamine. In: *Drugs and Lactation Database (LactMed®)*.Bethesda (MD): National Institute of Child Health and Human Development; 2006. http://www.ncbi.nlm.nih.gov/books/NBK501163/ (accessed 20 Aug2024).

291 Salman S, Davis TME. **Regarding "Lactation Status and Studies of Pyrimethamine Pharmacokinetics in Pregnancy."** *CPT: Pharmacometrics & Systems Pharmacology* 2017; **6**:730–730.

292 de Kock M, Tarning J, Barnes KI, Denti P. **Response to "Lactation Status and Studies of Pyrimethamine Pharmacokinetics in Pregnancy."** *CPT: Pharmacometrics & Systems Pharmacology* 2017; **6**:731–731.